2013

INVENTORY OF MONGOLIAN GLACIERS FOR THE GLOBAL LAND ICE MEASUREMENTS FROM SPACE (GLIMS) PROGRAM

Caleb Gikai Pan
The University of Montana

INVENTORY OF MONGOLIAN GLACIERS FOR THE GLOBAL LAND ICE MEASUREMENTS FROM SPACE (GLIMS) PROGRAM

By

CALEB GIKAI PAN

Bachelor of Science in Geography, Appalachian State University, Boone, NC, 2010

Thesis

Presented in partial fulfillment of the requirements for the degree of

Master of Science in Geography

The University of Montana
Missoula, MT

June 2013

Approved by:

Sandy Ross, Associate Dean of The Graduate School
Graduate School

Ulrich Kamp, Chair
Department of Geography

Kevin McManigal
Department of Geography

Jeffery Colby
Department of Geography and Planning
Appalachian State University

ABSTRACT

Pan, Caleb, M.S., Spring 2013 Geography

Inventory of Mongolian Glaciers for the Global Land Ice Measurements from Space (GLIMS) Program

Committee Chair: Ulrich Kamp

Glaciers in the Altai Mountains of Mongolia provide an estimated 10 % of the total water resources within the country. Yet, the number and area of glaciers within the Altai Mountains is inconsistent and conflicting. Glacier mapping attempts by previous author groups did not mention their mapping methods, data source, and/or date of analysis. Therefore, making it difficult to analyze and compare glacier base data. Due to a combination of climate change and land use management practices, the necessity of inventorying glaciers in the Altai Mountains of Mongolia is of great importance. The practice of glacier monitoring using remote sensing data provides the foundation for enlightened water resource management, vulnerability and adaptations to water shortages, climate change assessment, and glacier change detection. Implementing data acquired from Landsat Thematic Mapper, this glacier inventory developed an intuitive, robust, and inexpensive methodology to map glaciers in the Altai Mountains during 1990, 2000, and 2010. Along with the developed methodology, this study also defined a glacier definition, glaciated extents, and date of acquisition to ensure consistency for the future of glacier monitoring in the Altai Mountains. Furthermore, this study parameterized the glacier outlines using SRTM data, including equilibrium line altitude, mean slope, mean glacier terminus elevation, and aspect. Including data acquired from ASTER GDEM, this study found that surface lowering occurred on 82.3 % of all glaciers from between 2000 to 2008. The inventory includes an estimated total surface area of 540.57 km^2 in 1990, 428 km^2 (±17.20 %) in 2000, and 372.30 km^2 (±17.17 %) in 2010. All glacier datasets will be made available to the public free of charge at www.glims.org for further analysis of glaciers in the Altai Mountains of Mongolia.

"O, how incomprehensible everything was, and actually sad, although it was also beautiful. One knew nothing. One lived and ran about the earth and road through forests, and certain things looked so challenging and promising and nostalgic: a star in the evening, a blue harebell, a reed-green pond, the eye of a person or a cow. And sometimes it seemed that something never seen yet long desired was about to happen, that a veil would drop from it all; but then it passed, nothing happened, the riddle remained unsolved, the secret spell unbroken, and in the end one grew old and looked cunning… or wise… and still one knew nothing perhaps, was still waiting and listening."

——Herman Hesse, *Narcissus and Goldmund* in
The Snow Leopard by Peter Matthiessen

ACKNOWLEDGEMENTS

I should start by saying that it has been a great privilege to work with my advisor Dr. Ulrich Kamp. I am forever grateful to him for being an amazing mentor and giving me this opportunity.

I would also like to thank my committee members Mr. Kevin McManigal and Dr. Jeff Colby for taking time out of their busy days to assist me with my perpetual questions and for providing their technical expertise.

To my fellow graduate students, thank you for the moral support and more importantly, your friendships.

Finally, I want to thank my family for their unconditional support throughout this adventure.

ABBREVIATIONS

A_{er}	Percent Error of Area Determination
ARC	Anisotropic Reflectance Correction
ASTER	Advanced Spaceborne Thermal Emission and Reflection Radiometer
AWS	Automated Weather Stations
CSI-CGIAR	Consortium for Spatial Information - Consultative Group for International Agricultural Research
CWD	Cold Wave Duration
DEM	Digital Elevation Model
EBA	Ecosystem-Based Adaptations
ECPA	Energy Partnership for the Americas
ELA	Equilibrium Line Altitude
ENSO	El Niño Southern Oscillation
GLIMS	Global Land Ice Measurement from Space
GLOVIS	Global Visualization Viewer
HWD	Heat Wave Duration
ICIMOD	International Centre for Integrated Mountain Development
IPCC	Proposed resource management plan
MDG	Millennium Development Goals
MEA	Millennium Ecosystem Assessment
MNE	Ministry Nature and Environment
MTRI	Michigan Tech Research Institute
NDS	National Development Strategies
NDSI	Normalized Difference Snow Index
NDWI	Normalized Difference Water Index
NIR	Near-Infrared
NPS	National Park Service
NSIDC	National Snow and Ice Data Center
RC	Regional Center
RESTEC	Remote Sensing Technology Center of Japan
RGI	Randolph Glacier Inventory

SRTM	Shuttle Radar Topography Mission
SWE	Snow Water Equivalent
SWIR	Short-Wave Infrared
TM	Thematic Mapper
USGS	United States Geological Survey
WGI	World Glacier Inventory
WGMS	World Glacier Monitoring Service

CONTENTS

FIGURES

TABLES

APPENDICES

1. INTRODUCTION

Mountains provide an essential source of freshwater to millions of people. Global water resources can be affected by climate change due to the sensitive nature of mountain ecosystems, specifically alpine glaciers (Zemp *et al*. 2010, Viviroli *et al.* 2011). In order to help mitigate risk and vulnerability in future water shortages, the practice of monitoring glaciers helps contribute to enlightened water resource management. These management issues become even more important as the issue of water security and geopolitcal stability are discussed (Bishop *et al*. 2008). To assist in these resource management decisions the World Glacier Monitoring Service (WGMS) was established in 1986 (Raup *et al.* 2007a, Gjermundsen *et al*. 2011). The WGMS took responsibility for collecting information on global glacier fluctuations from the World Glacier Inventory (WGI) (Racoviteanu *et al.* 2009, Gjermundsen *et al.* 2011).

In 1999, the Global Land Ice Measurements from Space (GLIMS) program was developed. GLIMS is an international consortium of global universities and research institutes, and is coordinated by the University of Arizona and the National Snow and Ice Data Center (NSIDC) (Kargel *et al*. 2005, Bishop *et al*. 2008). GLIMS's mission is to assess the condition of the world's land glaciers by coupling remote sensing and GIS technologies to produce glacier base data (Bishop *et al*. 2008, Racoviteanu *et al.* 2009). All imagery and glacier data can be accessed via the internet and downloaded free of charge (Raup *et al*. 2007a, Bishop *et al.* 2008, Racoviteanu *et al*. 2009). From evaluating the data on the GLIMS website, it is evident that mountain areas such as the Alps, Andes, Himalayas, and Alaska receive most of the research interest while other mountain ranges are underrepresented. It was only in 2010 that scientists at the National University of

Mongolia and The University of Montana together established the GLIMS Regional Center for Mongolia (Kamp *et al.* in press). In order to study global patterns of glacier changes, GLIMS distributes the responsibility for a particular glaciated region to Regional Centers (RC). RC's are tasked with coordinating mission planning for their designated region, including data acquisition and analysis. It is important for the RC to have a strong understanding of seasonal weather conditions and general familiarity with the region in order to utilize the best available data (www.glims.org).

Glacier monitoring efforts in the Altai Mountains of Mongolia play an integral role in pastoralist mitigation and adaptations to climate change and water resource conservation. Data generated from a glacier inventory will contribute to a greater understanding of how climate change and land use management have impacted glaciers as an invaluable water resource in Mongolia. When Mongolia was introduced to a free market economy in 1990, rapid urbanization and economic development exponentially increased Mongolia's demand for water (Priess *et al.* 2010). Mongolia is a naturally water-restricted nation, but through a combination of climate change and land use management practices the necessity of inventorying glaciers is of great importance. Kamp *et al.* (in press) explained that only a few studies involving the mapping of glaciers exist for Mongolia and only recently has systematic mapping begun. Since there are so few studies concerning glaciers in Mongolia, the exact number is conflicting. Davaa *et al*. (2005) put the number of glaciers at 262, while Klinge (2001) estimated the number to be as high as 731. In addition, Kamp *et al*. (in press) discussed the importance in approaching previous glacier studies in Mongolia with extreme caution, because methods of glacier mapping, source data type, and/or date of acquisition are often not mentioned.

Previous Mongolia mapping projects have been performed by multiple scientific teams (Selivanov 1972, Lehmkuhl 1998, 2012, Baast 1998, Klinge 2001, Kadota and Davaa 2004, 2011, Davaa and Basandorg 2005, Enkhtaivan 2006, Krumwiede et al. in press). These authors used various sources including topographic maps, repeat photography, aerial photos, and satellite images from CORONA Landsat, and ASTER.

As part of GLIMS, this study will report observations in glacier length, number, and area in the Altai Mountains of Mongolia, based on multi-spectral analysis of Landsat Thematic Mapper (TM) imagery for 1990, 2000, and 2010. Knowledge of the complex glacier-climate dynamic and history of glacier mass is essential to the long-term management of water resources in Mongolia. Due to the high spatial variability of glacier ablation and accumulation, glacier parameters were produced and examined, including glacier slope, aspect, and hypsometry.

Multiple author groups have used satellite imagery to examine glaciers at a massif/range scale. Most of these author groups only examined glacier area and number, and few examined hypsometric parameters. To gain a stronger understanding of glacier spatial variability within the Altai Mountains, this paper will examine two massifs in detail; Tavan Bogd and Munkh Khairkhan. These two massifs are excellent study sites because they include a wide spread of glacier types, distribution, previous research, and high quality Landsat TM data for all three time periods.

This glacier inventory also attempts to establish a glacier monitoring network within the Altai Mountains of Mongolia by creating a simple, inexpensive, and robust method for mapping and attributing glaciers from remote sensing imagery. The final inventory will be made available to the public through the GLIMS online database.

2. STUDY AREA

Mongolia lies between of 41° 35'N and 52° 09'N and of 87° 44'E and 119° 56'E and is a landlocked country that experiences extreme continentality which is expressed in diurnal (±30˚C) and seasonal variation (Batima 2006, Shahgedanova *et al.* 2009). January tends be the coldest month with average temperatures ranging from -15°C to -35°C. July is the warmest month with average temperatures around 15°C - 20°C in the mountainous regions and average temperatures ranging from 20°C - 25°C in the eastern steppe and Gobi desert (Batima *et al.* 2005).

In general, Mongolia is semi-arid to arid (Batima *et al.* 2005). The drier climate is due to strong influence of the Siberian High during the winter time allowing for about 250 days of clear skies (Gong *et al.* 2001, Shahgedanova *et al.* 2009). In summer, Mongolia is controlled by the westerlies which bring precipitation from the Atlantic and Mediterranean. The influence of the moisture brought from the Atlantic and Mediterranean results in decreasing precipitation from west to east (Shahgedanova *et al.* 2009). Mongolia only receives 230 mm of precipitation annually. Precipitation amounts tend to be highest in the north region and decreases towards the south. Northern regions can receive between 350-500 mm/year while areas in the south, such as the Gobi Desert, receive precipitation as low as 50 mm/year (Davaa *et al.* 2007) Precipitation in Mongolia is spatially variable and highly seasonal with 60-90 % falling during the summer months. During the winter months, mountainous regions above 2,500 m receive precipitation totals between 400-500 mm (Endo *et al.* 2006, Davaa *et al.* 2007, Khrutsky and Golubeva 2008). Yet at lower elevations, precipitation is dominated by the Mongolian anticyclone (Siberian High), which promotes cold weather, infrequent

precipitation and drying winds, causing fallen snow to quickly evaporate (Khrutsky and Golubeva 2008). Batima and Dagvadorj (2000) have revealed that on average 70-90% of fallen precipitation evaporates, while the rest will recharge rivers and groundwater. The distribution of available water and precipitation gradient has created a gradient in ecotones of forest-steppe-desert (Davaa *et al.* 2007).

Mongolia is an upland country with an average altitude of 1,580 m and 85% of the country is located above 1000 m (Gilberg *et al.* 1996, Stumpp *et al.* 2005, Batima 2006). There are four mountain ranges within Mongolia including; Khan-Khokhii Mountains, Khanghai Mountains, Khentii Mountains, and the Altai Mountains. The Altai is the only range supporting glaciers, and it has the highest peak of Mongolia at 4,653 m (Khuiten Peak). Klinge (2001) divided the Altai Mountains into north and central sub-regions, within the northern Altai are the following ranges/massifs: Ikh Turgen, Turgen, Kharkhiraa, Tavan Bogd Khuiten, Tsagaan Khairkhan, Asgat, Dongoron, and Tsengel. In the central Altai are Tsambagarav, Sair, Khokh Serhiyn, Munkh Khairkhan, and Suitai. Because the Altai is such a large area, this study follows the lead of Bolch *et al*. (2010a) and separates the ranges into regions based on climate characteristics and natural boundaries (Figure 1 & Table 1).

Table 1. Glaciated regions in the Mongolian Altai and their assigned sub-regions.

Sub-region	**Range**
Northwest Interior	Tavan Bogd Hoton Sirgali Unkur Khairkhan
Northern Altai	Kharkhiraa Turgen Ikh Turgen
Southern Altai	Munkh Khairkhan Sutai Batar Khairkhan
Central Altai	Tsambagarav Sairiin Khukh Serkhyn Khrumuni Khairkhan
Central Interior	Tsengel Khairkhan Buyantiin Uul Kharit Nuruu Dushiin Uul

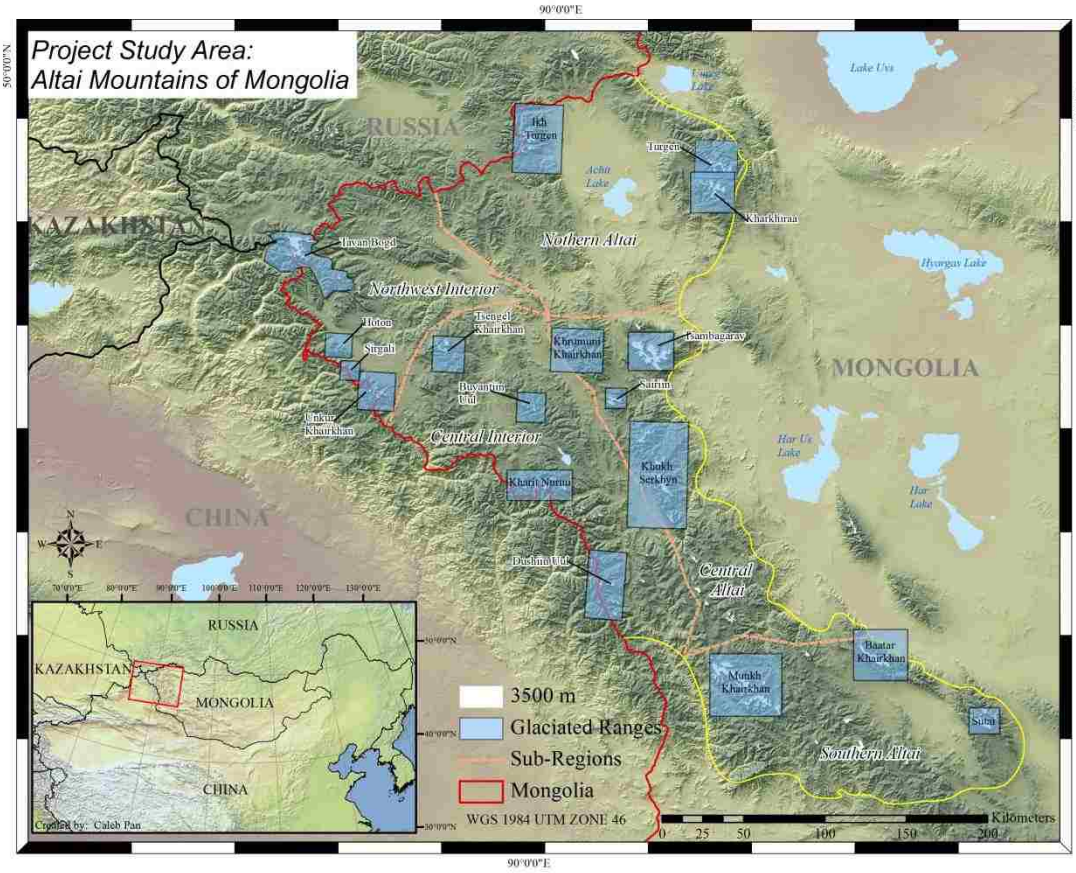

Figure 1. Study area showing the defined sub-regions and elevations higher than 3,500 m.

3. BACKGROUND

3.1 Glaciers in Mongolia

Glaciers in Mongolia can be found at elevations starting at 2,750 m with mean annual air temperature of -8°C. The distribution of glaciers follows a north-west to south-east trend, between 46°25' and 50°50'N and between 87°40' and 100°50'E (Davaa *et al*. 2007). The Mongolian glaciers can be divided into three types: 75% mountain slope glaciers, 21 % valley glaciers, and 4% flat top glaciers (WWF 2004). Dashdeleg *et al.* (1983) put the total number of glaciers in Mongolia at 262 with a total area of 659 km^2. It is difficult to say how far glaciers have retreated due to inconsistent records, but Baast (1998) believed that from 1945 to 1985 total glacier area has decreased by 6%. Kadota and Gombo (2007) inventoried 91 glaciers in the Mongolian Altai and found that glaciers lost between 10-30% of their surface area since the 20th century. The variation in glacier retreat is credited to the high spatial variability between individual glaciers (Shahgedanova *et al.* 2009).

3.2 Water Resources

Mongolia has an estimated total water resource of 599 km^3/year. The overwhelming majority of the water resource is stored in freshwater lakes (500 km^3/year; 83.4%) and glaciers (62.9 km^3/year; 10.8%). Rivers do not play a significant role in water resources and only store an estimated 34.6 km^3/year (5.8%). The insignificant role in rivers is because 60 % of the river runoff formed in Mongolia flows into China and Russia, only 40% flow into the Gobi. Mongolian rivers are less consistent and experience limited flow for half of the year. During the winter months, river flows are drastically reduced due to freezing. Surface water in Mongolia during summer months is

susceptible to being lost to evaporation due to the arid environment and lost to groundwater infiltration (Davaa *et al.* 2007). In Mongolia, because of the lack of surface water, ground water is invaluable for livestock and human settlements. Besides wells, the only access to water that wildlife have are oases and natural springs (Dugarjav *et al.* 2003). The importance of ground water is emphasized by the fact that 31% and 25% of the total population of Mongolia receive their water from the tap or tank distribution, which mostly comes from the ground (Davaa *et al.* 2007). A Mongolian water inventory conducted in 2007 concluded that there are 5,138 rivers in Mongolia and among those, 884 (17.2%) have dried-out. Mongolia also has 3,747 lakes, but 1,189 (31.6%) of them have dried out (Bayasgalan *et al.* 2008). The distribution of water availability is also unevenly distributed throughout Mongolia. Myagmarajav *et al.* (1999) explained that in northern Mongolia the available water per capita is 4-5 times more than the world average, while in southern Mongolia, the available water per capita is 10 times less than the world average.

3.3 Environmental Change Adaptation Strategies and Projects

Alam (2010) explained the importance of Ecosystem-Based Adaptation (EBA) drawing from Millennium Ecosystem Assessment (MEA) examples conducted in 2005. Throughout the world over one billion people in over 100 developing countries are locked in the cycle of poverty and environmental degradation made worse by climate change. Currently, Mongolia is stuck in the cycle mentioned in the MEA. Over half of Mongolia's population is dependent on livestock production and as 2007, 830,000 (32.2%) Mongolians are living in poverty (Bayasgalan *et al.* 2008, Tsedendamba 2010). This large dependence on a singular economy puts Mongolia in a precarious situation due

to the effects of climate change and land use management (Davaa *et al*. 2007). It should also be noted that up to 1990, Mongolia had pursued intensive utilization of its natural resources to accelerate economic development. Therefore, conservation efforts were heavily neglected (Dugarjav *et al.* 2003). Fortunately, pastoralist vulnerability to climate change has been recognized by many research groups since the 1990s. The National Action Plan for Climate Change in Mongolia was approved in 1999, however had not been implemented due to lack of financial resources and political commitment (Bayasgalan *et al.* 2008). Finally, in 2007 the President of Mongolia requested that the government to create Millennium Development Goals (MDG) based on the long-term National Development Strategy (NDS) up to 2021; these goals were ratified on January 31st, 2008 (Tsedendamba 2010). The MDG-based assessment identified multiple concerns including, insufficient poverty reduction, decreasing population growth, utilization of land, mineral resources and environmental protection, and economic development.

3.3.1 Pastoralist Adaptations to Environmental Change

Herders need to develop the ability to adapt to a changing landscape, specifically a reduced water supply and desertification. Togtokh (2010) noted that the increase in livestock and decrease in water availability has led to the collapse of pastoral systems in central and western Mongolia. Adaptation strategies to sustain the Mongolian livestock sector include encouraging communities living in riparian regions to economically diversify to industries such as farming and ecotourism. By reducing the amount of livestock and mitigating degradation in ecologically fragile and integral ecosystems, valuable springs and water resources will be protected. Adaptation strategies also need to

be implemented in regions where water is not as readily available as it is in the western Altai. Outside of the Altai, irrigation and wells are the dominant source of water for livestock throughout Mongolia. Since the privatization of herds, the condition of wells has disintegrated because private herders do not take responsibility for maintaining wells. Bayasgalan *et al.* (2008) suggested the concept that each family has their own well needs to be rejected and replaced with ideology that collects families to one centralized water distribution center that works like a gas station. Naidansuren (2007) suggested government involvement to maintain the state of pastoral wells. This includes the expensive task of digging new wells or increasing well-depth as the water table lowers. The proposed mitigation strategies by Bayasgalan *et al.* (2008) and Naidansuren (2007) are valuable initiatives and need to be consolidated to be most beneficial. Davaa *et al.* (2010) suggested to capturing glacier melt in reservoirs and existing lakes at high altitudes to minimize evaporation loss. The created reservoirs can be utilized for hydropower, drinking water, industrial water use, and pastoral watering.

3.3.2 Agricultural Adaptations

With the success of the government program Third Campaign for Reclaiming Virgin Lands and the possible cultivation of hay, Mongolia needs to implement environmentally sustainable agricultural practices to continue intensive agriculture. Since intensive agriculture only began in 2008 in Mongolia, the long-term effects are still not fully understood. However, Tsogoo *et al.* (2010) emphasized the need for implementing high-efficiency water-saving agro-technologies, including spray and drip irrigation and also the development of fertilizers and pest controls technology.

4. METHODS

4.1 Defining 'Glacier'

Prior to any image processing, it is important to define the object of the mapping study, i.e. to define 'glacier'. This is crucial in order to sustain consistent multi-temporal analysis by different scientific teams. GLIMS defines a glacier in terms of remote sensing, thus does not involve motion of ice. A glacier or perennial snow mass, identified by a single GLIMS glacier ID, consists of a body of ice and snow that is observed at the end of the melt season (Müller *et al*. 1977, Paul and Andreasen. 2009, Rau *et al*. 2005, Racoviteanu *et al*. 2009, Raup *et al.* 2007a). Many scientific groups using remote sensing data to map glaciers have used the GLIMS definition but have varying glacier area (km^2) to define what constitutes a glacier. When inventorying glaciers in western Canada, Bolch *et al*. (2010a) decided to only map glaciers larger than 0.05 km^2. Bolch *et al*. (2010b) mapped glaciers that were 0.01km^2, but they only compared glaciers larger than 0.1km^2. Paul *et al*. (2010) believed the lower limit of what constitutes a glacier is 0.01 km^2, because a glacier any smaller would be too difficult to accurately identify through a platform with a spatial resolution of 15m to 30m. Frey *et al.* (2012a) defined a glacier as being larger than 0.2 km^2. Krumwiede *et al.* (in press) applied a 0.1 km^2 size filter when mapping glaciers on Munkh Khairkhan and Tavan Bogd massifs, believing anything smaller represents only transient snow patches. This study puts the threshold for identifying a glacier at 0.01 km^2. However, to filter out potential snow patches, glacier parameters were only developed for glaciers larger than 0.1 km^2.

For water resource management it is important to map even transient snow patches because they contribute to local hydrology. Further, it is assumed that when mapping glaciers through a remote sensing platform that the implemented image is obtained at the absolute end of the melt season. Therefore, any snow patches in the image will remain until the first season's snow.

In this study, five classes of glacier size were created to further analyze glacier parameters based on glacier size. In the Altai Mountains, most of the glaciers are of small scale; therefore, a geometrical classification was used for the derivation of size classes (Table 2).

Table 2. Glacier class sizes based on a geometrical classification.

Class Size	Area (km^2)
1	< 0.025
2	.026-.125
3	.126-.85
4	.86-5.5
5	> 5.5

4.2 Creating a GLIMSID

Glaciers are identified in the GLIMS database using a unique ID composed of the glacier's longitude and latitude coordinates, known as the GLIMSID (Paul *et al.* 2009). The actual generation of the GLIMSID is made simple thanks to the "GLIMS glacier ID generation tool" which can be found at http://glims.colorado.edu/tools/lonlat2id/. To create the GLIMSID, the analyst needs to calculate the centroid for all the glaciers in longitude and latitude using the Feature to Point tool within ArcMap Desktop. Next, the coordinates for each centroid needs to be imported to the online tool. The tool then transforms the coordinates into an ID, identifiable by placing a "G" in front of the ID and

an “E” and “N” designating easting or northing in the centroid coordinates (e.g. G225691E58672N) (Raup *et al.* 2007b).

On occasion, depending on the glacier outline shape, the centroid can fall outside of the glacier polygon. In these instances it is necessary for the user to manually move the point to reside within the polygon. Also, it should be noted that the point needs to be located within the glacier polygon for all time periods. Due to the rapid retreat of glaciers and high frequency of small glaciers in the Altai Mountains, assigning GLIMSIDs became even more challenging due to the disintegration of many glaciers. As a glacier disintegrates from a larger glacier, the new glacier receives a new GLIMSID but also retains the old GLIMSID in a new field, designated as a Parent_ID. Raup *et al.* (2007b) described the retention of parent-child glacier relationships as being valuable to a user for updating or repeating original analyses.

4.3.1 Satellite Imagery

Landsat TM imagery is the main satellite data source for the Mongolian glacier inventory. In this study, Landsat TM imagery from 1989 to 1991, 1998 to 2002, and 2010 to 2011 was utilized and presents twenty years of glacier changes in the Altai Mountains. The scenes are made available at the USGS using the Global Visualization Viewer (GLOVIS); as Level 1t products which provide radiometric and geometric corrections based from ground control points or Level 1Gt products using SRTM DEM for radiometric and geometric corrections (http://landsat.usgs.gov/products_productinformation.php, Bolch *et al*. 2010a) (Table3). For this study, Landsat TM imagery was ordered and selected based on multiple criteria:

1) percent of cloud cover; 2) atmospheric noise; 3) date availability; and 4) end of melt season.

Table 3. Utilized Landsat TM imagery.

	Date	Path/Row	Sensor	Entity ID
1990 Inventory	09/03/89	143/26	TM4	LT41430261989246XXX02
	09/13/89	141/26	TM5	LT51410261989256BJC00
	07/17/91	141/26	TM5	LT51410261991198XXX0
	07/17/91	141/27	TM5	LT51410271991198XXX03
	08/04/91	139/28	TM5	ETP139R28_5T19910804
2000 Inventory	08/19/98	143/25	TM5	LT51430251998231BIK00
	08/21/98	141/26	TM5	LT51410261998233BIK00
	08/26/98	144/26	TM5	LT51440261998238BIK00
	09/04/98	143/26	TM5	LT51430261998247BIK00
	08/03/00	140/27	TM5	LT51400292000216BJC00
	08/08/00	143/26	TM5	LT51430262000221BJC00
	08/17/00	142/27	TM5	LT51420272000230BJC00
	08/27/00	140/27	ETM	LE71400272000240SGS00
	09/18/00	142/26	TM5	LT51420262000262BJC00
	07/28/01	141/26	TM5	LT51410262001209BJC00
	09/05/01	142/25	TM5	LT51420252001248BJC00
	09/07/01	140/28	TM5	LT51400282001250BJC00
2010 Inventory	08/29/10	147/25	TM5	LT51420252010241IKR00
	07/26/11	141/27	TM5	LT51410272006207IKR00
	08/07/11	143/26	TM5	LT51430262011219KHC01
	08/25/11	141/26	TM5	LT51410262011237IKR00
	09/01/11	142/27	TM5	LT51420272011244IKR00
	09/01/11	142/26	TM5	LT51420262011244IKR00
	09/03/11	140/28	TM5	LT51400282011246IKR00
	09/03/11	140/27	TM5	LT51400272011246IKR00
	09/08/11	143/25	TM5	LT5143025201125IKR00

4.3.2 Cloud-Cover Model

Due to the orographic nature of mountains, collecting high quality Landsat TM imagery during three time periods is challenging. To increase the number of good Landsat TM scenes and use all available data, a cloud-cover model was developed using Model Builder inside the ArcMap environment. This model requires two separate

satellite scenes and was used in the few instances when certain parts of mountain ranges were inundated with clouds, but still had regions where glacier data could be utilized. Within a short time-frame a separate image was captured and where the earlier image was covered in clouds (Figure 2a), the new image was cloud-free (Figure 2b).

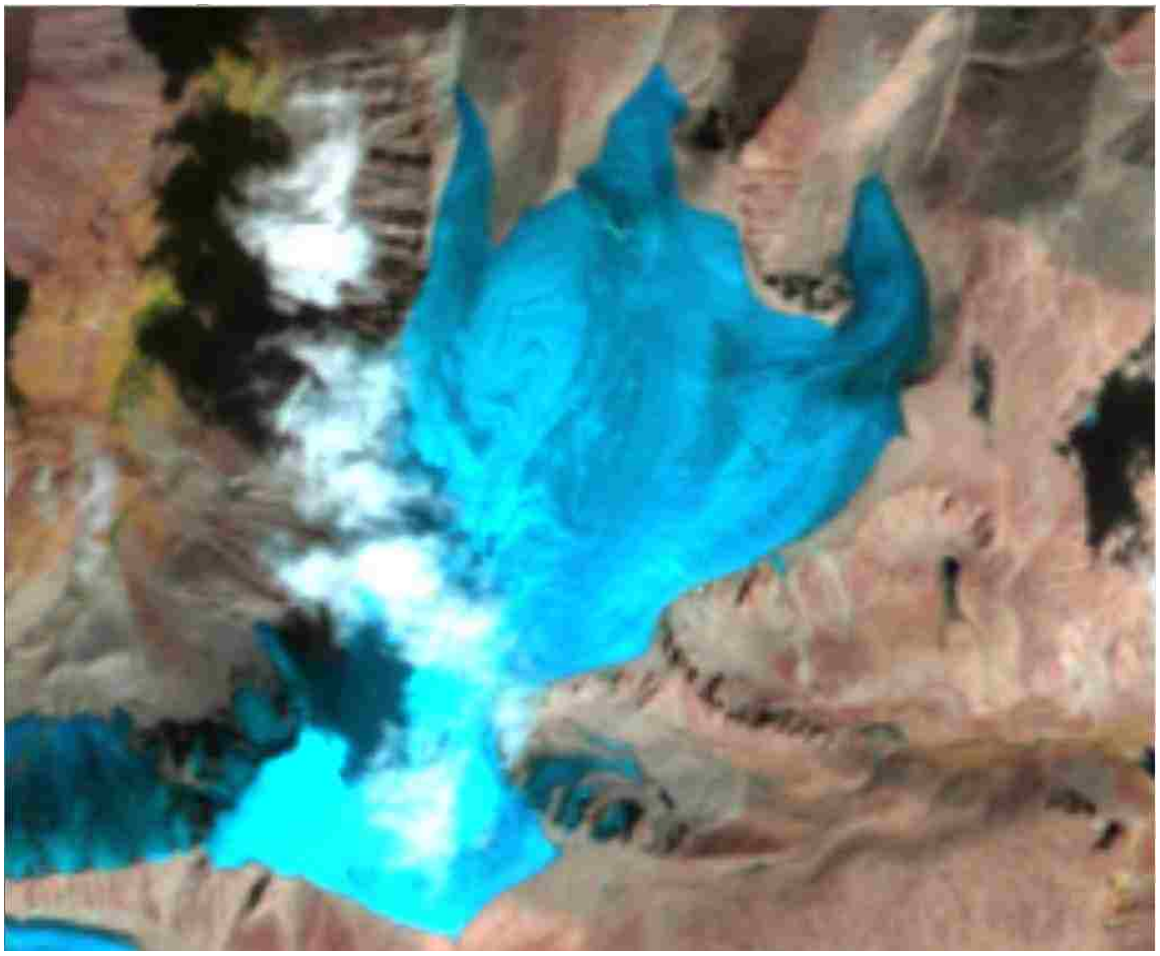

Figure 2a. Utilized image in the cloud-cover model, acquired on 8/25/2011 over Tsambagarav.

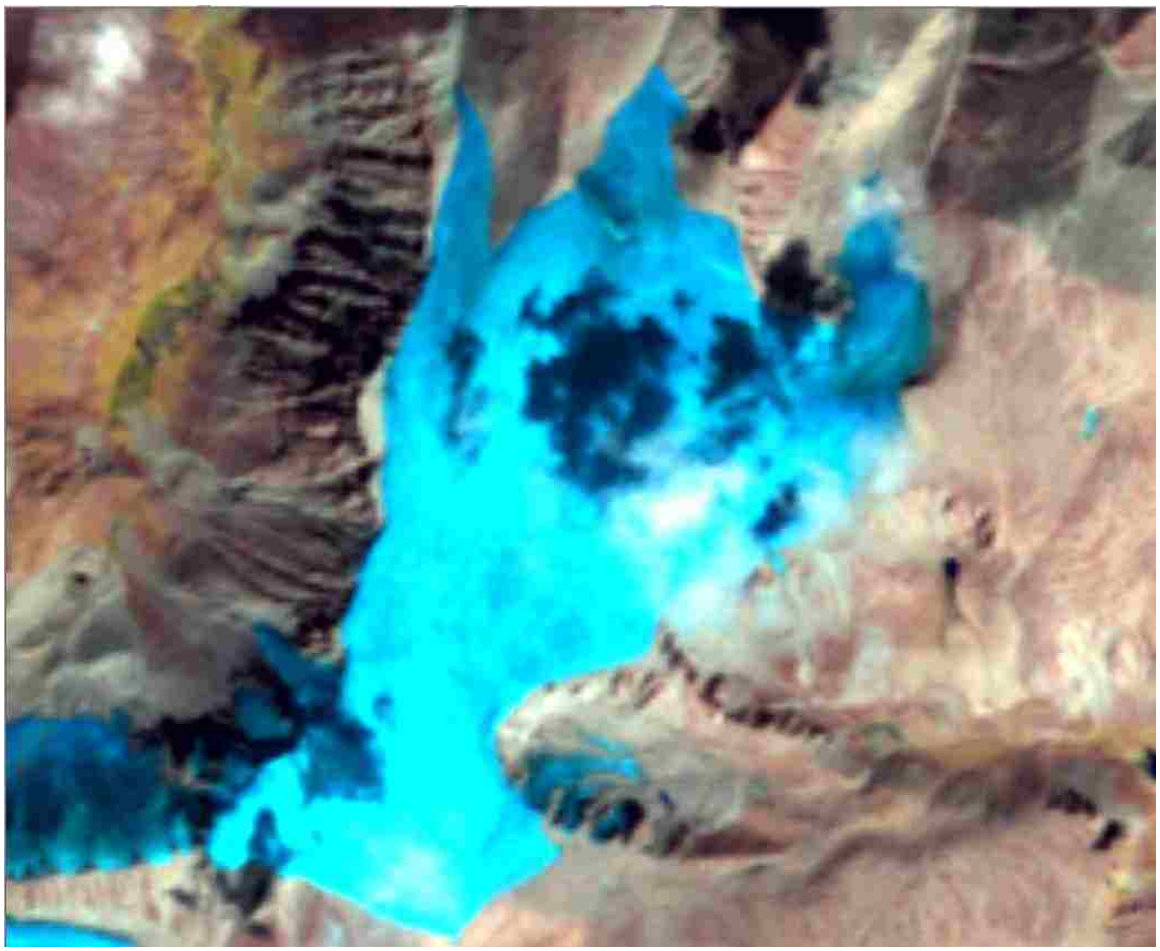

Figure 2b. Utilized image in the cloud-cover image, acquired on 9/1/2011 over Tsambagarav. Comparing Figure 2a & 2b, western half of Figure 2a is inundated with clouds while Figure 2b is not. Yet Figure 2b is inundated with clouds and shadows on its eastern half. When the two images are combined they equal a high quality Landsat TM scene for the time period.

The cloud cover model utilizes two input glacier polygons extracted from two images acquired at separate times, using a band ratio. Once the input data is processed, they are converted to a raster and appended to each other. The two appended rasters now represent the combined glacier land cover between the two images; they are then converted back to polygons and smoothed (Figure 3). It is important that the images used in this model do not have a significant difference in temporal resolution. If the time span is large, the newly created polygon will not be representative of the state of glaciers at the

particular time. For the Mongolian glacier inventory, the cloud cover model was only used in instances where the time span was two weeks apart.

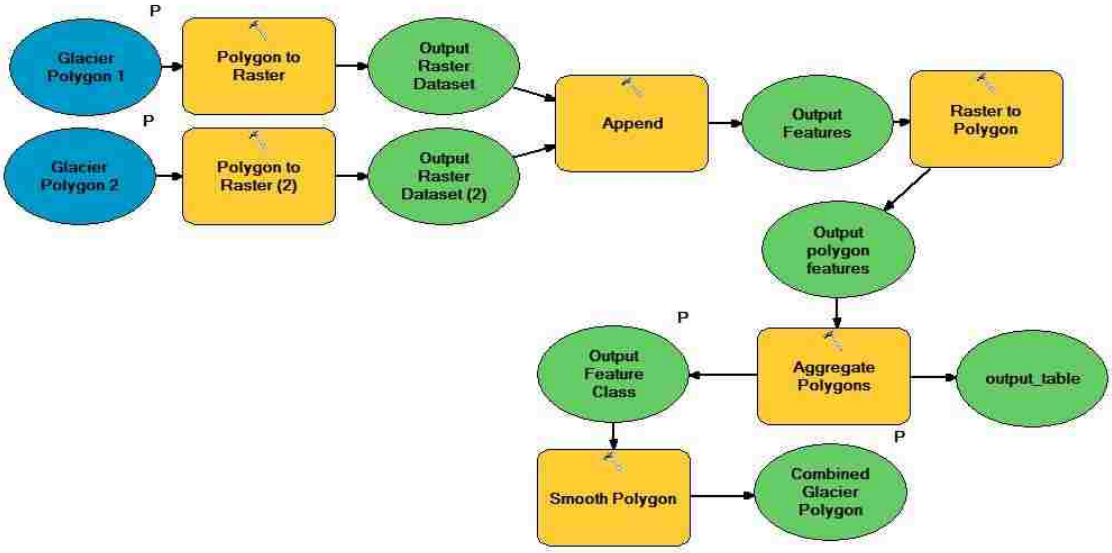

Figure 3. Cloud Cover Model developed in Model Builder within the ArcMap environment.

4.4.1 Glacier Mapping Methodology

There have been many methods developed to map glaciers using remote sensing techniques. Raup *et al*. (2007a) and Bhambri and Bolch (2009) described five classification methods: manual digitization (Sarikaya *et al.* 2011, Paul *et al.* 2013), spectral band ratio and threshold, Normalized Difference Snow Index (NDSI), geomorphometric-based, and thermal band methods. In the inventory of the Southern Alps of New Zealand by Gjermundsen *et al*. (2011), a supervised classification method was tested and the results were not promising: bright rocks and small disconnected snow patches classified as glacier area resulted in high error percentage. The NDSI is an unsupervised classification method that utilizes the brightness of snow and ice in the visible band 2 and is contrasted against the low reflectivity in the SWIR band 5 (Hall *et*

al. 1995, Bishop *et al.* 2008). When mapping glaciers in the Cordillera Blanca, Peru, Racoviteanu *et al.* (2008) found the NDSI was superior to other band ratios based on visual inspection. However, the NDSI method is still susceptible to erroneously mapping shadowed regions (Bishop *et al.* 2008).

$$NDSI = \frac{TM2 - TM5}{TM2 + TM5}$$

In order to classify debris-covered glaciers, Raup *et al.* (2007a) suggested a geomorphometric-based method. Automated delineations of debris-covered glaciers using geomorphometric-based methods have been implemented by many author groups including, Bolch *et al.* 2006, Bolch *et al.* 2007, Bhambri *et al.* 2011, and Kamp *et al.* 2011, however these studies discussed high errors (>5%) requiring editing during post-processing. Geomorphometric methods also require a DEM of sufficient accuracy. When developing a new glacier inventory for the European Alps and mapping glaciers in the Cordillera Blanca of Peru, Paul *et al.* (2011) and Racoviteanu *et al.* (2008) both respectively manually edited their glacier outlines to include debris-covered glaciers using contrast-enhanced false-color composite satellite images. The Mongolian glacier inventory will not follow the lead of Racoviteanu *et al.* (2008) and Paul *et al.* (2011) and map debris-covered glaciers via manual digitization because Paul *et al.* (2010) discussed that human, as opposed to automated, delineation of glacier outlines tended to digitize only parts of glaciers. Due to the human input required and inconsistent nature of the aforementioned methods, this study implements a band ratio technique that is described by Bolch *et al.* (2010a), Bhambri and Bolch (2009) and Paul *et al.* (2013) as a robust and time-effective approach to map clean glacier ice.

A Landsat TM scene has a spatial coverage of 170 x 185km^2, with a spatial resolution of 30 x 30 m, except for the thermal band (band 6) which has a spatial resolution of 120 x 120 m. Each scene is comprised of seven separate spectral bands. Determining which spectral band to use in the band ratio technique is important in order to understand the relationship between the glacier and its associated spectral signature. As described by Rees (2006), the concept of a spectral signature is the association between specific land cover and the variation of pixel values representative across different bands of an image. Figure 4 shows that clean glacier land cover is highly reflective in the visible and NIR wavelengths (0.45 μm – 0.90 μm). On the contrary, high absorption occurs in SWIR between the ranges of 0.6 to 0.7 μm and 2.08 – 2.35 μm in the electromagnetic spectrum. Identifying bands with high and low reflectance is important to select the bands for the band ratio analysis. The greater the difference in pixel values, the higher the contrast between glacier ice and other land covers (Dozier 1989, Lillesand *et al.* 2000, Paul *et al.* 2011).

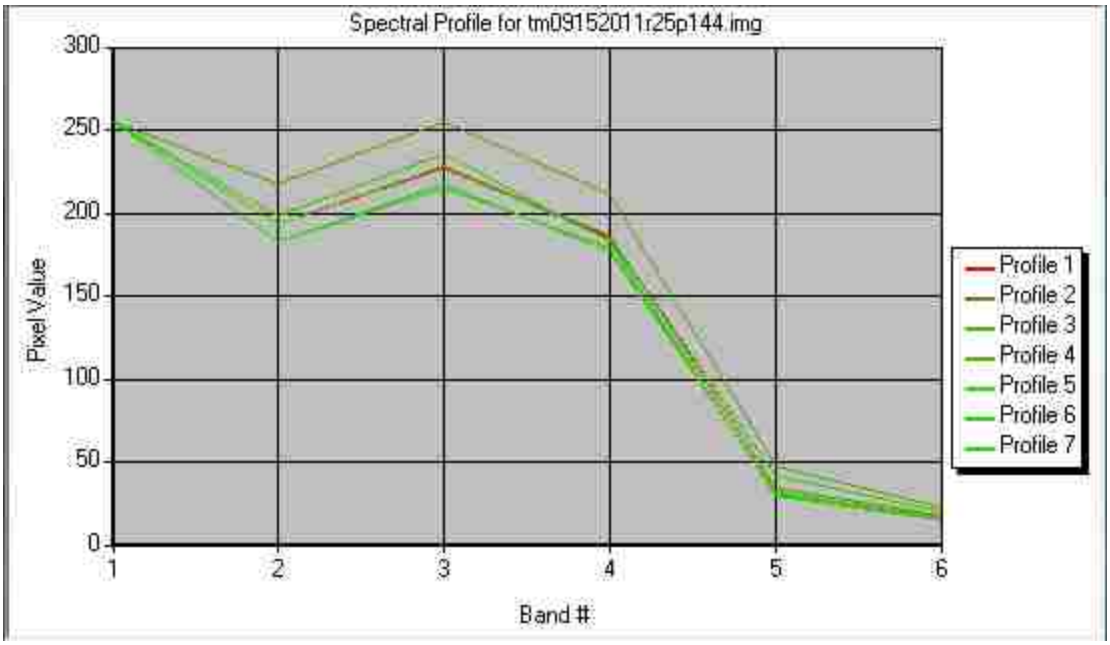

Figure 4. Landsat 5 spectral characteristics. Profiles 1-7 were all sampled on clean glacier ice.

4.4.2 Satellite Band Ratios

Predominately, two band ratios to map glaciers have been proposed in the literature (Andreassen *et al.*2008, Bhambri *et al.* 2011, Bolch *et al.* 2006, 20010a, 2010b, Frey *et al.* 2012a, Gjermundsen *et al.* 2011, Paul *et al.* 2002, 2011, 2013). When using a Landsat TM scene, the most common band ratios used are TM3/TM5 and TM4/TM5 (Figure 5). Paul *et al*. (2002) compared TM3/TM5 and TM4/TM5 band ratios and found that TM4/TM5 was the only combination that did not have problems in shadow regions. Yet, in Paul *et al.* (2011) a TM3/TM5 band ratio was used to map glaciers in the Alps and the author group applied an additional threshold in TM1 to improve classification in shadow regions. One of the disadvantages of the TM4/TM5 ratio is that it often identifies turbid lakes and vegetation as being glacier ice. Along with land cover, sun angle can also be influential on a band ratio classification. At low sun angles, TM3/TM5 produced better results for glacier areas in shadow, yet more turbid lakes are mapped as

glacier ice (Bishop *et al.* 2008, Frey *et al.* 2012a). Bolch (2006, 2007, 2010a) suggested using the Normalized-Difference Water Index (NDWI) to correct band ratio mapping errors. It should also be mentioned that the TM4/TM5 band ratio has been proven to be effective at mapping thin debris-covered glaciers (Paul *et al.* 2005, Bolch *et al.* 2010b). Bolch (2007) used a TM4/TM5 band ratio with a threshold of 2 when mapping glacier retreat in the Tien Shan. However, Bolch *et al*. (2010a, 2010b) used a TM3/TM5 band ratio when creating an inventory for western Canada and the western Nyainqentanglha Range and the Nam Co Basin. The reasons were that the TM3/TM5 band ratio was appropriate for larger study areas and by using a 3 x 3 median filter the isolated pixels were effectively eliminated (Bolch *et al*. 2010b, Gjermundsen *et al.* 2011, Frey *et al.* 2012a).

$$Band\ Ratio = \frac{TM(x)}{TM(y)}$$

Along with determining spectral bands to use in a band ratio, the threshold is equally important. Deciding the correct threshold is important because if the threshold is too small more manual editing will be required and if the threshold is too large, glaciers will be underrepresented. Bishop *et al.* (2008) explained that thresholding ratio images are most sensitive in regions with ice in shadows and suggested a threshold of 2 when using any band ratio method. Furthermore, Paul *et al.* (2013) recommended using the smallest threshold available when using an automated method such as a band ratio or NDSI. A small threshold will include most of the slightly dirty glacier ice surrounding the glacier margins.

4.5 Satellite Band Combinations

When using remote sensing imagery, it is important to use reference images to increase user's confidence when interpreting images. To first identify glaciers within a Landsat TM scene, band combinations are utilized. Multiple band combinations have been created to emphasize clean glacier ice. Klein *et al.* (1998) suggested a 5-4-2 combination to discriminate between glacier and water bodies. A 5-4-3 combination (Figure 7) is effective at deciphering between clean glacier ice with vegetation (Bolch *et al.* 2007). By using this combination, the band ratios can be interpreted more effectively. The use of high-resolution imagery such as Google Earth has also been recommended to confirm debris-cover manual delineation and visual interpretation of automated mapping accuracies (Paul *et al.* 2013).

Figure 5 TM4/TM5 band ratio (7/17/1991)

Figure 6. TM4/TM7 band ratio (7/17/1991)

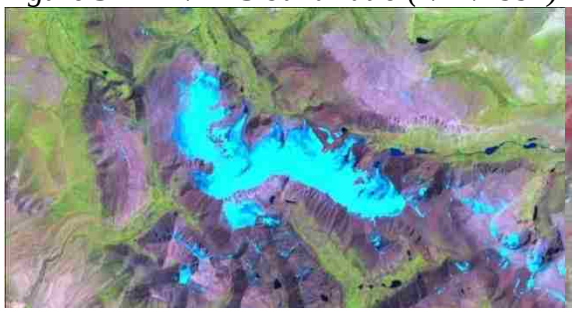

Figure 7. TM composite 5-4-3 (717/1991).

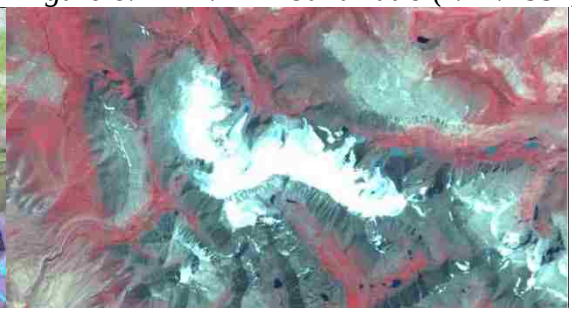

Figure 8. TM composite 4-3-2 (7/17/1991).

4.6 Anisotropic Reflectance

The use of remote sensing in high mountain environments is heavily influenced by variations in irradiant and radiant flux caused by the atmosphere, topography, and land cover. There have been multiple anisotropic reflectance correction (ARC) methods developed to reduce the influence of topography in a satellite image. However, no one method has proven as a suitable best method (Colby 1991, Colby and Keating 1998, Bishop and Colby 2002). Given the nature of glaciers developing at high altitudes and in typically complex topography, it is important to attempt to understand the influence of topography within an image when using remote sensing to map glaciers. This study compared the Cosine and Minnaert corrections for ARC of satellite imagery within the Altai Mountains (Appendix D).

4.7 Digital Elevation Model

For most regions, SRTM digital elevation model (DEM) data of 90 m resolution is available. A DEM is necessary in order to generate glacier parameters such as mean median, minimum and maximum elevation, range, mean slope, and mean aspect. In order to generate these parameters, SRTM data were downloaded from the Consortium for Spatial Information - Consultative Group for International Agriculture Research (CSI-CGIAR). However, Bishop *et al.* (2008) found that SRTM data are greatly affected by shadows caused by high topographic relief, and that the lack of repeat coverage presents problems of DEM quality. Therefore CGIAR designates the vertical error of the DEM's to be less than 16 m (Jarvis *et al.* 2008). Furthermore, Frey and Paul (2012b) described the vertical and horizontal error of SRTM data to be approximately 10 m based on ground control points.

When developing a glacier inventory, DEMs provide a pivotal role in creating ice divides. Racoviteanu *et al.* (2008) described the purpose of ice divide mapping is to identify glacier entities in an objective and consistent manner, and Bolch *et al*. (2010a) showed that SRTM data did provide sufficient results to calculate ice divides, which are important for defining individual glaciers, and will help automate the process of delineating glaciers. Integrating ice divides with glacier delineations enables for hydrologic applications and change detections. Once glaciers are properly divided into their hydrologic entity, parameters can be extracted and used for spatial analysis. Racoviteanu *et al.* (2008) and Bolch *et al.* (2010a) suggested calculating the drainage basin from a DEM and clipping the basin with the glacier outlines (Figure 9). However, Bolch *et al.* (2010a) discussed gross errors are often produced and require manual editing.

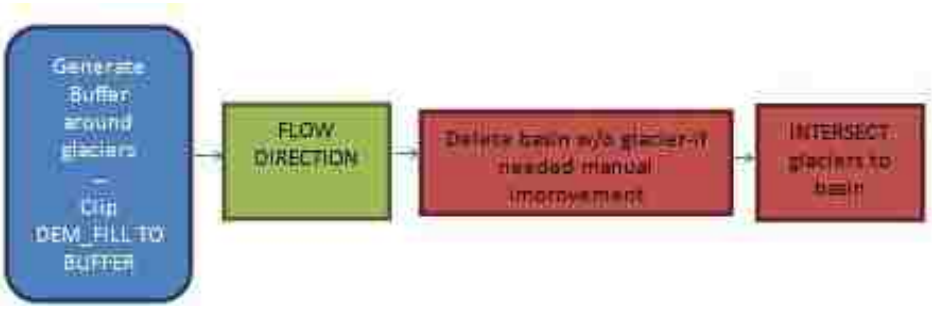

Figure 9. Workflow to generate ice divides as described by Bolch et al. (2010a).

Due to the erratic records of glacier area and numbers, there have been very few studies that have examined glacier parameters in the Altai Mountains. Racoviteanu *et al.* (2009) stated the importance of glacier parameters is needed to assess spatial patterns of glacier change and their connections with climate fluctuations at multiple scales. One of the strongest metrics to show glacial change is to quantify the change in percent of a

specific parameter, for example the percent change in glacial area. The percent change metric can measure changes at an individual glacier scale, range scale, sub-region scale, and at temporal scales. The percent change is defined by the following equation:

$$\text{Percent Change} = \frac{old\ value - new\ value}{old\ value}$$

This study measured multiple parameters including hypsometric measurements, slope, aspect, different scales and for glaciers larger than 0.1 km^2. The parameters were derived for each individual glacier then aggregated into larger regions based on massifs and finally sub-regions.

ASTER imagery has the capability to generate DEMs at a higher spatial resolution of 30 m and is available for most areas of the world at the ASTER Global Digital Elevation Model (GDEM) project website for free of charge (http://gdem.ersdac.jspacesystems.or.jp/). However, even though GDEM has a higher spatial resolution than SRTM, Frey and Paul (2012b) found that glacier parameters derived from SRTM yielded more accurate results than parameters derived from GDEM. Kääb (2002) found the vertical accuracy of ASTER GDEM to be as high as ±60 m in rugged terrain. Yet, in areas of less topographically complex regions, Toutin (2008) found more a more reasonable vertical accuracy for ±15-30 m.

ASTER GDEM may not be necessary for the derivation of glacier parameters, however when coupled with SRTM data, changes in glacier elevation can be examined and therefore inferences towards glacier mass balance can be assessed. The SRTM data was acquired in the year 2000 and will represent the elevation of glaciers during that year. ASTER GDEM data was acquired during 2008 and will represent the state of glacier elevation during 2010. Before the changes in elevation can be calculated, both

datasets need to have a common spatial resolution and were resampled to 60 m (Wagner and Hoelzle 2010). After the DEM data are resampled they can be simply subtracted using map algebra to find the change in elevation (Figure 10). The new raster dataset is then clipped to the glacier outlines to find the changes in glacier thickness for each glacier.

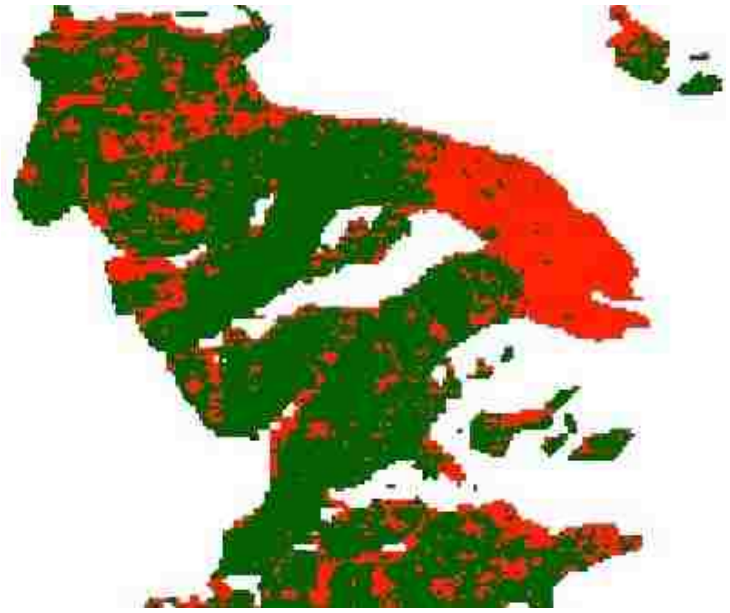

Figure 10. Changes in glacier elevation from 2000 to 2008 using SRTM and ASTER GDEM. Red indicates surface lowering. Green indicates no gain in surface elevation.

4.8 Mapping Uncertainty

The main sources of uncertainty when mapping glaciers using satellite imagery derive from 1) positional errors; 2) classification errors; 3) processing errors; 4) conceptual errors (Racoviteanu *et al.* 2008, Bolch *et al.* 2010a). Frey *et al.* (2012a) and Krumwiede *et al.* (in press) applied an uncertainty of ±1 pixel (30 m) when mapping clean glacier ice for the glacier outline position. A more precise quantitative assessment is not possible due to the lack of ground truth data as performed by Granshaw and Fountain 2006, Bolch *et al* 2006, Bolch *et al.* 2010a, 2010b, and Bhambri *et al.* 2011.

Yet, Frey *et al.* (2012a) continues to justify the absence in ground truth data with the ±1 pixel (30 m) uncertainty because other author groups have proven the band ratio approach yields similar results (Andreassen *et al.* 2008, Paul *et al.* 2005). The Mongolian Glacier Inventory will apply an uncertainty of ±1 pixel (30 m) for clean glacier ice and glaciers larger than 0.1 km^2 and will apply an additional ±0.5 (15 m) pixel for glaciers smaller than 0.1 km^2.

It is possible to quantify the percent error of area determination (A_{er}). The A_{er} represents a maximum estimated error and is however an error biased towards underestimation of glacier area (Krumwiede *et al.* in press). The A_{er} is defined by the following equation:

$$Aer = \frac{100\%(n \cdot m)}{Agl}$$

where: n = number of pixels defining the perimeter of the glacier area
m = pixel resolution (e.g., 900 m^2 for a 30 m x 30 m TM pixel)
Agl = glacier area (m^2)

5. RESULTS

5.1 Band Ratio Test Results

Surprisingly, in the literature there is no mention of using the SWIR band between the 2.08 – 2.35 μm wavelengths (Figure 6) even though it exhibits the highest absorption rates concerning glacier land cover (Figure 4). This study independently tested five separate band ratios including TM3/TM5, TM4/TM5, TM4/TM7, and NDSI. All ratios used a threshold of 2 with the exception of NDSI which had a threshold of 0; in addition a TM4/TM7 ratio with a threshold of 3 was also tested. All mapping methods were tested using a Landsat TM image acquired on September 3, 2011 with 0% cloud cover and very limited remnant snow patches.

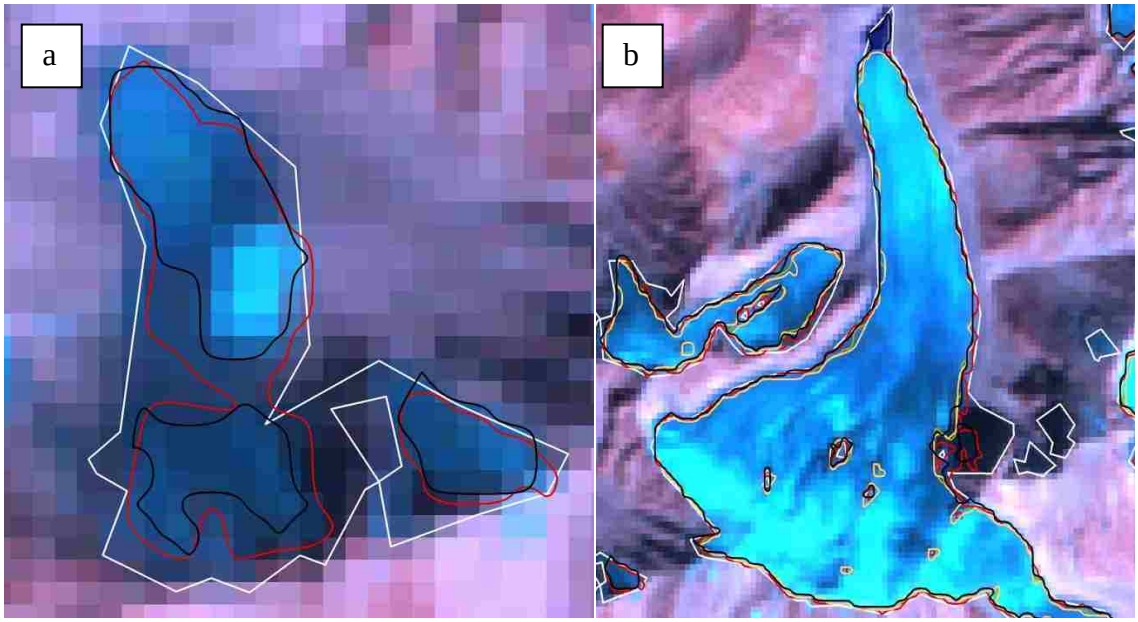

Figure 11. Only three out of the five methods mapped the glacier in Image A including, TM4/TM7-thresh2, NDSI, and TM3/TM5. Each method produced a different glacier area and number (see Image D for associated method).
Figure 12. Image B demonstrates which methods are susceptible to mapping proglacial lakes and shadows.

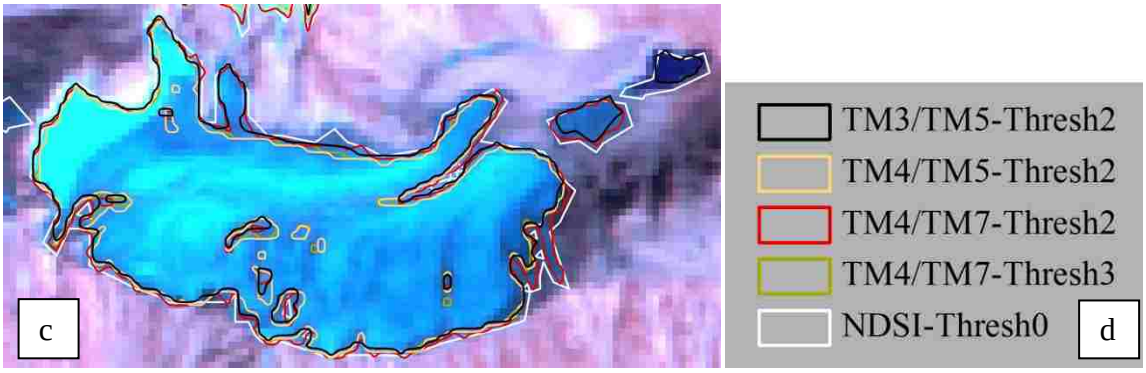

Figure 13. Image C represents how certain ratios only map parts of glaciers, these include TM4/TM5 and TM4/TM7-thresh3. Also, again TM3/TM5, NDSI, map water bodies. Similar to Image A, Image C shows certain ratios mapping small disconnected glaciers.

Figure 14. Image D is a legend for utilized ratios in the ratio tests. Except for TM4/TM7, each ratio has been utilized in glacier mapping projects for GLIMS.

Visual interpretation of preliminary band ratio results immediately demonstrates the variability in mapping results amongst different mapping methods. This variability is exemplified in Figure 11a, only three out of the five methods mapped the designated glaciated region in the image. More importantly, of the three that mapped glacier ice (NDSI, TM3/TM5, TM4/TM7 threshold 2); each method mapped a different glacier area (km^2) and glacier number. Figure 12b illustrates TM3/TM5 and NDSI mapping both turbid water and shadowed regions. Figures 11-13 all demonstrate TM4/TM5 underrepresenting glacier area, especially noted with the inability for TM4/TM5 to map the glaciers in Figure 11a. These preliminary mapping tests further endorse the validity in using a band ratio with a SWIR band between the 2.08 – 2.35 μm wavelengths. TM4/TM7 with a threshold of 2 did not underrepresent glaciers, map turbid water, or heavily map shadowed regions, therefore will be implemented in the Mongolian glacier inventory.

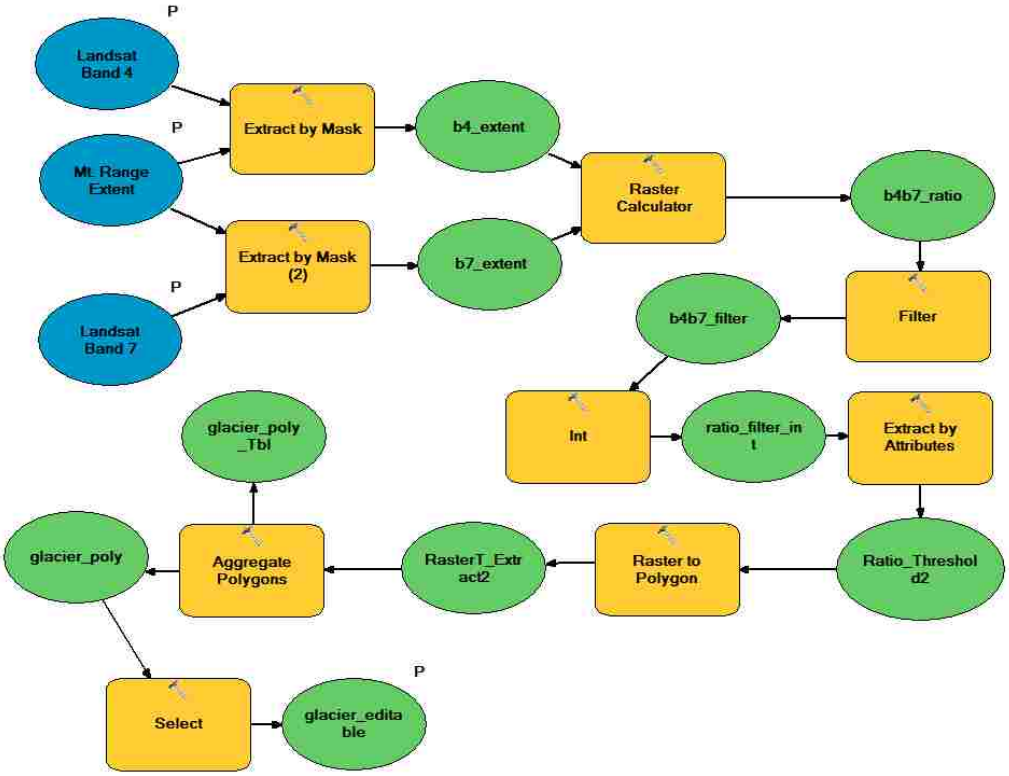

Figure 15. Developed model created to delineate glacier outlines. The model requires three inputs; NIR and SWIR Landsat TM bands and defined spatial extent of the mountain range.

5.2 Anisotropic Reflectance Results

The Minnaert correction was the most effective ARC method when mapping glaciers in the Turgen Range and Munkh Khairkhan Range. However, integrating an ARC method into the developed mapping workflow would negate any attempts in creating an intuitive and inexpensive method. Furthermore, scale was identified as being an important parameter when applying an ARC method in glacier mapping: at smaller scales the results are unsatisfactory. ARC methods are effective only if the area of an individual glacier is large enough to be identified in a Landsat TM image with 30 m resolution. However, for the Mongolian glaciers ARC methods would need to be conducted using imagery of higher spatial resolution (Appendix E).

5.3 Ice Divide Delineation

Figure 16 was derived from a SRTM DEM based on techniques discussed by Racoviteanu *et al.* (2008), Bolch *et al.* (2010a), and Frey *et al.* (2012a) (Figure 9). Ice divides and glacier entities proved to be successfully delineated and time invested in correcting gross errors is still superior to manually identifying and digitizing ice divides. It is important to note that the ice divides are divided in a hydrologic way. For example, Figure 11 maps Potanin and Alexandra glaciers as one entity because they both contribute to the same localized hydrology. Kadota *et al.* (2011) appear to have mapped Potanin and Alexandra glacier based on geomorphological features as indicated by the ridge dividing the two glaciers (Figure 17). However, strictly defining glaciers on geomorphological features is not in-line with GLIMS protocols. Not only does the area (km^2) need to be considered when defining a glacier but tributary glaciers that contribute to a larger glacier's mass and glacier runoff (hydrology) needs to be considered (Racoviteanu *et al.* 2008).

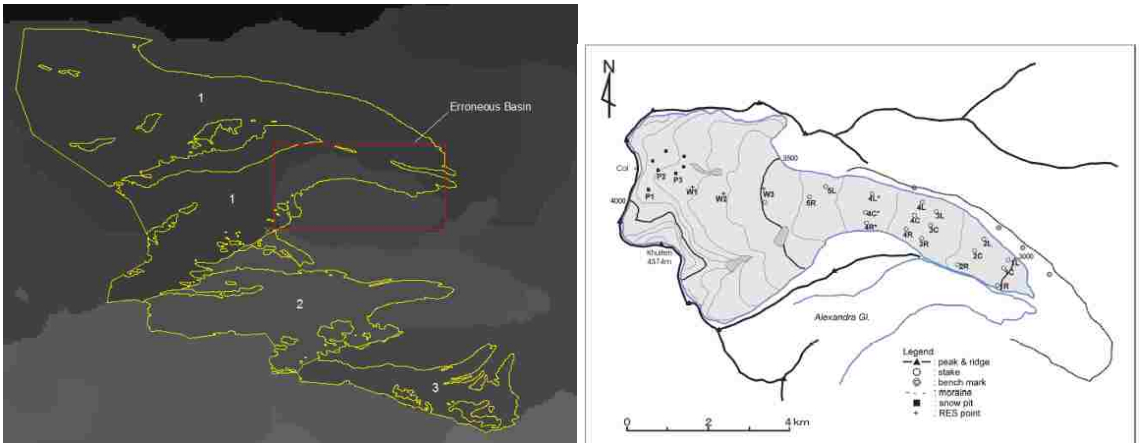

Figure 16 (left). Glaciers outline clipped with derived ice divides resulted in three individual glaciers. Kadota et al. 2011 (Figure 17, right) used topographic maps to divide Potanin glacier form Alexandra glacier. However, as observed in Figure 9., Potanin and Alexandra glacier are mapped as one.

5.4 Mongolia Glacier Inventory Error Estimation

The Percent Error of Area Determination (A_{er}) was calculated for each massif, sub-region, and the entire Altai range (Appendix A, B, and C). As expected, as the scale became larger, the A_{er} increased. Also, the A_{er} was only calculated for glaciers greater than 0.1km^2 because smaller glaciers dramatically impacted the $A_{er.}$ Due to the high A_{er} and the fact that small glaciers in steep and shadowed slopes are more susceptible to DEM artifacts (Frey *et al.* 2012), glacier parameters will only be calculated for glaciers larger than 0.1 km^2.In 1990, Tsengel Khairkhan in the Central Interior had the highest overall A_{er} at 27.68% and the Central Altai had the lowest A_{er} with 11.90%. The A_{er} for glacier mapping increased after 1990, and in 2000 the A_{er} ranged between 24.24% in the Central Interior to as low as 14.91% in the Central Altai. The A_{er} from 2000 to 2010 changed little from sub-region to sub-region. The highest A_{er} was in the Central Interior at 26.27%, an increase of 2.03% from 2000. The lowest A_{er} was again in the Central Altai at 14.15%, a decrease of 0.75% from 2000 (Figure 18).

The Central Interior consistently had the highest A_{er} because the sub-region contains the Altai's smallest glaciers and most complex topography. While the Central Altai consistently had the lowest $A_{er,}$ even though it does not contain the Altai's largest glaciers, it does contain the most flat-top glaciers, therefore decreasing the influence of topography. When the A_{er} is calculated based on the entire Altai Mountains, the overall A_{er} is 13.54% in 1990 and increases to 17.17% in 2010 (Figure 19). The increase in A_{er} is due to the disintegration of larger glaciers into smaller glaciers from 1990 to 2010. Glaciers with small surface area increase the A_{er} (Krumwiede *et al.* in press, Paul *et al.* 2013). The lower A_{er} during 1990 is also due to an overall smaller number in mapped

glacier regions, specifically, the exclusion of mountain regions with small glaciers. Therefore, larger glaciers were mapped during 1990 improving the overall A_{er}.

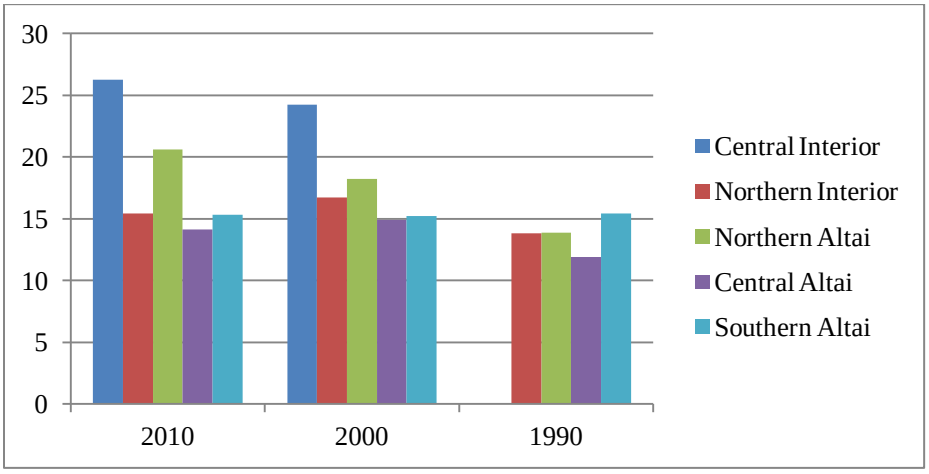

Figure 18. Graph displaying the Percent Error of Area Determination for glaciers >0.1km^2 by sub-region. Central interior is not shown for 1990 because only Tsengel Khairkhan was mapped during that time period.

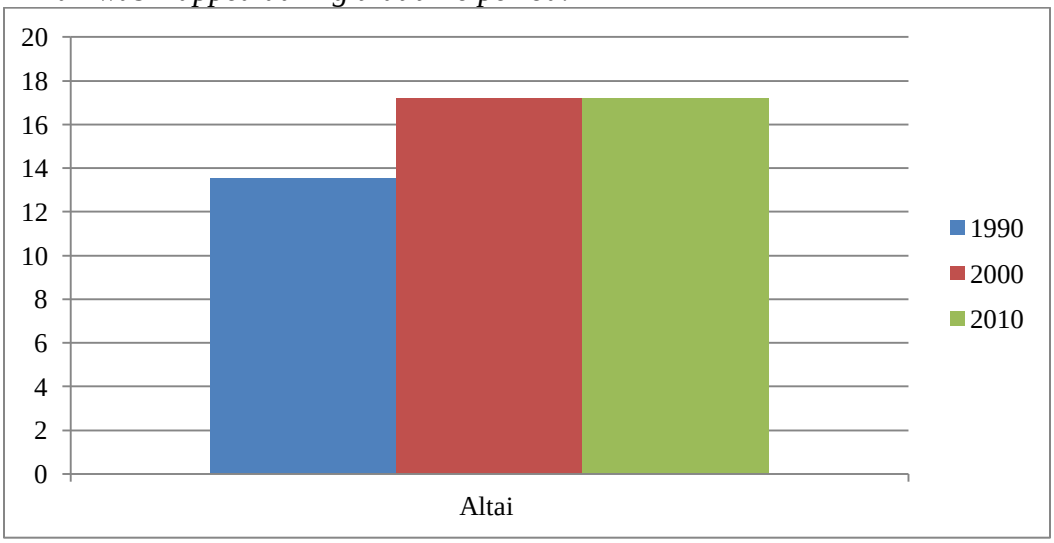

Figure 19. Graph displaying the Percent Error of Area Determination for glaciers >0.1km^2 for the entire Altai region.

5.5 Glacier Mapping Results

The availability of quality Landsat scenes during 1990 only provided enough images to map 11 out of the 18 glaciated massifs in the entire Altai Mountains. Based on this study's definition of a glacier and methodology, the total area mapped in 1990 was 443.12 km^2 (±13.54%) and the total number of glaciers was 690. By examining the

percent change between the mapped regions in 1990 and the sub-sectioned ranges in 2000, a percent change in glacier area was calculated and applied to the mapped glacier area in 1990. The 22 percent change was applied to the mapped area of 443.12 km^2 leading to a corrected estimated total glacier area of 540.57 km^2 in 1990. Enkhtaivan (2006) calculated 514 km^2 which is close to the average of both of our figures for 1990, but unfortunately, the author did not designate the year. In 2000, the total glacier area was 428.60 km^2 (±17.20%) and the total glacier number was 716. Our glacier area is in strong agreement with Kadota *et al.* (2004) who calculated a total glacier area of 425 km^2 and with Ohata *et al.* (2009) who calculated a total glacier area of 423 km^2 during the same time period. Davaa (2010) calculated a total area 417 km^2 and a total number of 580 using Landsat data from between 2000 to 2002. In 2010, 671 glaciers covered an area of 372.30 km^2 (±17.17%). The Northwest Interior sub-region contains the largest glacier area, throughout all time periods. In 1990, the Northern Altai and Central Altai had close to the second largest glaciated regions and were only separated by 1.40 km^2 in total glacier area. However, in 2010 the Central Altai had a total glacier area 20 km^2 greater than the Northern Altai, suggesting a faster rate of retreat in the Northern Altai (Figure 20).

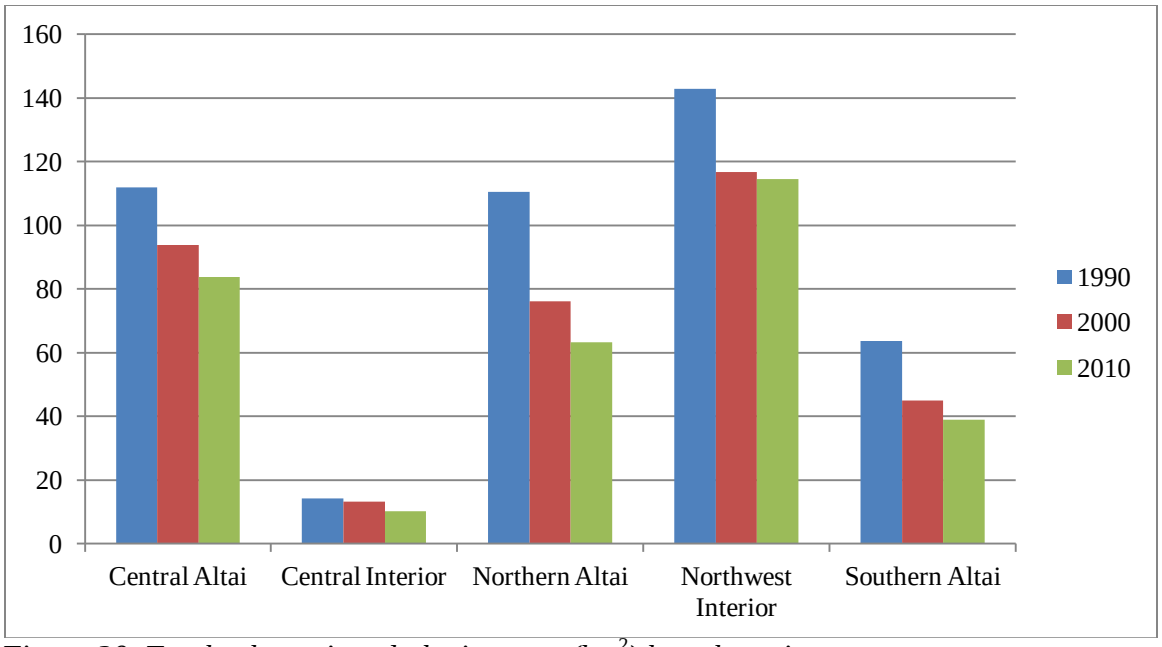

Figure 20. Total sub-sectioned glacier area (km^2) by sub-region.

In the entire period between 1990 and 2010, the total glacier area decreased by 117.85 km^2 or 29.86%; when using the corrected total area of 540.57 km^2 for 1990, the decrease in area is even higher at 31.13% (Figure 21). From 1990-2000, the decrease in total glacier area was 20.17%, and from 2000-2010 it was 13.14%. Figure 21 depicts the greatest loss of glacier area occurring in the Northern Altai (42.96%), which includes Ikh Turgen, Turgen, and Kharkhiraa ranges. The Southern Altai had the second highest rate of glacier loss (38.84%); glaciers in the Northwest Interior had the lowest percent change in area (19.81%). Glacier area changes are further summarized in Appendix D.

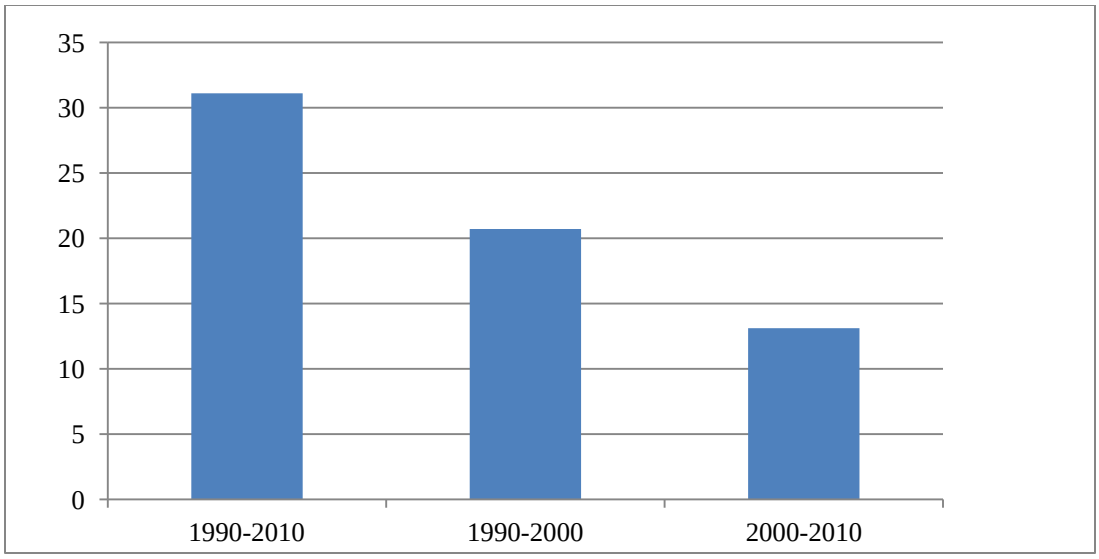

Figure 21. Decrease in Glacier Area in percent change.

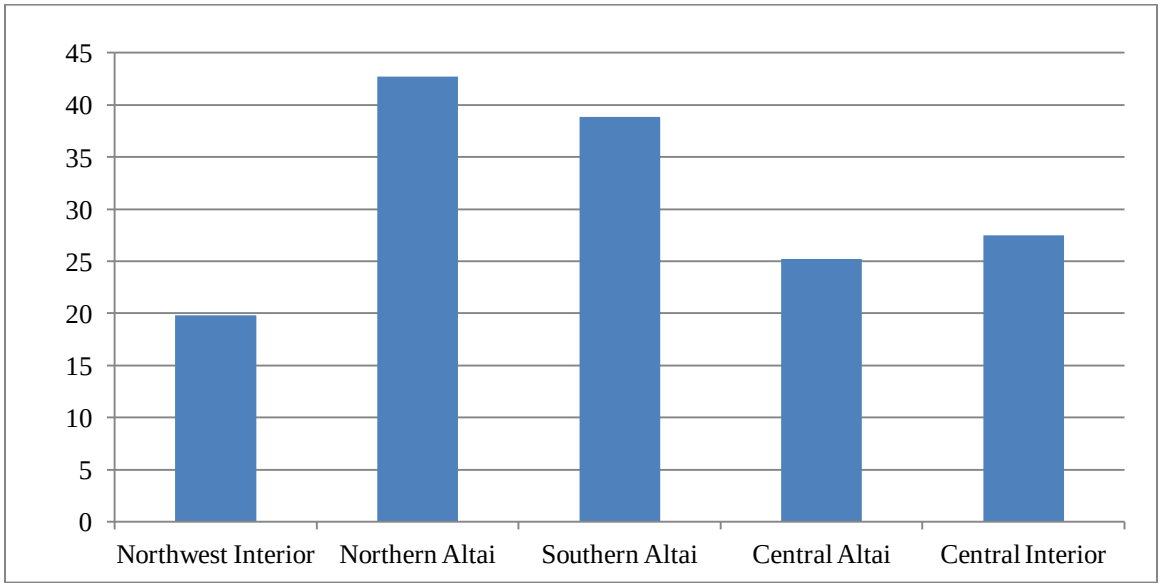

Figure 22. The percent change in glacier area from 1990-2010 using sub-sectioned regions. The Northern Altai had the greatest decrease in glacier area while the Northwest Interior had the lowest decrease in glacier area.

Glaciers in class size 5 (>5.5 km^2) consistently had the lowest total frequency of glaciers but represented 35-44% of the total glacier area through each time period. Class size 2 (0.26 km^2 – 0.125 km^2) consistently had the highest frequency of glaciers but never had a percent total area greater than 3.56%. Throughout the Altai Mountains, there is a consistent decrease in the total glacier frequency in class size 5. From 1990 to 2010 the

frequency of glaciers in class size 5 decreased by 45% (Figure 23). There are observed increases in glacier frequency within class sizes 3 (0.126 km^2 – 0.85 km^2) and 4 (0.86 km^2 – 5.5 km^2). However, during the time period of 2000-2010, increase in glacier frequency in class sizes 3 and 4 ceases and a decrease in frequency occurs.

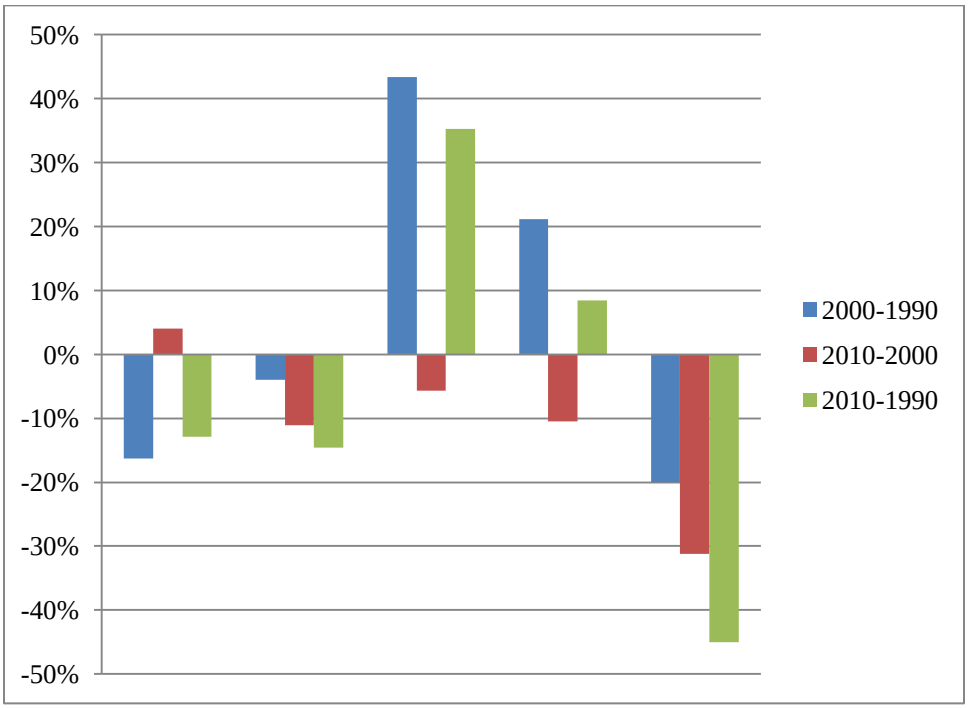

Figure 23. Percent change in total glacier frequency by class size.

The comparison of hypsometric parameters suggests an overall decrease in glacier area. Using the mean minimum glacier elevation (aggregated by sub-region) to represent glacier terminus, it is evidenced that glaciers in the Northwest Interior have the lowest glacier terminus elevation ranging from 3065 m in 1990 to 3117 m in 2010, an increase of 52 m over the twenty years. The Southern Altai has the highest terminus elevation starting at 3504 m in 1990 and increasing further to 3534 m in 2010, an increase of 30 m. Even though an observed overall decrease in glacier area occurred in the Central Altai, the terminus elevation decreased from 3378 m in 1990 to 3371 m in 2010, a decrease of 7 m (Figure 24).

The average median elevation has an increasing trend with the lowest elevations in the northwest and an increasing elevation moving towards the southeast. In 1990 the median elevations was ~474.7 m and increased to ~511 m in 2010. The wide variation in median glacier terminus elevation reinforces the high spatial variability of glacier retreat and growth.

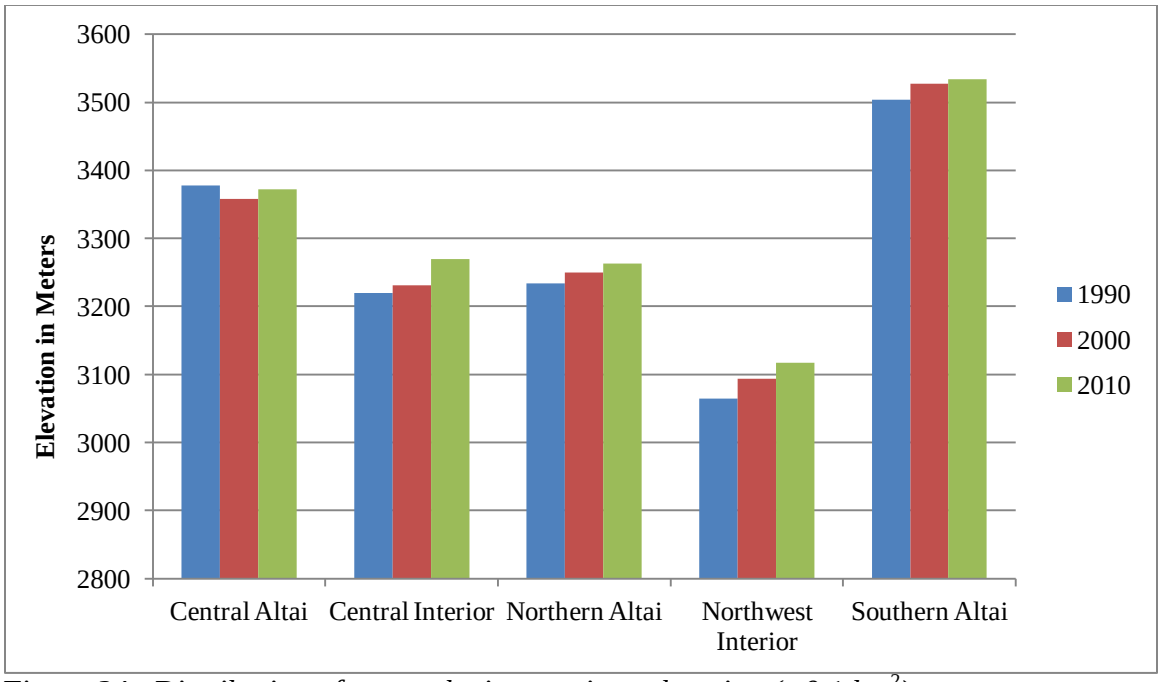

Figure 24. Distribution of mean glacier terminus elevation (>0.1 km^2).

The mean slope of glaciers in the Altai Mountains shows an increasing trend over the twenty year time period. In 1990 the mean slope of glaciers ranged from 18^o to 21.46^o and in 2010 the glaciers had an average slope of 17.49^o to 22.29^o. Further, from between 2000 to 2010 glacier thickness reduced in the Altai Mountains by ~11 m on average and thinning occurred on 82.3% of all glaciers.

In the Mongolian Altai, glaciers overwhelmingly face east, evidenced through all three time periods. Northern aspects had the lowest frequency of glaciers followed by western aspects (Figure 25). However, the northeast facing glaciers observed the

smallest decrease in frequency through 1990-2010, while southeastern and eastern aspects experienced the largest reduction in glacier frequency.

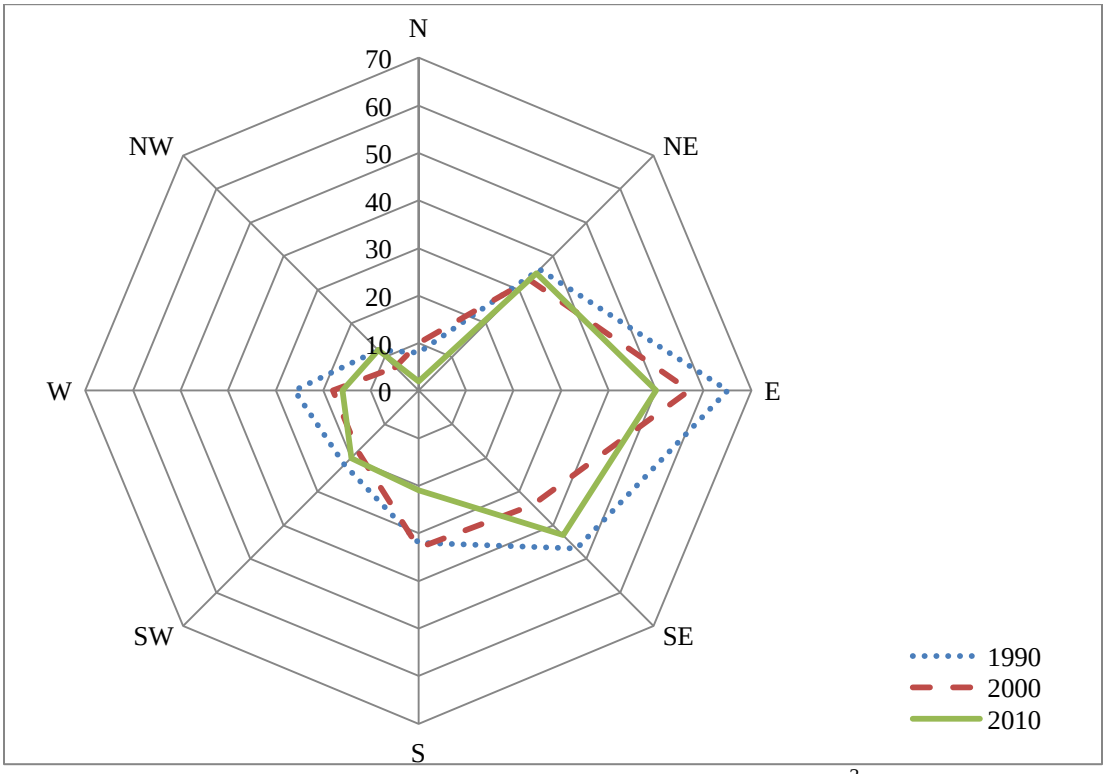

Figure 25. The frequency and aspect of glaciers larger than 0.1 km$^{2.}$ Aspect frequencies are in 22.5^{o} bins following Racoviteanu et al. (2008)

5.6 Case Studies: Tavan Bogd and Munkh Khairkhan Massifs

Tavan Bogd (Figure 26a) is located in the northwest corner of the Altai Mountains and is classified as being in the Northwest Interior sub-region. The region has an elevation ranging as high as 4,374 m a.s.l. (Khuiten Peak) to as low as 2,870 m a.s.l. (Krumwiede *et al.* in press). Tavan Bogd contains the largest glacier in the Altai with an area of 38.13 km^2 as of 2011, anecdotally, this glacier is known as Potanin and Alexandra glaciers. Kadota *et al.* (2011) documented the maximum thickness of Potanin glacier as 229 m and the surface velocity being spatially and seasonally variable, ranging from 0.8-2.6 m a^{-1} at the tongue to 17-31 m a^{-1} in the middle and being highest in the summer rather than the winter. The region also contains the largest total area of glaciers; 115.29

km^2 (±12.32%) in 1990, 95.86 km^2 (±12.49%) in 2000, and 94.67 km^2 (±12.65%) in 2010 (Figure 28). From 1990 to 2000, Tavan Bogd observed a large decrease in area of approximately 16.85%. The rapid ablation was significantly reduced to an area loss of 1.24% from 2000 to 2010 (Figure 29) The aforementioned retreat in glacier terminus calculates to a retreat of only 1.75 km (±90 m) over the next 100 years.

Figure 26a. Tavan Bogd study site and mapping extent, indicated by the red polygon (1:200,000). The dashed black line is the Mongolian border, glacier outside of the border were included in the analysis if the watershed flowed into Mongolia. Figure 26b. Munkh Khairkhan study site and mapping extent, also indicated by the red polygon (1:150,000).

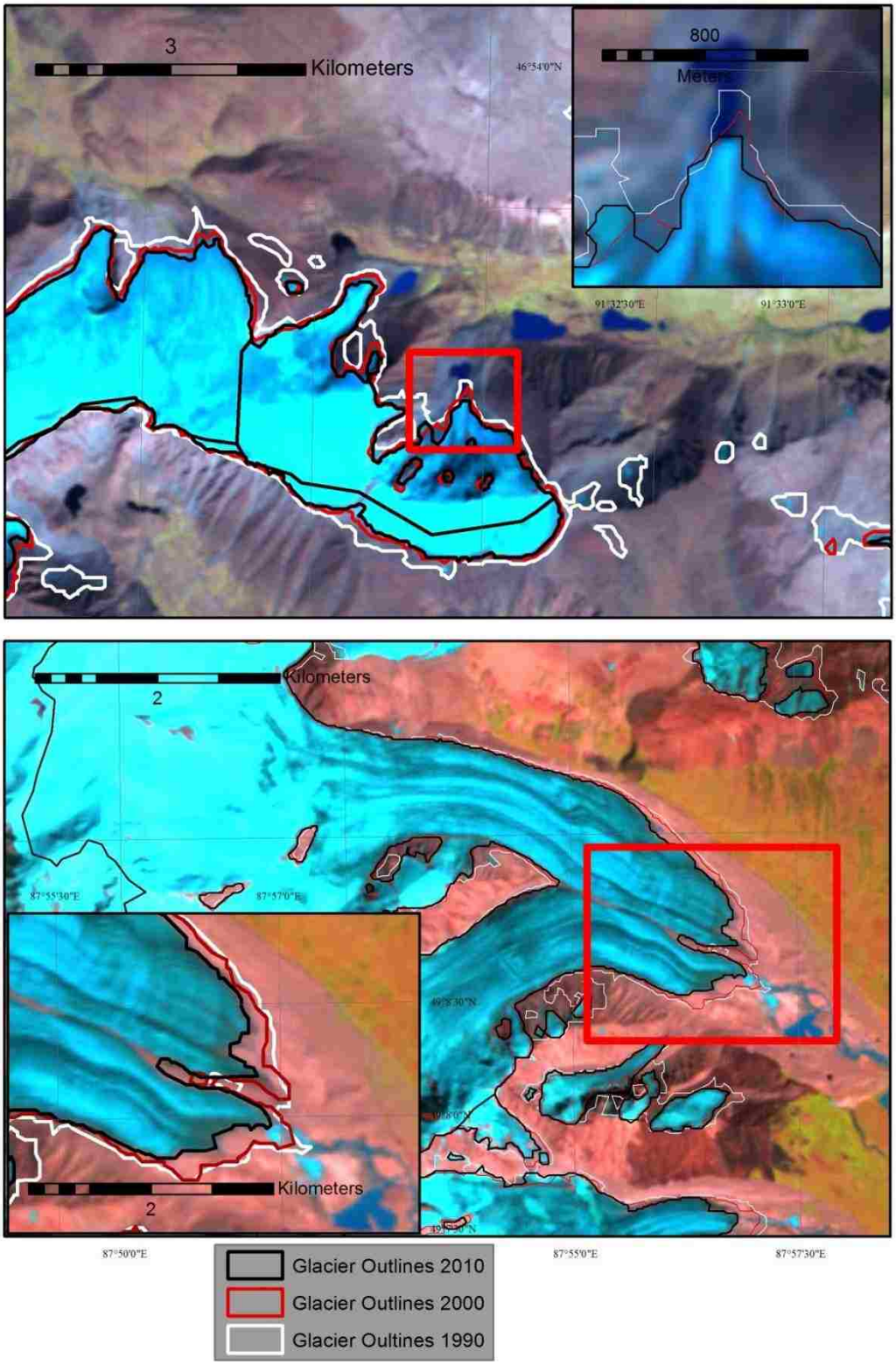

Figure 27. The top map is Munkh Khairkhan with glacier outlines demonstrating an overall reduction in glacier area. The bottom map is Tavan Bogd range, specifically Potanin and Alexandria glaciers with glacier outlines also demonstrating an overall reduction in glacier area.

Munkh Khairkhan (Figure 26b) is located in the central Altai and is the largest massif in the Southern Altai sub-region. Munkh Khairkhan Uul is the second highest peak in the Altai Mountains with an elevation of approximately 4,208 m a.s.l. (Krumwiede *et al.* in press). Glaciers in the range are observed to elevations as low as 3528 m a.s.l. in 1990. Based on this project's definition of a glacier, the largest glacier in Munkh Khairkhan range was 8.90 km^2 as of 2011. The total glacier areas in the region were 48.86 km^2 (±15.74%) in 1990, 31.12 km^2 (±11.34%) in 2000, and 27.37 km^2 (±13.13%) in 2010 km^2. Similar to Tavan Bogd and throughout the Altai, Munkh Khairkhan observed the largest decrease in glacier area from 1990 to 2000, within these ten years ~36.3% of glacier area was lost. However, from 2000 to 2010, the rapid retreat of glaciers reduced to 12%, almost a decrease of two-thirds of glacier retreat from the previous decade. Overall, from 1990 to 2010 an observed retreat in glacier area totaled 43.98% decrease (Figure 27). Our results are similar to Krumwiede *et al.* (in press), who documented a retreat of ~12 km^2 from 1990 to 2006. Only Turgen and Kharkhiraa ranges exceeded Munkh Khairkhan in glacier area loss.

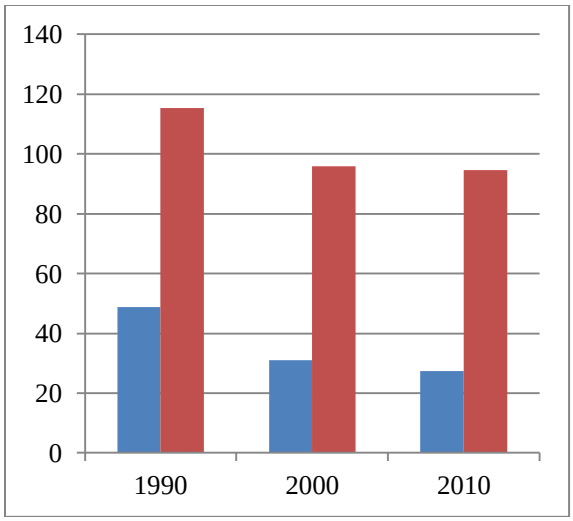

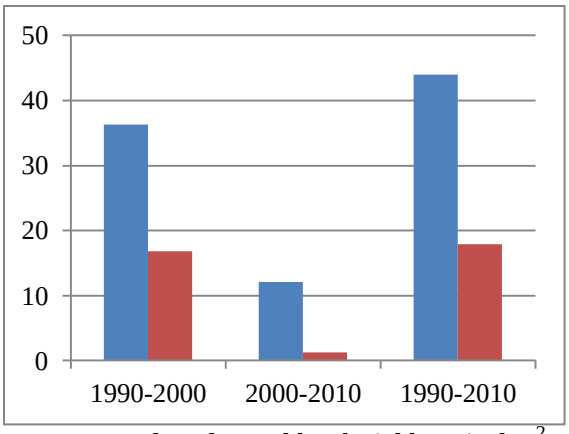

Figure 28 (left). The Total Glacier Area for Tavan Bogd and Munkh Khairkhan in km^2. Figure 29 (right). Changes in glacier area for Tavan Bogd and Munkh Khairkhan, expressed as a percent. In Figures 28 & 29, Tavan Bogd is represented in Red and Munkh Khairkhan is represented Blue.

For both Tavan Bogd and Munkh Khairkhan the average slope of glaciers has an increasing trend. The slopes ranged from; 23.95^o in 1990, 23.96 in 2000, and 24.16^o in Tavan Bogd and 20.03^o in 1990, 22.97^o in 2000, and 23.06^o in 2010 for Munkh Khairkhan. The trend of average slopes by sub-regions does not indicate an increase in slopes, like Munkh Khairkahn and Tavan Bogd. Not only has the glacier surface area on Tavan Bogd and Munkh Kkhairkhan reduced but their mean glacier thickness has also decreased, as indicated by the increase in glacier slope.

The mean glacier terminus elevation for Tavan Bogd shows an increase from 1990 to 2000 but a slight decrease from 2000 to 2010 (Figure 30). But the overall change of terminus elevation from 1990 to 2010 is only 24 m and inaccuracies need to be considered since the base data has a spatial resolution of 90 m. The same pattern is observed at Munkh Khairkhan. From 1990 to 2000 there is a noticeable increase in glacier teminus elevation but from 2000 to 2010 the glacier terminus elevation decreases by 3 m.

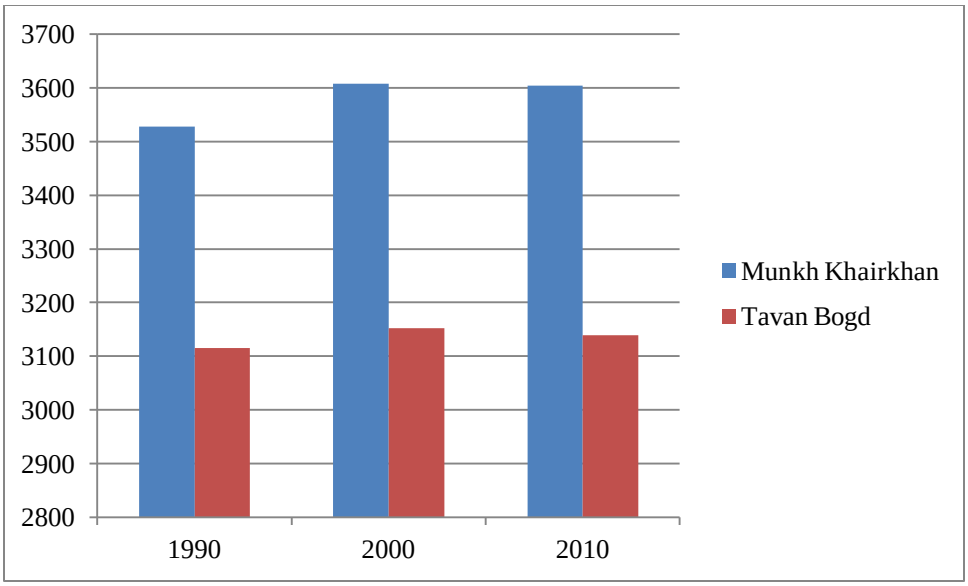

Figure 30. The mean glacier terminus elevation in both Munkh Khairkhan and Tavan Bogd ranges.

The majority of glaciers in both Tavan Bogd and Munkh Khairkhan ranges reflect the same average glacier aspects as the sub-regions. However, Tavan Bogd has a majority with an eastern aspect followed by a northeast then southeast aspect (Figure 31), while Munkh Khairkhan has a significant majority of glaciers with a northeast aspect followed by a northern then eastern aspect (Figure 32). From 1990 to 2010, there was only a noticeable reduction in glaciers with a southeast aspect. Yet, in Munkh Khairkhan from 1990 to 2010 glaciers with a northeast aspect reduced from 31 to 12 and glaciers with an eastern aspect reduced from 26 to 7 respectively.

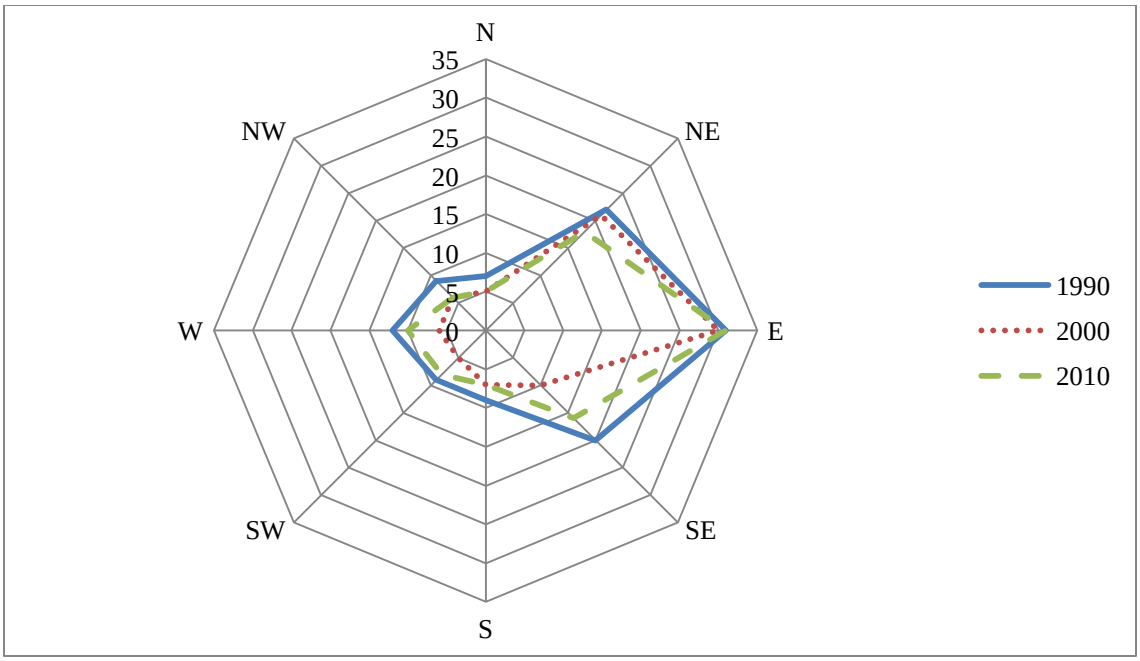

Figure 31. The glacier aspect and frequency for Tavan Bogd range from 1990 to 2010.

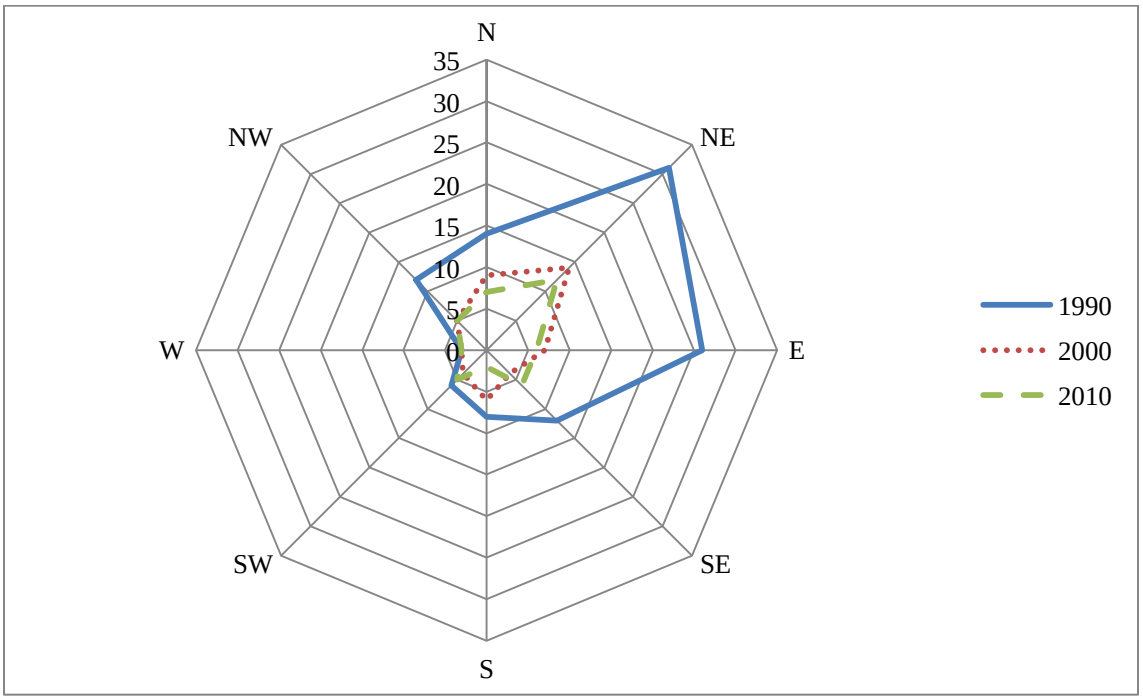

Figure 32. The glacier aspect and frequency for Munkh Khairkhan rnage from 1990 to 2010. Observable is the dramatic reduction in glacier frequency for northeast and eastern aspects.

6. DISCUSSION

6.1 Effectiveness of Developing a Glacier Inventory by Remote Sensing

The methodology developed to inventory glaciers in the Altai Mountains of Mongolia was highly time efficient and simple once the model schema was determined. By developing and implementing models to automate the glacier mapping method, two to three mountain ranges within the Altai complex could be mapped in one day. This includes glacier outlines for all three time periods, parameters, and the assignment of GLIMSIDs to individual glaciers. The only process in the work flow that requires any manual digitization is in the few instances where the Cloud-Cover Model is necessary. The most important aspect of the applied methodology is the ability to replicate glacier outline results created by different parties. The ability to replicate results is achieved because the models only allow for Landsat TM4 and Landsat TM7 inputs and do not allow for human subjectivity. Built into the model is the ratio threshold, polygon aggregation distance, median filter, and minimum glacier size (km^2). Also, glacier parameters should retain consistency as long as the SRTM DEM is used to derive the parameters. Different results are possible if a DEM derived from ASTER imagery is used (Frey and Paul 2012b).

Unfortunately, the methodology schema is not entirely automated. After the model produced the glacier outlines, the first step was to manually remove all misclassified water bodies as glaciers. This method is in line with Bolch *et al.* (2010a) who found that manual removal is much quicker and effective than using the Normalized Difference Water Index (NDWI). Misclassified vegetation was also removed. Due to the relatively coarse spatial resolution of SRTM data, when ice divides are clipped to glacier

outlines, sliver polygons are frequently produced. Sliver polygons are polygons that have an area smaller than the minimum glacier definition (<0.01 km^2) and so rather than deleting the sliver polygon; the slivers are merged to the larger adjacent glacier. In regions where the topography is complex, sliver polygons became more prevalent (Figure 33a). However on Tsambagarav and Sutai ranges, sliver polygons are not common due to the flat-top nature of the glaciers and the plateau nature of the local topography, thus indicating high spatial variability when monitoring glaciers using satellite imagery (Figure 33b).

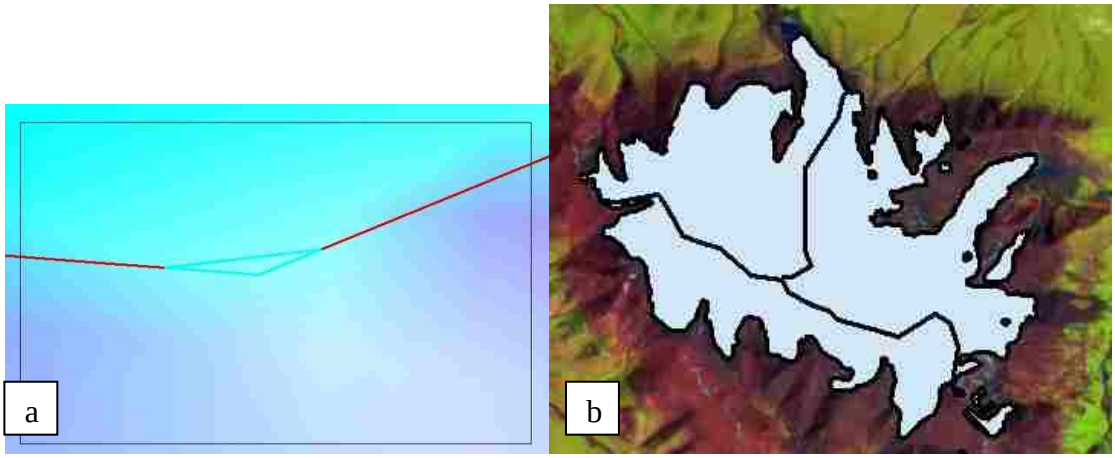

Figure 33. (a) Example of a Sliver polygon on Dushin Massif, indicated by the highlighted polygon. The area of the sliver polygon was only 58 m^2. (b) Sub-section of Tsambagarav massif where no slivers were produced after intersecting the Ice Divide with the glacier outline.

6.2 Previous Glacier Studies in the Altai Mountains

As mentioned in the results section, there have been many author groups who have used satellite imagery to map glaciers in the Altai Mountains; however, there are few similarities or agreement of glacier number and area between author groups. As a consequence, a complete inventory of glaciers in Mongolia does not exist.

Upon completion of the Mongolian glacier inventory, possible causes for glacier area and number discrepancies were recognized. The most glaring distinction between

the here developed inventory and other author group's attempts in mapping ranges in the Altai Mountains is Landsat TM scene selection. Glacier mapping attempts on Kharkhiraa, Tsambagarav, Turgen, and Sair, by Erdenetuya *et al*. (2006) used a Landsat TM scene acquired on June 25, 1992 (Figure 33a); however, it is of insufficient quality: snow patches indicate that the date of acquiring the image was not the end of the melt season also, due to the orographic nature of mountainous terrain, Tsambagarav is inundated with clouds. This study only used high quality images from between 1991 (Figure 34b) and 2011.

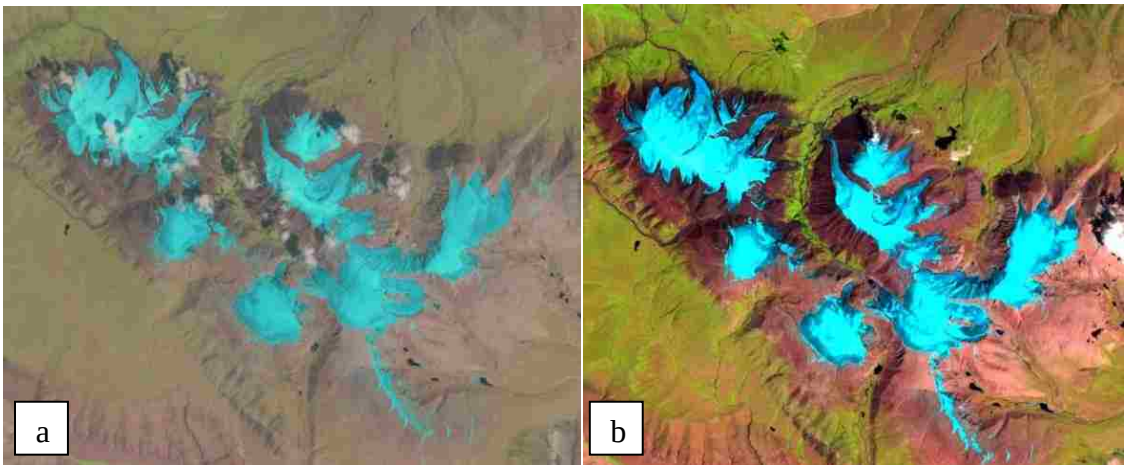

Figure 34a. A Landsat TM image acquired on 06251992 used by Erdenetuya et al. (2006). As evidenced by light now patches, the image was not acquired at the end of the melt season, skewing glacier area. Also, much of the glaciated region is covered by clouds. Figure 34b. The Mongolian Glacier Inventory chose to use a Landsat TM image acquired on 07171991 rather than 06261992. Figure 34b is clearly at the end of the melt season and has acceptable cloud cover.

When producing a glacier inventory, it is important to document the coordinates (Lat/Long) of the extent that binds the study region; otherwise calculations of glacier number and area can be negatively affected. This is evidenced when Krumwiede *et al.* (in press) mapped glaciers in the Tavan Bogd range. In their glacier mapping efforts an area of 213 km^2 was mapped in 1989 and 204 km^2 in 2009. Their numbers far exceed the area of glaciers in this inventory, which is due to each group's defined glacier extent.

Krumwiede *et al.* (in press) mapping approach did not pay attention to national boundaries with the result that also cross-boundary glaciers were entirely mapped. On the contrary, in the study at hand, the mapping approach only included glaciers and glacier parts within the boundaries of Mongolia, and the glacier extent was defined local watersheds and hydrological parameters. Therefore, our extent included a smaller area of glaciers. In addition, some glaciers and glacier parts that were located within Mongolian boundaries were excluded from the inventory, because their waters flowed into Russia and Kazakhstan. The binding coordinates for each range in the Mongolian Altai will be uploaded to the GLIMS database and downloaded as a shapefile.

The presented results illustrate the importance of glacier size. Kamp *et al.* (in press) first noted that previous glacier studies in Mongolia never disclosed their definition of a glacier. When determining a glacier inventory's definition of a glacier, the proposed size (km^2) can profoundly affect the total glacier number and area. Had this inventory only mapped glaciers >0.02 (km^2) like Frey *et al.* (2012a) the area and total number of glaciers would be much lower. The size of glaciers mapped is also important to consider when assessing the accuracy of the selected mapping methodology. As noted in (APPENDIX A, B, and C) the larger the glacier, the higher the accuracy.

Examining changes in glacier frequency by class size (km^2) is a strong indicator of glacier retreat or stagnation. From 1990 to 2000, glaciers in the Altai Mountains observed the strongest retreat in all sub-regions and ranges. At the same time, there was also a strong increase in glacier frequency in class size 3 (0.126 – 0.85 km^2), which indicates a strong disintegration of larger glaciers into smaller glaciers. When creating an inventory in the Tian Shan, Bolch (2007) also documented the disappearance of small

glaciers and the disintegration of larger glaciers after 1979. Yet, when small glaciers become less frequent, glaciers are considered in a state of stagnation. From 2000-2010, the intensity of glacier retreat decreased significantly from the previous decade and in some ranges, like Tavan Bogd, only minor loss in glacier area was documented. As evidenced by the reduction in the frequency of small glaciers from 2000 – 2010 (Figure 23). Many author groups state the importance of glacier sizes vary with changing climate and have been a good indicator of climate change. Furthermore, the rate of glacier retreat is mostly influenced by glacier size and smaller glaciers shrink faster than larger glaciers (Bolch 2007, Bolch *et al.* 2010a, Granshaw and Fountain 2006, Kadota *et al.* 2011).

The Mongolian glacier inventory reflects the overall global retreat of alpine glaciers; as observed in glacier inventories developed by Granshaw and Fountain (2006) in the North Cascades, Paul *et al.* (2007) in the Alps, Racoviteanu *et al.* (2009) in the Cordillera Blanca, Moussavi *et al.* (2009) in Iran, Yafeng *et al.* (2009) in China, Haritashya *et al.* (2009) in the Pamir mountains of Afghanistan, Bolch *et al.* (2010a) in western Canada, and by Bhambri *et al.* (2011) in the Garhwal Himalaya, India. Yet, glaciers in Mongolia are retreating at different rates than other regions. For example, from between 1958 to 1998 Granshaw and Fountain (2006) only found a decrease of 7% in total ice-covered area in the North Cascades National Park in Washington, USA. Also, from between 1985 – 2005 Bolch *et al.* (2010a) documented a rate of retreat of 25.4 ± 4.1% in the southern Rock Mountains of Alberta.

However, there are also documented glacier advances and surges in regions such as the Karakorum (Barrand and Murray 2006, Copland *et al.* 2011). In the Altai

Mountains the observed decrease of glacier terminus by 7 m in the Central Altai should be approached with caution before a glacier advance can be proclaimed. The decrease in terminus elevation can be attributed to either a relative stagnation of glacier area or because the 90 m SRTM DEM, no measureable change in mean glacier terminus elevation occurred ±90 m

The Mongolian inventory is in agreement with other author groups who have examined glacier mass balance within the Altai (Table 4) which have demonstrated a retreat in glacier termini. Kadota *et al.* (2011) estimate Potanin Glacier may retreat up to 3 km in the next 100 years. Using the change in glacier terminus elevation, this study recorded a retreat at a rate of 350 m (±90 m) over 20 years for Potanin glacier. At a rate of 350 m over 20 years a retreat of only 1,750 m over 100 years is estimated. Batima (2005) calculated a glacier retreat of 6 % from between 1945 to 1985. This study shows an accelerated rate of retreat from 1990 to 2010 of close to 30 % throughout the entire Altai.

Table 4. Previous and current author groups who have surveyed glaciers based on ranges in the Altai Mountains.

MASSIF	AUTHOR GROUP
Tavan Bogd	Pan et al 2012 Krumweide et al 2012 Kadota et al 2011
Turgen	Pan et al 2012 McManigal et al 2012 Lemhkuhl 2012 Erdenetuya et al 2006 Kadota et al 2004
Kharkhiraa	Pan et al 2012 Lehmkuhl 2012 Erdenetuya et al 2006 Kadota et al 2004
Munkh Khairkhan	Pan et al 2012 Krumweide et al 2012 Erdenetuya et al 2006
Sairiin	Pan et al 2012 Erdenetuya et al 2006
Tsambagarav	Pan et al 2012 Kadota et al 2011 Erdenetuya et al 2006 Kadota et al 2004

In Tavan Bogd region from the 1940s to 2000, Kadota *et al.* (2007) found a total decrease in glacier area of 10.2 %. In the same region, Krumwiede *et al* (in press) found an overall decrease in glacier area of only 4 % from 1989 to 2009. This study found an overall decrease in glacier area on Tavan Bogd to be 16.84 % from between 1990 to 2010. Furthermore, the percent change in glacier area drastically reduced to only 1.24 % from 2000 to 2010. This is in line with Krumwiede *et al.* (in press) who also found the glaciers in Tavan Bogd to be in a state of stagnation. On Munkh Khairkhan massif, Krumwiede *et al.* (in press) also found a decrease of glacier area of close to 12 km^2 (30

%) from between 1990 to 2006. In this study, the total change in glacier area from 1990 to 2010 was 17 km^2 (38.6 %).

Paul *et al.* (2009) found that mean slope is an excellent proxy for mean glacier thickness. In theory, the glacier thickness and mean slope have an inverse relationship. As the mean slope increases, the mean glacier thickness is decreasing. Analysis of mean glacier slope in the Altai Mountains, demonstrate an increasing slope from 1990 to 2010, suggesting glacier thinning. Examination of surface lowering using DEM analysis show a mean reduction of 9.3 meters on Potanin Glacier in the Tavan Bogd Region, 2 m less than the mean reduction for the entire Altai Mountains from 1990 to 2010. Kadota *et al.* (2011) measured the surface lowering on Potanin Glacier using stake observations from 2004 to 2009. At three locations on Potanin Glacier, Kadota *et al.* (2011) found a surface lowering of 15.8 m, 13.5 m, and 9.5 m.

Glacier inventories performed by Bolch *et al.* (2010a, 2010b) and Frey *et al.* (2012a) in western Canada, Tibetan Plateau, and western Himalaya all had glaciers with a predominately northern aspect followed by a northeast aspect. Khrutsky and Golubeva (2008) stated that northern slopes in the Altai Mountains had the most extensive glacierization due to the higher moisture contents on the northern slopes. The results from this study are not in line with their results, in fact when analyzing glaciers larger than 0.1 km^2, there were no more than 10 glaciers with a northern aspect during any time period.

6.3 Climate – Glacier Interaction in the Mongolian Altai.

Few places in the world have as strong of a continental climate as Mongolia (Jacoby *et al.* 1996, Lehmkuhl and Lang 2001, Batima *et al.* 2009), therefore is an ideal

location to attempt in better understanding glacier-climate dynamics, specific to a continental climate. Examining climatic data will also ideally lead to a resolution of the rapid glacier retreat observed from 1990 to 2000. The systematic collection of meteorological data in Mongolia began in the 1940s. Yet, there is very little recorded or published information concerning historical climate data in Mongolia. Batima (2006) described that only some spot points on short period extremes have been recorded. Currently there are four meteorological stations in or within close proximity to the Altai Mountains; Ulaangom ~500-1000 m a.s.l., Ulgii ~1600-2200 m a.s.l., Khovd ~ 1000-1600 m a.s.l., and Baitag ~ 1000-1600 m a.s.l.. By using the aforementioned stations, Batima (2006) concluded that the climate in Mongolia is getting warmer and slightly drier, this trend is more pronounced in the Altai Mountains.

There have been no significant changes in precipitation in Mongolia over the last 70 years, but overall it has been noted by multiple author groups that precipitation has decreased by 7 % (Bayasgalan *et al.* 2008, Sarantuya *et al.* 2010). However, the nature of change in precipitation has a highly localized character (Batima *et al.* 2005, Stumpp *et al.* 2005). For example, annual precipitation decreased by 30-90 mm on the north-eastern slope of the Khanghai mountains. While in the Mongol Altai, annual precipitation increased by 2-60 mm (Batima *et al.* 2005).

Air temperature is one of the most influential factors contributing to fluxes in glacier mass balance. However, the amount of influence is spatially variable. For example, when examining energy balance on Antizana Glacier in the Ecuadorian Andes, Francou *et al.* (2004) found that an increase in air temperature favors rainfall over snowfall, insufficient snowfall to maintain high glacier albedo, low wind speeds, which

limits the transfer of energy from melting to sublimation, and reduced cloud cover, which increased incoming solar radiation, all of the aforementioned influences were dictated by El Niño phases. Francou *et al.* (2004) mentioned that Antizana Glacier is a tropical glacier, and that glaciers found in the outer tropics will respond differently to ENSO phases and climate change. Therefore, in the case of the Altai Mountains it will be very challenging to make any strong inferences of how influential air temperature is to glacier mass balance because of the lack of localized weather stations.

Temperature records in Mongolia dating from 1940-1990 show that mean annual air temperature has increased by 1.56˚C. Winter temperatures have increased by 3.6˚C, spring/fall temperatures increased by 1.5˚C, and interestingly summer temperatures have decreased by 0.3˚C (Jacoby *et al.* 1999, Sarantuya and Natsagdorj. 2010). The increase in temperatures for Mongolia is in agreement with other locations in the Northern Hemisphere; however between the 1950s through 1970s, Mongolian temperatures are slightly above the Northern Hemisphere trends (Jacoby *et al.* 1999). Using temperature data collected from 48 meteorological stations throughout Mongolia, the mean annual air temperature in Mongolia has increased by 2.1 ˚C (Bayasgalan *et al* 2008, Sarantuya and Natsagdorj. 2010). The current change in increased annual air temperature indicates a stronger warming phase compared to the change from 1940-1990. Also, the study performed by Batima *et al.* (2005) indicates a summer warming trend of 1.1 ˚C, whereas previous studies found a much lower increase (Bayasgalan *et al.* 2008). The here presented glacier inventory spans twenty years from 1990 to 2010; within this time frame published climatological data exists from 1940 to 2001. Batima *et al.* (2006) notes a

clear warming beginning in the 1970s and intensifies towards the end of the 1980s (Figure 35 & 36).

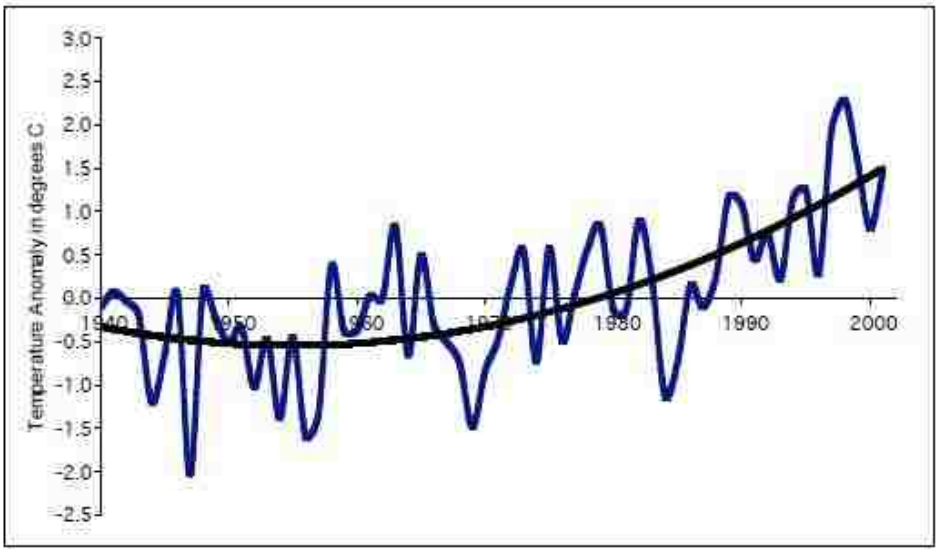

Figure 35. Temperature trend from 1940 – 2001 in the Mongolian Altai. Black line indicates a second order polynomial trend (Batima et al. 2006).

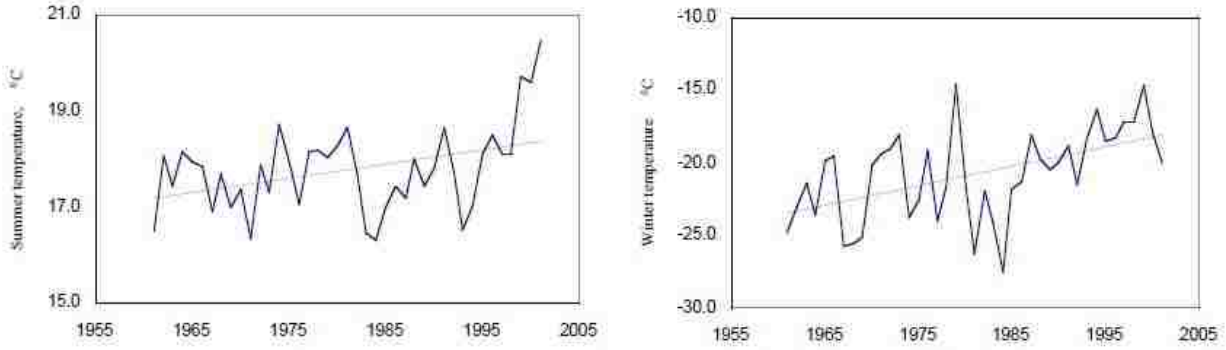

Figure 36. Recorded temperature trends during the summer and winter, recorded from a meteorological stations in Khovd, Mongolia (Batima et al. 2006).

As the trend in mean temperatures increase in Mongolia, the trend in Heat Wave Duration (HWD) also increased (Figure 37). It has been noted that the most extreme HWD event occurred in 1998, reaching 70 days in the mountain regions and 30 days in the Gobi desert (Batima *et al.* 2005). At the opposite end, there is a clear trend in decreasing Cold Wave Duration (CWD) by about 13 days. Following extreme HWD events in 1998, Mongolia experienced severe drought between 1999-2002, subsequently

causing the most severe dzud (zud) in recorded history (Batima *et al.* 2005, Bayasgalan *et al.* 2008).

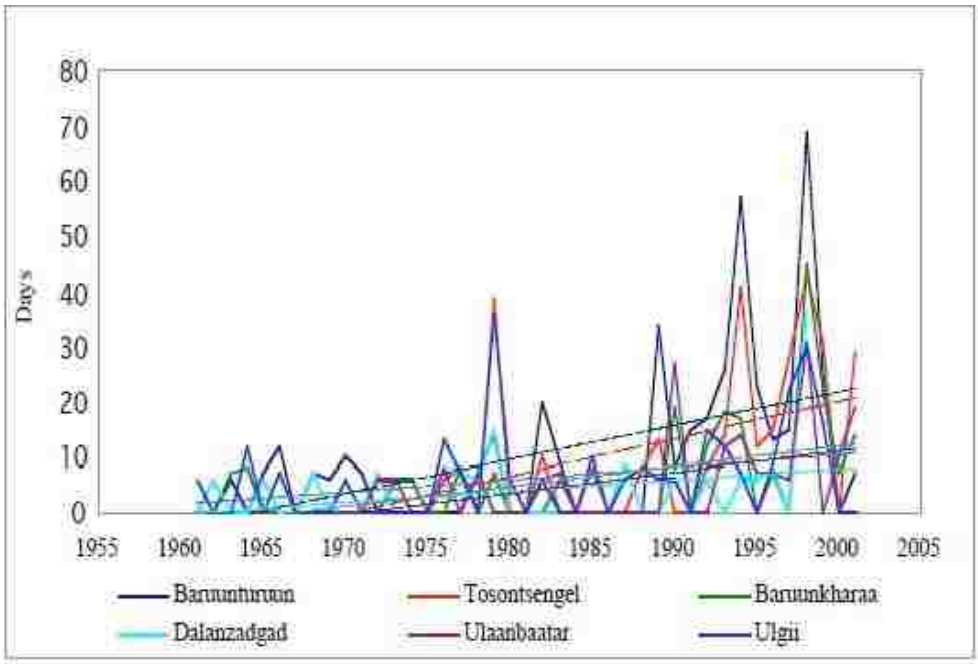

Figure 37. Trend in increasing HWD days from 1960 to 2000 measured at six separate meteorological stations. Ulgii is located in the Altai Mountains and shows a positive trend (Batima et al. 2006).

The Mongolian glacier inventory has demonstrated an overall decrease in glacier area from 1990 to 2010 and an accelerated loss from 1990 to 2000 compared to the latter decade, this trend is also recognized by Krumwiede *et al.* (in press). As the glaciers have receded in the Altai Mountains, there has been an overall trend in warming temperatures in Mongolia and increasing HWD. The intensified temperature anomalies towards the end of the 1980s and into the 1990s (Figure 35) are a strong indicator of why there was such rapid glacier retreat from 1990 to 2000. Changes in glacier snout are a good indicator of mass balance and thereby a good indicator of climate. However, the response time of a glacier to climate is dependent on glacier size and intensity of the current climate (Barry 2006). However, research conducted to estimate glacier response

time is highly limited. Yet, mass balance measurements are un-delayed and strong climate indicators (ICIMOD 2013). Mass balance metrics can include the equilibrium line altitude (ELA) which is characterized by Frey *et al.* (2012a) as the mean glacier elevation. However, other author groups used the median glacier elevation to denote ELA (Braithwaite and Raper 2009, Paul *et al.* 2009, Bolch *et al.* 2010a). The ELA is described as the most important characteristic altitude because it divides the glacier into ablation and accumulation areas (Armstrong *et al.* 1973, Braithwaite and Raper 2009). For this inventory, the ELA will be defined as the median glacier elevation.

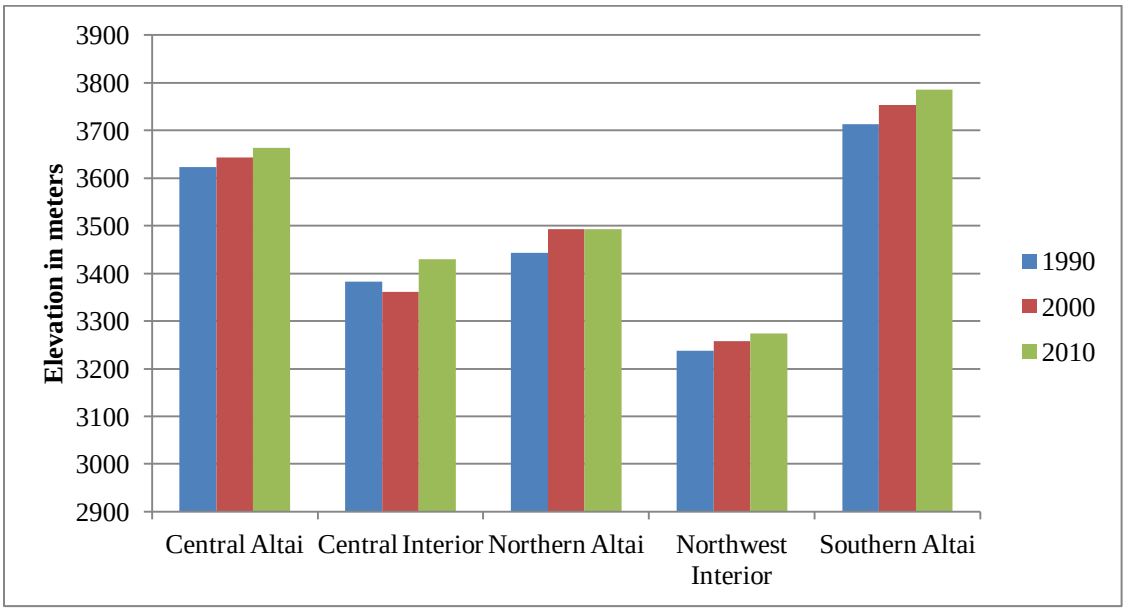

Figures 38. The glacier ELA in the Altai Mountains by sub-region and greater than 0.1 km^2.

Figure 38 indicates an overall increase in ELA throughout the Altai Mountains from 1990 to 2010. The highest increases in ELA are observed in the Southern Altai followed by the Central and Northwest Interior. The maximum elevation of glaciers in the Southern Altai is ~3959 m a.s.l. and currently the ELA is 3785 m. Over the twenty year time period, the mean glacier terminus elevation has retreated from 3504 m to 3533 m change of 29 m. The ELA increased by 73 m over the same time period which is much

faster compared to mean glacier terminus elevation. Braithwaite and Raper (2009) stated that once the ELA has risen above the glacier, the glacier will loose its accumulation zone and might disappear. If Mongolia's climate continually trends towards a warmer climate and longer HWD, the ELA increase by 73m/20 years in the Southern Altai will lead to a loss of accumulation zones of individual glaciers by 2058.

Unfortunately though, the climatological and even glaciological records in the Altai Mountains are too sparse and inconsistent to make any strong inference between glacier and climate with confidence at this point in time. As part of the IPCC 2012 report, a supplemental global glacier inventory was submitted known as the Randolph Glacier Inventory (RGI). Submitted in the report are glacier outlines digitized from Soviet military maps between 1968 and 1983 for Mongolia. Unfortunately, these outlines are not made available to the public yet and will be an important asset when combined with our glacier outlines (Arendt *et al.* 2012). Once the older glacier outlines are made available, it will be possible to create a glaciological record of up to 42 years and make stronger inferences of glacier-climate interactions in the Altai Mountains.

6.4Land Use Management and Glacier Retreat

Climate change can impact glacier mass balance in other ways than direct air temperature or precipitation. As mentioned in the chapter *Background* through a combination of climate change and shifts in land use management in Mongolia, there has been a rapid increase in the desertification of pasture lands. Increased drought coupled with desertification has increased the frequency of dust storms and drifting dust in the Altai. Natsagdorj *et al.* (2003) found that the number of dusty days has tripled from the 1960s to 1990s within Mongolia. Their study also found that the number of "dusty

days" in the south side of the Altai Mountains ranged from 91-120 days. When examining glaciers in the Karakorum, Hewitt (2005) discussed that a thin layer of wind-blown dust can increase the rate of ablation by up to 40%. In the Swiss Alps, Oerlemans *et al.* (2009) found that a decrease in glacier albedo of 0.32 to 0.15 by surface dust caused an additional removal of 3.5 m of ice. The decrease in albedo is equal to retaining a glacier albedo of 0.32 but increasing the air temperature by 1.7 K. Currently, there are no studies in the Altai Mountains examining the occurrence of dusty days and its impact on glacier surface albedo in the region. However, when examining the Turgen Mountains, Kamp *et al.* (in press) did observe glaciers with a thin layer of dust (Figure 39). Further research will need to be performed to identify the origin of the dust found on the Turgen glaciers and the cause for the increase in dusty days since the 1990s.

Figure 39. Panoramic photo in the Turgen Mountains. It is possible that there is evidence of wind-blown dust on the glacier surface, indicated by red boxes. Photo by Kevin McManigal 2010.

6.5 Future of the Glacier Monitoring Efforts in Mongolia.

The most powerful component of any environmental monitoring effort is the temporal component. This study has created and compiled glacier outlines and parameter

data over a twenty-year period which is a strong foundation for future efforts in glacier monitoring in the Altai Mountains. Furthermore, this inventory presents a mapping approach that only require a limited number of data inputs and produces glacier outlines. This study also promotes consistency and community participation in glacier monitoring efforts in the Mongolian Altai. By involving Mongolians in the glacier monitoring, the inventory will continue to grow, if mapping efforts continue on a 5 to 10 year time-scale (Fountain *et al*. 1997).

It is evident that glacier monitoring efforts are imperative for Mongolia, in terms of water resources as local climate changes and industry transitions to more water intensive industries. But also, due to the nature of nomadic livelihoods being highly dependent on the environment, it is important to incorporate glacier monitoring data in adaptation and mitigation strategies for sustainable livelihoods. With that said, throughout the globe, the most successful glacier monitoring efforts stemmed from government funding and support. For example, in 2011, President Barack Obama supported the partnership between U.S. and Chilean scientists to strengthen regional glacier monitoring efforts through the Energy Climate Partnership of the Americas (ECPA) and Andean Glacier Monitoring Center. The United States Geological Survey (USGS) along with academic institutions such as Michigan Tech Research Institute (MTRI) provided scientific assistance for glacier monitoring technology (http://chile.usembassy.gov/2012press0831-glacier.html).

In the United States, the majority of regions in the contiguous 48 states that contain glaciers are protected as National Parks. Among these parks are Mount Rainier National Park, Glacier National Park, and North Cascades National Park. All three

National Parks have strong glacier monitoring programs supported by park employees and lead by the USGS (Fountain *et al* 1997). Similar to the United States, Mongolia has also taken steps in preserving their glaciated regions with National Parks, including Munkh Khairkhan National Park, Altai Tavan Bogd National Park, and Tsambagarav Uul National Park. It is in these National Parks where steps need to be initiated for the development in a strong glacier monitoring network. Figure 40 outlines important funding and support entities to achieve a successful glacier monitoring program in Mongolia. Similar to the U.S. – Chilean partnership, the here proposed network relies on academic institutions, specifically The University of Montana and the National University of Mongolia for the training of NPS employees in monitoring glaciers remotely and with in-situ observations.

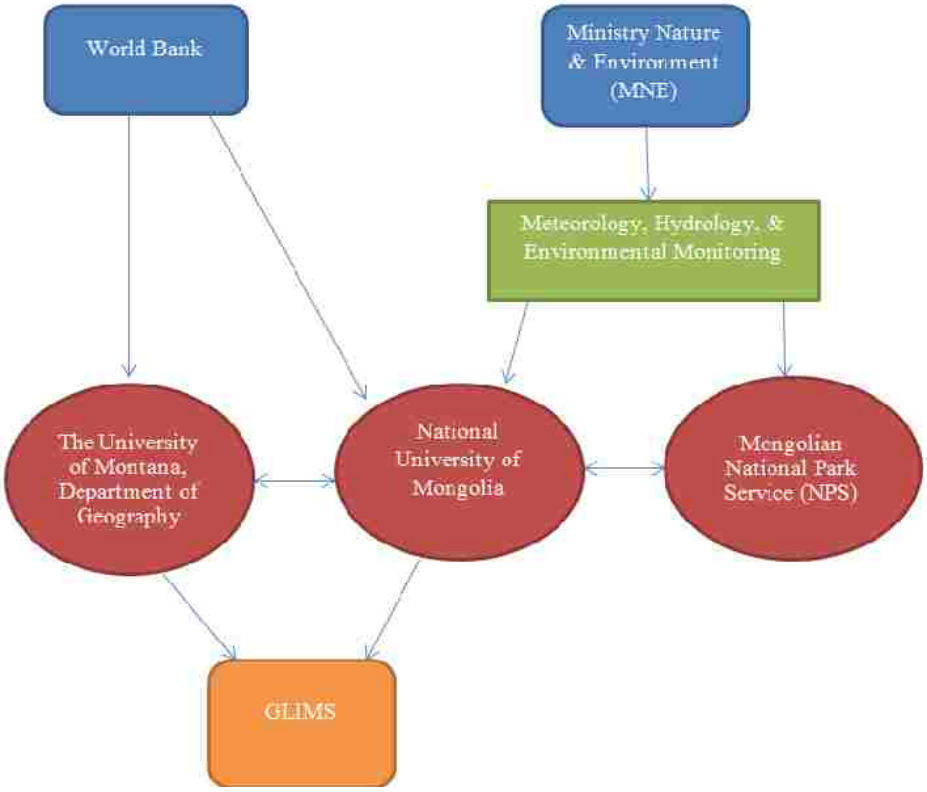

Figure 40. The flowchart identifies private and government entities to be involved in a glacier monitoring program for the Mongolian Altai. Blue indicates major sources of funding to be dispersed amongst the entities in red. The red entities will be responsible for training and the collection of data. Orange indicates the medium to disseminate information concerning Altai glaciers to the public.

The next step in establishing a strong glacier monitoring program in the Altai Mountains would be the installation of Automatic Weather Stations (AWS) on or in close proximity to glaciers. These efforts have already been initiated by Kadota *et al.* (2011), who have installed AWSs on glaciers in Tavan Bogd and Tsambagarav Massif. As climate data and records for glaciated regions become more abundant and reliable, stronger inferences about climate change, weather trajectories, and their relationship to glaciers can be made. Kadota *et al.* (2011) also have stakes and snow-pit observations being carried out on glaciers in Tavan Bogd and Tsambagarav massif.

AWS and in situ glacier measurements include but are not limited to (Alford *et al.* unpublished report):

- Temperature
- Wind
- Radiation
- Humidity
- River flows
- Observation of glacier ablation
- Solid Precipitation
- Snow (snow water equivalent (SWE), depth, extent, density, albedo

The research presented in this paper was designed around the creation of a simple and inexpensive method for mapping and managing glacier data, derived from remote sensing. Even though some regions in the Altai have a high percent error of area determination, it is still effective in mapping and inventorying glaciers and should be used in future Mongolian glacier mapping endeavors. Not only was a method created for mapping glaciers, but a product was created to physically exchange to Mongolian National Park employees or researchers to continue the glacier inventory. The methodology created in this glacier inventory should be the foundation for glacier monitoring workshops which can be administered by scientists at The University of Montana and National University of Mongolia. Depending on funding, the current method is created using the ArcGIS Desktop environment, but can be easily adapted to more affordable software packages such as IDRISI Selva. In the case of highly restricted funding, the GLIMS program has developed their own software specific to digitize

glaciers and provide attributes through GLIMSView; it can be downloaded for free at http://www.glims.org/GLIMSView/.

Figure 39 also outlines large funding sources as being the Mongolian Ministry Nature and Environment (MNE) and the World Bank. The World Bank is a strong contributor towards projects with international development objectives, specifically glacier monitoring efforts. In 2008 the World Bank partnered with the Adaptation to Rapid Glacier Retreat in the Tropical Andes Project to provide technical assistance through training to scientists from Ecuador, Bolivia, Columbia, and Peru on monitoring their glaciers through satellite imagery. Scientists from the Remote Sensing Technology Center of Japan (RESTEC) prepared eleven topics related to glacier monitoring using remote sensing technology and spent approximately one month giving local scientist's hands-on training with a teacher : student ratio of 1:14 (Haruyama *et al.* 2008). Following the lead of Haruyama *et al.* (2008) and the US-Chilean partnership, scientists from The University of Montana and National University of Mongolia, in their role of presenting the GLIMS RC for Mongolia, should assume the role of instructors in facilitating the education of Mongolian NPS employees in glacier monitoring techniques through remote sensing when funding has been procured.

The RC for Mongolia allows for downloading satellite (ASTER, Landsat TM) and DEM free of charge from the USGS. As the glacier monitoring program in the Altai progresses, if National Park employees would like to acquire ASTER imagery, they can submit a request to the RC. Again, the developed methodology can be easily adjusted to utilize ASTER imagery rather than Landsat TM.

Ultimately, as these data and inventory grow, Mongolians will have a strong understanding and be able to anticipate how their glaciers will react during a particular climate phase. Therefore mitigating and adapting to any impacts climate may have on up to 10% of the nation's water resource.

7. CONCLUSION

Multiple conclusions can be drawn from this study. The first conclusion is a concise and conclusive number and area of glaciers in the Altai Mountains of Mongolia for three time periods, including 1990, 2000, and 2010. We mapped a glacier area of 443.12 km^2 (±13.54%) in 1990 and a total number of 690, the total estimated area totaled 540.57 km^2. The total glacier area in 2000 was 438.72 km^2 (±17.20%) and a total number of 716. And the most current state of glaciers, in 2010, the total glacier area was 372.30 km^2 (±17.17%) and a total number of 671. These data will be the foundation for future glacier change assessments, water resource conservation analysis, and climatological studies within the Altai Mountains of Mongolia.

Multi-decadal analyses of glacier change in the Altai Mountains show spatial and temporal trends with the highest rate of retreat occurring in the Northern Altai and the fastest rate of total retreat occurring from between 1990 – 2000 at 20.17%. From 1990 to 2010 glacier area loss was 29.86%, this is a significant increase from a glacier decrease of only 6% from 1945 to 1985 as described by Kadota and Gombo (2007). Annually, from 1990 to 2010, glacier area changed 5.89%.

From what little climatological data is available in the Altai Mountains, the climate is generally becoming warmer and dryer based on data from the 1940s to 1990s. During the 1990s, Mongolia experienced its worst droughts and a strong increase in temperature and can be responsible for the rapid retreat of glaciers during that time period. However, the climate is highly variable within mountain environments, therefore more research needs to be conducted pertaining to glacier – climate interaction in the Altai, specifically the relationship between glacier aspect and localized weather

trajectories. Also, the occurrence and distribution of dust on glaciers in the Altai is a topic that has not been researched but can have powerful societal and environmental impacts if the increased dust can be linked to land use management.

For future glacier monitoring endeavors in Mongolia, this study also developed clearly defined guidelines for the continuation of glacier monitoring through remote sensing imagery. These guidelines include the definition of a glacier, ideal date of acquisition of satellite imagery, and mountain range extents as defined by shapefiles. But most importantly, as the RC within the GLIMS program, we designed and created multiple models using a TM4/TM7 ratio to replicate, limit human induced error, accurately, and inexpensively monitor glaciers using remote sensing and GIS technology. These models are an important component in the long term objective for a successful glacier monitoring network program in the Altai Mountains of Mongolia and glacier inventories on a 5 to 10 year time scale.

Compared to other mountain ranges in the world, the Altai Mountains may seem insignificant. There are no glamorous 8,000 m peaks or even 5,000 m peaks. The Altai has no immediate glacier hazards like the glacier lakes in Nepal. There are no glorified glaciers that are spawned in the Altai and have a grand finale by calving into an ocean. Yet, the importance of glaciers in the Altai should never be understated. Glaciers in Mongolia provide a precious source of water to millions of nomadic herds that sustain Mongolian livelihoods, water for a newly initiated and promising agricultural sector, and booming mining industry. But also, glaciers in Mongolia truly contribute to the greater knowledge of our understanding of glaciers in a continental climate, effectiveness in

glacier monitoring methods through remote sensing, and link between land use management and glacier mass balance.

8. REFERENCES

Alam, M. "Mainstreaming of Climate Change Adaptation into Sustainable Development." (paper presented at the meeting on Integration of Climate Change Adaptation into Sustainable Development in Mongolia, Ulaanbaatar, Mongolia, June 17-18, 2010).

Andreassen, L.M., Paul, F., Kääb, A., & Hausberg, J.E. (2008). Landsat-derived glacier inventory for Jotunheimen, Norway, and deduced glacier changes since the 1930s. *Cryosphere, 2*, 131-145

Arendt, A., T. Bolch, J.G. Cogley, A. Gardner, J.-O. Hagen, R. Hock, G. Kaser, W.T. Pfeffer, G. Moholdt, F. Paul, V. Radić, L. Andreassen, S. Bajracharya, M. Beedle, E. Berthier, R. Bhambri, A. Bliss, I. Brown, E. Burgess, D. Burgess, F. Cawkwell, T. Chinn, L. Copland, B. Davies, H. de Angelis, E. Dolgova, K. Filbert, R. Forester, A. Fountain, H. Frey, B. Giffen, N. Glasser, S. Gurney, W. Hagg, D. Hall, U.K. Haritashya, G. Hartmann, C. Helm, S. Herreid, I. Howat, G. Kapustin, T. Khromova, C. Kienholz, M. Koenig, J. Kohler, D. Kriegel, S. Kutuzov, I. Lavrentiev, R. LeBris, J. Lund, W. Manley, C. Mayer, E. Miles, X. Li, B. Menounos, A. Mercer, N. Moelg, P. Mool, G. Nosenko, A. Negrete, C. Nuth, R. Pettersson, A. Racoviteanu, R. Ranzi, P. Rastner, F. Rau, J. Rich, H. Rott, C. Schneider, Y. Seliverstov, M. Sharp, O. Sigurðsson, C. Stokes, R. Wheate, S. Winsvold, G. Wolken, F. Wyatt, & N. Zheltyhina. (2012). Randolph Glacier Inventory [v2.0]: A Dataset of Global Glacier Outlines. Global Land Ice Measurements from Space, Boulder Colorado, USA. Digital Media.

Baast, P. (1998). Modern glaciers of Mongolia. Ulan Bator, Unpublished Report, Institute of Meteorology and Hydrology, 162 p. (In Russian).

Barrand, N.E., & Murray, T. (2006). Multivariate controls on the incidence of glacier surging in the Karakoram Himalaya. *Arctic Antarctic and Alpine Research, 38*, 489-498

Barry, R.G. (2006). The status of research on glaciers and global glacier recession: a review. *Progress in Physical Geography, 30*, 285-306

Batima, P. (2006). *Climate Change Vulnerability and Adaptation in the Livestock Sector of Mongolia*. Washington, D.C.: Assessments of Impacts and Adaptations to Climate Change (AIACC) Project Office, 84 p.

Batima, P., Natsagdorj, L., Gombluudev, P., & Erdenetsetseg, B. (2005). *Observed Climate Change in Mongolia*. Nairobi: Assessments of Impacts and Adaptations to Climate Change (AIACC) Working Papers, No. 13, 26 p. [online at http://www.aiaccproject.org/]

Bedunah, D.J., & Schmidt, S.M. (2004). Pastoralism and protected area management in Mongolia's Gobi Gurvansaikhan National Park. *Development and Change, 35*, 167-191

Bhambri, R., & Bolch, T. (2009). Glacier mapping: a review with special reference to the Indian Himalayas. *Progress in Physical Geography, 33*, 672-704

Bhambri, R., Bolch, T., & Chaujar, R.K. (2011a). Mapping of debris-covered glaciers in the Garhwal Himalayas using ASTER DEMs and thermal data. *International Journal of Remote Sensing, 32*, 8095-8119

Bhambri, R., Bolch, T., Chaujar, R.K., & Kulshreshtha, S.C. (2011b). Glacier changes in the Garhwal Himalaya, India, from 1968 to 2006 based on remote sensing. *Journal of Glaciology, 57*, 543-556

Bishop, M.P., & Colby, J.D. (2002). Anisotropic reflectance correction of SPOT-3 HRV imagery. *International Journal of Remote Sensing, 23*, 2125-2131

Bishop, M.P., Kargel, J.S., Kieffer, H.H., MacKinnon, D.J., Raup, B.H., & Shroder, J.F. (2000). Remote-sensing science and technology for studying glacier processes in high Asia. *Annals of Glaciology, Vol 31, 2000, 31*, 164-170

Bishop, M.P., Schroder, J.F., & Colby, J.D. (2003). Remote sensing and geomorphometry for studying relief production in high mountains. *Geomorphology, 55*, 345-361

Bishop, M. P., J. A., Olsenholler, J. F., Schroder, R. G., Barry, B. H., Raup, A. B. G., Bush, L., Copland, J. L., Dwyer, A. G., Fountain, W., Haeberli, A., Kääb, F., Paul, D. K., Hall, J. F. Kargel, B. F., Molnia, D. C., Trabant, & R., Wessels. (2008). Global land ice measurements from space (GLIMS): remote sensing and GIS investigations of the Earth's cryosphere. *Geocarto International, 19 (2)*, 57-84.

Bolch, T. (2007). Climate change and glacier retreat in northern Tien Shan (Kazakhstan/Kyrgyzstan) using remote sensing data. *Global and Planetary Change, 56*, 1-12

Bolch, T., Menounos, B., & Wheate, R. (2010a). Landsat-based inventory of glaciers in western Canada, 1985-2005. *Remote Sensing of Environment, 114*, 127-137

Bolch, T., Yao, T., Kang, S., Buchroithner, M.F., Scherer, D., Maussion, F., Huintjes, E., & Schneider, C. (2010b). A glacier inventory for the western Nyainqentanglha Range and the Nam Co Basin, Tibet, and glacier changes 1976-2009. *Cryosphere, 4*, 419-433

Braithwaite, R.J., & Raper, S.C.B. (2009). Estimating equilibrium-line altitude (ELA) from glacier inventory data. *Annals of Glaciology, 50*, 127-132

Bronge, L.B., & Bronge, C. (1999). Ice and snow-type classification in the Vestfold Hills, East Antarctica, using Landsat-TM data and ground radiometer measurements. *International Journal of Remote Sensing, 20*, 225-240

Bulag, U.E. (2009). Mongolia IN 2008 From Mongolia to Mine-golia. *Asian Survey, 49*, 129-134

Bulley, H.N.N., Bishop, M.P., Shroder, J.F., & Haritashya, U.K. (2013). Integration of classification tree analyses and spatial metrics to assess changes in supraglacial lakes in the Karakoram Himalaya. *International Journal of Remote Sensing, 34*, 387-411

Chuluun, T. "Climate Change and Sustainable Development of Mongolia: Summary of Papers." (paper presented at the meeting on Integration of Climate Change Adaptation into Sustainable Development in Mongolia, Ulaanbaatar, Mongolia, June 17-18, 2010).

Colby, J.D. (1991). Topographic normalization in rugged terrain. *Photogrammetric Engineering and Remote Sensing, 57*, 531-537

Colby, J.D., & Keating, P.L. (1998). Land cover classification using Landsat TM imagery in the tropical highlands: the influence of anisotropic reflectance. *International Journal of Remote Sensing, 19*, 1479-1500

Consortium for Spatial Information (CGIAR-CSI). (2013). http://www.cgiar-csi.org/data/srtm-90m-digital-elevation-database-v4-1. (accessed May 15, 2013).

Copland, L., Sylvestre, T., Bishop, M.P., Shroder, J.F., Seong, Y.B., Owen, L.A., Bush, A., & Kamp, U. (2011). Expanded and Recently Increased Glacier Surging in the Karakoram. *Arctic Antarctic and Alpine Research, 43*, 503-516

Dagvadorj, D. "The Climate Change Policy and Measures in Mongolia." (paper presented at the meeting on Integration of Climate Change Adaptation into Sustainable Development in Mongolia, Ulaanbaatar, Mongolia, June 17-18, 2010).

Davaa. G. "Climate Change Impacts on Water Resources in Mongolia." (paper presented at the meeting on Integration of Climate Change Adaptation into Sustainable Development in Mongolia, Ulaanbaatar, Mongolia, June 17-18, 2010).

Davaa, G., Oyunbaatar, D. & Sugita, M. (2007). Surface Water of Mongolia. In: Konagaya, Y. (ed.), *A Handbook of Mongolian Environments*, 55-68.

Dozier, J. (1989). Spectral signature of alpine snow cover from the Landsat thematic mapper. *Remote Sensing of Environment, 28*

Dugarjav C., & B. Tsetseg. (2003). *Conservation and sustainable use of biodiversity in the Trans-Altai Gobi desert of Mongolia.* In J. Lemons, R. Victor, and D. Shaffer, *Conserving biodiversity in arid regions; best practices in developing nations.* pg. 137-156. Norwell MA: Kluwer Academic Publishers.

Enkhtaivan, D. (2006). Physical-geographical characteristics of the Altai region. *In* Vogtmann, H., and Dobrestov, N. (eds.), *Environmental Security and Sustainable Land Use: With Special Reference to Central Asia*. Dortrecht: Springer, 349–351

Endo, N., Kadota, T., Matsumoto, J., Ailikun, B., & Yasunari, T. (2006). Climatology and trends in summer precipitation characteristics in Mongolia for the period 1960-98. *Journal of the Meteorological Society of Japan, 84,* 543-551

Erdenetuya, M., Khishigsuren, P., Gombo, D., Otgontogs, M. (2006). Glacier change estimation using Landsat TM data. *International Archives of the Photogrammetry, Remote Sensing and Spatial Information Science, 36,* Part 6.

Fountain, A. G., Krimmel, R. M., & Trabant, D. C. (1997). A strategy for monitoring glaciers. *U.S. Geological Survey circular 1132.*

Francou, B., Vuille, M., Favier, V., & Caceres, B. (2004). New evidence for an ENSO impact on low-latitude glaciers: Antizana 15, Andes of Ecuador, 0 degrees 28 ' S. *Journal of Geophysical Research-Atmospheres, 109,* 17

Frey, H., & Paul, F. (2012b). On the suitability of the SRTM DEM and ASTER GDEM for the compilation of topographic parameters in glacier inventories. *International Journal of Applied Earth Observation and Geoinformation, 18,* 480-490

Frey, H., Paul, F., & Strozzi, T. (2012a). Compilation of a glacier inventory for the western Himalayas from satellite data: methods, challenges, and results. *Remote Sensing of Environment, 124,* 832-843

Fritz, V. (2007). Democratisation and corruption in Mongolia. *Public Administration and Development, 27,* 191-203

Gao, J., & Liu, Y.S. (2001). Applications of remote sensing, GIS and GPS in glaciology: a review. *Progress in Physical Geography, 25,* 520-540

Gjermundsen, E.F., Mathieu, R., Kääb, A., Chinn, T., Fitzharris, B., & Hagen, J.O. (2011). Assessment of multispectral glacier mapping methods and derivation of glacier area changes, 1978-2002, in the central Southern Alps, New Zealand, from ASTER satellite data, field survey and existing inventory data. *Journal of Glaciology, 57,* 667-683

Global Land Ice Measurements from Space (GLIMS) Program. (2013). www.glims.org (accessed April 19, 2013).

Global Land Ice Measurements from Space (GLIMS) Program (2013). "GLIMS glacier ID generation tool." http://glims.colorado.edu/tools/lonlat2id/ (accessed April 19, 2013).

Granshaw, F.D., & Fountain, A.G. (2007). Glacier change (1958-1998) in the North Cascades National Park Complex, Washington, USA (vol 52, pg 251, 2006). *Journal of Glaciology, 53,* 723-723

Grunert, J., Lehmkuhl, F., & Walther, M. (2000). Paleoclimatic evolution of the Uvs Nuur basin and adjacent areas (Western Mongolia). *Quaternary International, 65-6,* 171-192

Hall, D.K., Foster, J.L., Verbyla, D.L., Klein, A.G., & Benson, C.S. (1998). Assessment of snow-cover mapping accuracy in a variety of vegetation-cover densities in central Alaska. *Remote Sensing of Environment, 66,* 129-137

Haritashya, U.K., Bishop, M.P., Shroder, J.F., Bush, A.B.G., & Bulley, H.N.N. (2009). Space-based assessment of glacier fluctuations in the Wakhan Pamir, Afghanistan. *Climatic Change, 94,* 5-18

Haruyama, Y., Makoto, O., Igarashi, T., Tomyama, N., Yamanokuchi, T., Furuta, R., & Ueno, R. (2008). Technical assistance and capacity building on satellite-based monitoring of ground cover in Andean glacier regions. *The International Archives of the Photogrammetry, Remote Sensing and Spatial Information Sciences, 37, Part 6a,* 101-106.

Hewitt, K. (2005). The Karakoram anomaly? Glacier expansion and the 'elevation effect,' Karakoram Himalaya. *Mountain Research and Development, 25,* 332-340

Hoelzle, M., Chinn, T., Stumm, D., Paul, F., Zemp, M., & Haeberli, W. (2007). The application of glacier inventory data for estimating past climate change effects on mountain glaciers: A comparison between the European Alps and the Southern Alps of New Zealand. *Global and Planetary Change, 56,* 69-82

Hofmann, J., Hurdler, J., Ibisch, R., Schaeffer, M., & Borchardt, D. (2011). Analysis of Recent Nutrient Emission Pathways, Resulting Surface Water Quality and Ecological Impacts under Extreme Continental Climate: The Kharaa River Basin (Mongolia). *International Review of Hydrobiology, 96,* 484-519

Hofmann, J., Venohr, M., Behrendt, H., & Opitz, D. (2010). Integrated water resources management in central Asia: nutrient and heavy metal emissions and their relevance for the Kharaa River Basin, Mongolia. *Water Science and Technology, 62,* 353-363

Honeychurch, W. (2010). Pastoral nomadic voices: a Mongolian archaeology for the future. *World Archaeology, 42,* 405-417

International Centre for Integrated Mountain Development (ICIMOD). (2013). "HKH Glaciers, Frequently Asked Questions." http://www.icimod.org/?q=1179 (accessed April 19, 2013).

IPCC (Intergovernmental Panel on Climate Change). "IPCC Fourth Assessment Report: Climate Change (2007)." http://www.ipcc.ch/publications_and_data/ar4/wg1/en/ch4s4-1.html (accessed March 3, 2012).

Jacoby, G., D'Arrigo, R., Pederson, N., Buckley, B., Dugarjav, C., & Mijiddorj, R. (1999). Temperature and precipitation in Mongolia based on dendroclimatic investigations. *Iawa Journal, 20*, 339-350

Jacoby, G.C., Darrigo, R.D., & Davaajamts, T. (1996). Mongolian tree rings and 20th-century warming. *Science, 273*, 771-773

Jarvis, A., Reuter, H. I., Nelson, A., & Guevara, E. (2008). Hole-filled SRTM for the globe Version 4. Available from the CGIAR-SXI SRTM 90m database. http://srtm.csi.cgiar.org

Kääb, A. (2002). Monitoring high-mountain terrain deformation from repeated air and spaceborne optical data: examples using digital aerial imagery and ASTER data. *Isprs Journal for Photogrammetry and Remote Sensing, Vol 57*, 39-52.

Kääb, A., Paul, F., Maisch, M., Hoelzle, M., & Haeberli, W. (2002). The new remote-sensing-derived Swiss glacier inventory: II. First results. *Annals of Glaciology, Vol 34, 2002, 34*, 362-366

Kadota, T., & Gombo, D. (2007). Recent glacier variations in Mongolia. *Annals of Glaciology, Vol 46, 2007, 46*, 185-188.

Kadota, T., Gombo, D., Kalsan, P., Namgur, D. &, Ohata, T. (2011). Glaciological research in the Mongolian Altai 2003-2009. *Bulletin of Glaciological Research, 29*, 41-50.

Kamp, U., Byrne, M., & Bolch, T. (2011). Glacier fluctuations between 1975 and 2008 in the Greater Himalaya Range of Zanskar, southern Ladakh. *Journal of Mountain Science, 8*, 374-389

Kamp, U., Krumwiede, B., McManigal, K., Pan, C., Walther, M., & Dashtseren, A. (in press). Glaciers of Mongolia. *Arctic, Antarctic, and Alpine Research (INSTAAR)*, Occasional Paper 61.

Kaplonski, C. (2008). Prelude to violence: Show trials and state power in 1930s Mongolia. *American Ethnologist, 35*, 321-337

Kargel, J.S., Abrams, M.J., Bishop, M.P., Bush, A., Hamilton, G., Jiskoot, H., Kääb, A., Kieffer, H.H., Lee, E.M., Paul, F., Rau, F., Raup, B., Shroder, J.F., Soltesz, D., Stainforth, D., Stearns, L., & Wessels, R. (2005). Multispectral imaging contributions to global land ice measurements from space. *Remote Sensing of Environment, 99*, 187-219

Katoh, T., Munkhbat, B., Tounai, K., Mano, S., Ando, H., Oyungerel, G., Chae, G.T., Han, H., Jia, G.J., Tokunaga, K., Munkhtuvshin, N., Tamiya, G., & Inoko, H. (2005). Genetic features of Mongolian ethnic groups revealed by Y-chromosomal analysis. *Gene, 346*, 63-70

Khrutsky, V.S., & Golubeva, E.I. (2008). Dynamics of the glaciers of the Turgen-Kharkhira mountain range (Western Mongolia). *Geography and Natural Resources*, *29*, 278–287.

Klein, A.G., & Isacks, B.L. (1999). Spectral mixture analysis of Landsat thematic mapper images applied to the detection of the transient snowline on tropical Andean glaciers. *Global and Planetary Change, 22*, 139-154

Klinge, M., Böhner, J., & Lehmkuhl, F. (2003). Climate pattern, snow- and timber-line in the Altai Mountains, Central Asia. *Erdkunde, 57*, 296–308.

Krumwiede, B.S., Kamp, U., Leonard, G.J., Dashtseren, A., &Walther, M. (in press). Recent glacier changes in the Altai Mountains, western Mongolia: case studies from Tavan Bogd and Munkh Khairkhan. In: Kargel, J.S., Leonard G.J., Bishop, M.P., Kääb, A., Raup, B. (eds.), *Global Land Ice Measurements from Space.* Praxis-Springer, Heidelberg.

Lamsal, D., Sawagaki, T., & Watanabe, T. (2011). Digital terrain modelling using Corona and ALOS PRISM data to investigate the distal part of Imja Glacier, Khumbu Himal, Nepal. *Journal of Mountain Science, 8*, 390-402

Lehmkuhl, F. (1998). Quaternary glaciations in central and western Mongolia. *Journal of Quaternary Science, 13*, 153-167

Lehmkuhl, F., & Haselein, F. (2000). Quaternary paleoenvironmental change on the Tibetan Plateau and adjacent areas (Western China and Western Mongolia). *Quaternary International, 65-6*, 121-145

Lehmkuhl, F., & Lang, A. (2001). Geomorphological investigations and luminescence dating in the southern part of the Khangay and the Valley of the Gobi Lakes (Central Mongolia). *Journal of Quaternary Science, 16*, 69-87

Li, S.G., Eugster, W., Asanuma, J., Kotani, A., Davaa, G., Oyunbaatar, D., & Sugita, M. (2008). Response of gross ecosystem productivity, light use efficiency, and water use efficiency of Mongolian steppe to seasonal variations in soil moisture. *Journal of Geophysical Research-Biogeosciences, 113*, 13

Lillesand, T.M., Kiefer, R.W., & Chipman, J.W. (2007) Remote Sensing and Image Interpretation (6^{th} ed.). (pp. 61-121). Hoboken: John Wiley & Sons, Inc.

Maroney, R.L. (2005). Conservation of argali Ovis ammon in western Mongolia and the Altai-Sayan. *Biological Conservation, 121*, 231-241

Mearns, R. (2004a). Pastoralism and sustainable livelihoods in Mongolia. *Development and Change, 35*, 105-106

Mearns, R. (2004b). Sustaining livelihoods on Mongolia's pastoral commons: Insights from a participatory poverty assessment. *Development and Change, 35*, 107-139

Menzel, L., Hofmann, J., & Ibisch, R. (2011). Studies of water and mass fluxes to provide a basis for an Integrated Water Resources Management (IWRM) in the catchment of the River Kharaa in Mongolia. *Hydrologie Und Wasserbewirtschaftung, 55*, 88-103

Miyazaki, S., Yasunari, T., & Adyasuren, T. (1999). Abrupt seasonal changes of surface climate observed in Northern Mongolia by an automatic weather station. *Journal of the Meteorological Society of Japan, 77*, 583-593

Moussavi, M.S., Zoej, M.J.V., Vaziri, F., Sahebi, M.R., & Rezaei, Y. (2009). A new glacier inventory of Iran. *Annals of Glaciology, 50*, 93-103

Müller, F., Caflisch, T., & Müller. G. (1977). Instructions for the compilation and assemblage of data for a world glacier inventory. Zürich, IAHS (ICSI)/UNEP/UNESCO. Temporary Technical Secretariat for the World Glacier Inventory, ETH-Zürich.

Myagmarjav, B., & Davaa, G. (eds.), (1999). *Surface Water of Mongolia*. Ulan Bator: Interpress, 345 p.

Natsagdorj, L., Jugder, D., & Chung, Y.S. (2003). Analysis of dust storms observed in Mongolia during 1937-1999. *Atmospheric Environment, 37*, 1401-1411.

Oerlemans, J., Giesen, R.H., & Van den Broeke, M.R. (2009). Retreating alpine glaciers: increased melt rates due to accumulation of dust (Vadret da Morteratsch, Switzerland). *Journal of Glaciology, 55*, 729-736

Ohata, T., Kadota, T., Konya, K., Yabuki, H., & Gombo, D. (2009). Glacier condition and variation studies in the Mongolian part of the Altai Mountains. *EOS Transactions*, 90, Fall Meeting Supplement, Abstract C23A-0484.

Paul, F., Barrand, N.E., Baumann, S., Berthier, E., Bolch, T., Casey, K., Frey, H., Joshi, S.P., Konovalov, V., Le Bris, R., Molg, N., Nosenko, G., Nuth, C., Pope, A., Racoviteanu, A., Rastner, P., Raup, B., Scharrer, K., Steffen, S., & Winsvold, S. (2013). On the accuracy of glacier outlines derived from remote-sensing data. *Annals of Glaciology, 54*, 171-182.

Paul, F., & Andreassen, L.M. (2009). A new glacier inventory for the Svartisen region, Norway, from Landsat ETM plus data: challenges and change assessment. *Journal of Glaciology, 55*, 607-618

Paul, F., Barry, R.G., Cogley, J.G., Frey, H., Haeberli, W., Ohmura, A., Ommanney, C.S.L., Raup, B., Rivera, A., & Zemp, M. (2009). Recommendations for the compilation of glacier inventory data from digital sources. *Annals of Glaciology, 50*, 119-126

Paul, F., Frey, H., & Le Bris, R. (2011). A new glacier inventory for the European Alps from Landsat TM scenes of 2003: challenges and results. *Annals of Glaciology, 52*, 144-152

Paul, F., Huggel, C., & Kääb, A. (2004). Combining satellite multispectral image data and a digital elevation model for mapping debris-covered glaciers. *Remote Sensing of Environment, 89*, 510-518

Paul, F., Kääb, A., & Haeberli, W. (2007). Recent glacier changes in the Alps observed by satellite: Consequences for future monitoring strategies. *Global and Planetary Change, 56*, 111-122

Paul, F., Kääb, A., Maisch, M., Kellenberger, T., & Haeberli, W. (2002). The new remote-sensing-derived swiss glacier inventory: I. Methods. *Annals of Glaciology, Vol 34, 2002, 34*, 355-361

Pratt, D.G., Macmillan, D.C., & Gordon, I.J. (2004). Local community attitudes to wildlife utilisation in the changing economic and social context of Mongolia. *Biodiversity and Conservation, 13*, 591-613

Priess, J.A., Schweitzer, C., Wimmer, F., Batkhishig, O., & Mimler, M. (2011). The consequences of land-use change and water demands in Central Mongolia. *Land Use Policy, 28*, 4-10

Racoviteanu, A.E., Arnaud, Y., Williams, M.W., & Ordonez, J. (2008). Decadal changes in glacier parameters in the Cordillera Blanca, Peru, derived from remote sensing. *Journal of Glaciology, 54*, 499-510

Racoviteanu, A.E., Paul, F., Raup, B., Khalsa, S.J.S., & Armstrong, R. (2009). Challenges and recommendations in mapping of glacier parameters from space: results of the 2008 Global Land Ice Measurements from Space (GLIMS) workshop, Boulder, Colorado, USA. *Annals of Glaciology, 50*, 53-69

Rau, F., Mauz, F., Vogt, S., Khalsa, J. S., and Raup, B. 2005. Illustrated GLIMS glacier classification manual. Glacier classification guidance for the GLIMS inventory. NSIDC, Boulder.

Raup, B., Kääb, A., Kargel, J.S., Bishop, M.P., Hamilton, G., Lee, E., Paul, F., Rau, F.,

Soltesz, D., Khalsa, S.J.S., Beedle, M., & Helm, C. (2007a). Remote sensing and GIS technology in the global land ice measurements from space (GLIMS) project. *Computers & Geosciences, 33*, 104-125

Raup, B., Racoviteanu, A., Khalsa, S.J.S., Helm, C., Armstrong, R., & Arnaud, Y. (2007b). The GLIMS geospatial glacier database: A new tool for studying glacier change. *Global and Planetary Change, 56*, 101-110

Rees, W. G. (2006). Remote Sensing of Snow and Ice. (pp.75-95). Boca Raton: CRC Press.

Reeves, J. (2011). Mongolia's Environmental Security Chinese Unconscious Power and Ulaanbaatar's State Weakness. *Asian Survey, 51*, 453-471

Rossabi, M. (2009). Mongolia: Transmogrification of a Communist Party. *Pacific Affairs, 82*, 231-+

Sarantuya, G. & L. Natsagdorj. "Climate Change Impact and Vulnerability." (paper presented at the meeting on Integration of Climate Change Adaptation into Sustainable Development in Mongolia, Ulaanbaatar, Mongolia, June 17-18, 2010).

Sarikaya, M.A., Bishop, M.P., Shroder, J.F., & Olsenholler, J.A. (2012). Space-based observations of Eastern Hindu Kush glaciers between 1976 and 2007, Afghanistan and Pakistan. *Remote Sensing Letters, 3*, 77-84

Schaller, M., Ehlers, T.A., Blum, J.D., & Kallenberg, M.A. (2009). Quantifying glacial moraine age, denudation, and soil mixing with cosmogenic nuclide depth profiles. *Journal of Geophysical Research-Earth Surface, 114*, 18

Schlutz, F., & Lehmkuhl, F. (2007). Climatic change in the Russian Altai, southern Siberia, based on palynological and geomorphological results, with implications for climatic teleconnections and human history since the middle Holocene. *Vegetation History and Archaeobotany, 16*, 101-118

Shahgedanova, M., Nosenko, G., Khromova, T. & Muraveyev, A. (2010). Glacier shrinkage and climatic change in the Russian Altai from the mid-20th century: An assessment using remote sensing and PRECIS regional climate model. *Journal of Geophysical Research-Atmospheres*, 115, 12

Sidjak, R.W., & Wheate, R.D. (1999). Glacier mapping of the Illecillewaet icefield, British Columbia, Canada, using Landsat TM and digital elevation data. *International Journal of Remote Sensing, 20*, 273-284

Sternberg, T. (2008). Environmental challenges in Mongolia's dryland pastoral landscape. *Journal of Arid Environments, 72*, 1294-1304

Sternberg, T., Middleton, N., & Thomas, D. (2009). Pressurised pastoralism in South Gobi, Mongolia: what is the role of drought? *Transactions of the Institute of British Geographers, 34*, 364-377

Sternberg, T., Thomas, D., & Middleton, N. (2011). Drought dynamics on the Mongolian steppe, 1970-2006. *International Journal of Climatology, 31*, 1823-1830

Stumpp, M., Wesche, K., Retzer, V., & Miehe, G. (2005). Impact of grazing livestock and distance from water sources on soil fertility in southern Mongolia. *Mountain Research and Development, 25*, 244-251

Tsedendamba, L. "Millenium Development Goals-based Comprehensive National Development Strategy of Mongolia (2007-2021) in Context of Climate Change Adaptation." (paper presented at the meeting on Integration of Climate Change Adaptation into Sustainable Development in Mongolia, Ulaanbaatar, Mongolia, June 17-18, 2010).

Tsogoo, B., D. Borchuluun, J. Dorjpure, and D. Sengelmaa. "Technology Transfer Role in Alleviation of Climate Change Impact in Mongolia." (paper presented at the meeting on Integration of Climate Change Adaptation into Sustainable Development in Mongolia, Ulaanbaatar, Mongolia, June 17-18, 2010).

U.S. Embassy. (2013). "U.S. – Chile Monitoring Cooperation." http://chile.usembassy.gov/2012press0831-glacier.html (accessed April 19, 2013).

USGS Landsat Missions. (2013). "Landsat Processing Details." http://landsat.usgs.gov/Landsat_Processing_Details.php. (accessed May 15, 2013).

Viviroli, D., Archer, D.R., Buytaert, W., Fowler, H.J., Greenwood, G.B., Hamlet, A.F., Huang, Y., Koboltschnig, G., Litaor, M.I., Lopez-Moreno, J.I., Lorentz, S., Schadler, B., Schreier, H., Schwaiger, K., Vuille, M., & Woods, R. (2011). Climate change and mountain water resources: overview and recommendations for research, management and policy. *Hydrology and Earth System Sciences, 15*, 471-504

Winkler, S., Chinn, T., Gartner-Roer, I., Nussbaumer, S.U., Zemp, M., & Zumbuhl, F.J. (2010). An introduction to mountain glaciers as climate indicators with spatial and temporal diversity. *Erdkunde, 64*, 97-118

Ykhanbai, H., Bulgan, E., Beket, U., Vernooy, R., & Graham, J. (2004). Reversing grassland degradation and improving herders' livelihoods in the Altai Mountains of Mongolia. *Mountain Research and Development, 24*, 96-100

Zemp, M., Hoelzle, M., & Haeberli, W. (2009). Six decades of glacier mass-balance observations: a review of the worldwide monitoring network. *Annals of Glaciology, 50*, 101-111

9. APPENDIX

Appendix A. Percent Error of Area Determination based on massifs.

Range	Date	Pixels (>.1km^2)	Glacier Area (km^2) (>.1km^2)	A_{er} (>.1km^2)
Buyantiin Uul	2010	1226	4.59	24.04
	2000	2914	10.71	24.48
Dushiin Uul	2010	921	3.23	25.68
	2000	1123	4.22	23.95
Khairt Nuruu	2010	2720	10.33	23.70
	2000	3432	13.40	23.05
Tsengel Khairkhan	2010	3082	9.09	30.52
	2000	3401	12.03	25.44
	1990	3906	12.70	27.68
Hoton	2010	1202	3.48	31.09
	2000	1230	5.32	20.81
	1990	1520	5.53	24.72
Sergali	2010	361	1.48	21.97
	2000	298	1.62	16.54
	1990	472	1.63	25.99
Tavan Bogd	2010	13071	92.98	12.65
	2000	13053	94.02	12.49
	1990	15411	112.56	12.32
Unkur Khairkhan	2010	3086	12.57	22.10
	2000	3057	12.62	21.79
	1990	3657	17.33	18.99
Ikh Turgen	2010	6402	25.94	22.21
	2000	7456	33.20	20.21
Kharkhiraa	2010	5620	30.23	16.73
	2000	6230	35.54	15.78
	1990	8656	54.41	14.32
Turgen	2010	6625	31.77	18.77
	2000	6718	38.70	15.63
	1990	8258	55.39	13.42
Khukh Serkhyn	2010	1695	7.98	19.12
	2000	1463	9.09	14.48
	1990	2872	13.77	18.77
Khrumuni Khairkhan	2010	1477	6.93	19.19
	2000	3206	10.30	28.01
Sairiin	2010	1253	5.67	19.88
	2000	1482	7.54	17.69

	1990	1750	9.00	17.49
Tsambagarav	2010	7997	68.99	10.43
	2000	8611	76.25	10.16
	1990	9644	85.08	10.20
Baatar Khairkhan	2010	466	5.15	8.14
	2000	419	5.87	6.42
Munkh Khairkhan	2010	3824	26.22	13.13
	2000	3760	29.85	11.34
	1990	7212	41.24	15.74
Sutai	2010	1934	11.45	15.20
	2000	2094	13.63	13.82
	1990	2237	13.94	14.44

Appendix B. Percent Error of Area Determination based on sub-regions.

Sub-Region	**Date**	**Pixels (>.1km^2)**	**Glacier Area (km^2) (>.1km^2)**	**A_{er} (>.1km^2)**
Central Interior	2010	7949	27.23	26.27
	2000	10870	40.36	24.24
	1990	NA	NA	NA
Northwest Interior	2010	20028	116.78	15.43
	2000	21202	114.11	16.72
	1990	21060	137.07	13.83
Northern Altai	2010	20659	90.17	20.62
	2000	22252	109.90	18.22

	1990	16914	109.80	13.86
Central Altai	2010	14330	91.16	14.15
	2000	17474	105.47	14.91
	1990	14266	107.85	11.90
Southern Altai	2010	7523	44.17	15.33
	2000	8555	50.61	15.21
	1990	9449	55.18	15.41

Appendix C. Percent Error of Area Determination based on entire Alta Mountains.

Mongolia	Date	Pixels (>.1km^2)	Glacier Area (>.1km^2)	A_{er} (>.1km^2)
Altai	2010	70489	369.52	17.17
	2000	80353	420.46	17.20
	1990	61689.00	409.	13.54

Appendix D. Glacier area and area change from 1990 to 2010 in the Altai Mountains of Mongolia by sub-region.

Region	NW Int	N. Altai	S. Altai	C. Altai	C. Int.	Complete Inv.
Area 1990 (km^2)	142.8	110.53	63.67	111.92	14.18	***443.10***
Area 2000 (km^2)	116.78	110.06	50.87	105.60	45.34	***428.65***
Sub-Section Area 2000 (km^2)	116.783	76.05	44.91	93.89	13.25	***344.88***
Area 2010 (km^2)	114.51	91.11	44.10	91.01	31.60	***372.33***
Sub-Section Area 2010 (km^2)	114.51	63.34	38.94	83.73	10.28	***310.80***
Number of Glaciers (90)	242	114	118	161	57	***692***
Number of Glaciers (00)	164	141	66	126	220	***717***
Sub-Section Number (00)	164	82	64	66	57	***433***
Number of Glaciers (10)	202	138	64	87	181	***672***
Sub-Section Number (10)	202	76	62	68	49	***457***
Mean Size 90 (km^2)	0.59	0.97	0.54	0.7	0.25	***0.61***
Mean Size 00 (km^2)	0.71	0.79	0.77	0.84	0.21	***0.66***
Sub-Section Mean 00 (km^2)	0.71	0.93	0.70	1.42	0.23	***0.80***
Mean Size 10 (km^2)	0.57	0.66	0.69	1.06	0.18	***0.63***
Sub-Section Mean 10 (km^2)	0.57	0.83	0.63	1.23	0.21	***0.69***
Area Change 90-10 (km^2)	-2.27	-46.72	-11.93	-21.87	-35.06	**-117.85**
Annual Change 90-10 (km^2)	-0.11	-2.34	-0.60	-1.09	-1.75	**-5.89**

Appendix E.

Anisotropic correction in Landsat TM-based mapping of glaciers in the Altai Mountains of Mongolia

CALEB G. PAN*†, ULRICH KAMP†, and JEFF D. COLBY‡

†Department of Geography, The University of Montana, Missoula, MT 59802, U.S.A.

‡Department of Geography and Planning, Appalachian State University, Boone, NC 28607, U.S.A.

Abstract. Anisotropic reflectance has hindered the validity of remote sensing derived data since the 1970s, specifically in high mountain areas due to extreme and variable topography. However, satellite data have been beneficial to studying alpine ecosystems and alpine landforms, glaciers in particular. To improve satellite derived base data and glacier mapping results, multiple anisotropic reflectance correction (ARC) methods have been developed. In this study we tested ARC methods including Cosine and Minnaert corrections in mapping glaciers in the Altai Mountains of Mongolia using Landsat TM imagery. Using multiple diagnostics to quantify an increase or decrease in anisotropy - including linear regression, improvements in glacier mapping error, and semivariograms we conclude that the Minneart correction was most effective. We also recognized that anisotropic reflectance is spatially variable and scale-dependent. Using Landsat TM data, ARC correction methods are more effective when mapping large glaciers versus small glaciers. We suggest using imagery acquired from a sensor platform with a higher spatial resolution when applying ARC methods to map glaciers smaller than 0.125 km^2.

1.Introduction

Since the launch of the Landsat Multi-Spectral Scanner (MSS) in 1972, scientists have been using satellite imagery from various platforms to intensely study cryospheric and geomorphic earth processes. Earth Observing Systems (EOS) allow the collection of land cover data from anywhere in the world including some of the most inaccessible regions, specifically high mountain areas.

Previous glacier mapping attempts in the Altai Mountains by separate author groups did not mention their data source, method, date of acquisition, glaciated extent,

and glacier definition. Therefore, the number and area of glaciers in the region are highly conflicting and inconsistent. Only recently has the first complete inventory of the Mongolian glaciers been compiled by Kamp and Pan (in prep) however it has not yet been made available to the public through the Global Land Ice Measurements from Space (GLIMS) website (Kamp *et al.* 2013).

The use of remote sensing in high mountain environments is heavily influenced by variations in irradiant and radiant flux caused by the atmosphere, topography, and land cover. There have been multiple anisotropic correction (ARC) methods developed to reduce the influence of topography in imagery. However no one method has proven as a suitable best method (Bishop and Colby 2002). Most existing glacier inventories such as the international program Global Land Ice Measurements from Space (GLIMS) do not include any anisotropic correction in their glacier mapping protocols

In this study we evaluate the Cosine and Minnaert corrections for ARC of Landsat TM satellite imagery for the Turgen Range and Munkh Khairkhan Range in the Altai Mountains of Mongolia. While the Turgen Range shows complex topography, the Munkh Khairkhan Range has more homogenous topography. We applied ARC methods in the analysis of Landsat images of the Turgen-Kharkhiraa Range from between 1992 and 2010 and of the Munkh Khairkhan Range from between 1991 and 2010.

2. Study Area

Mongolia is an upland country with an average altitude of 1580 m and 85% of the country is located above 1000 m (Gilberg *et al.* 1996, Stumpp *et al.* 2005, and Batima 2006). There are four mountain ranges within Mongolia including the Khan-Khokhii Mountains, Khanghai Mountains, Khentii Mountains, and the Altai Mountains. Only the Altai Mountains – home to Hüiten Peak at 4653 m is the highest peak of Mongolia – are supporting glaciers.

Glaciers in Mongolia can be found between 46°25' and 50°50'N and between 87°40' and 100°50'E in elevations above 2750 m with mean annual air temperature of -8°C (Davaa *et al*. 2007). Mongolian glaciers can be divided into three types: 75% mountain slope glaciers, 21 % valley glaciers, and 4% flat top glaciers (WWF 2004). Dashdeleg *et al.* (1983) put the total number of glaciers in Mongolia at 262 with a total area of 659 km^2. The total water resources accumulated in glaciers is approximately 62.6 km^2 (Davaa *et al.* 2007). Baast (1998) showed that from 1945 to 1985 the total glacier area decreased by 6%. Kadota and Gombo (2007) inventoried 91 glaciers in the Mongolian Altai (figure 1) and found that they lost between 10-30% of their surface area since the 20th century. The variation in glacier retreat is credited to the high spatial variability between individual glaciers.

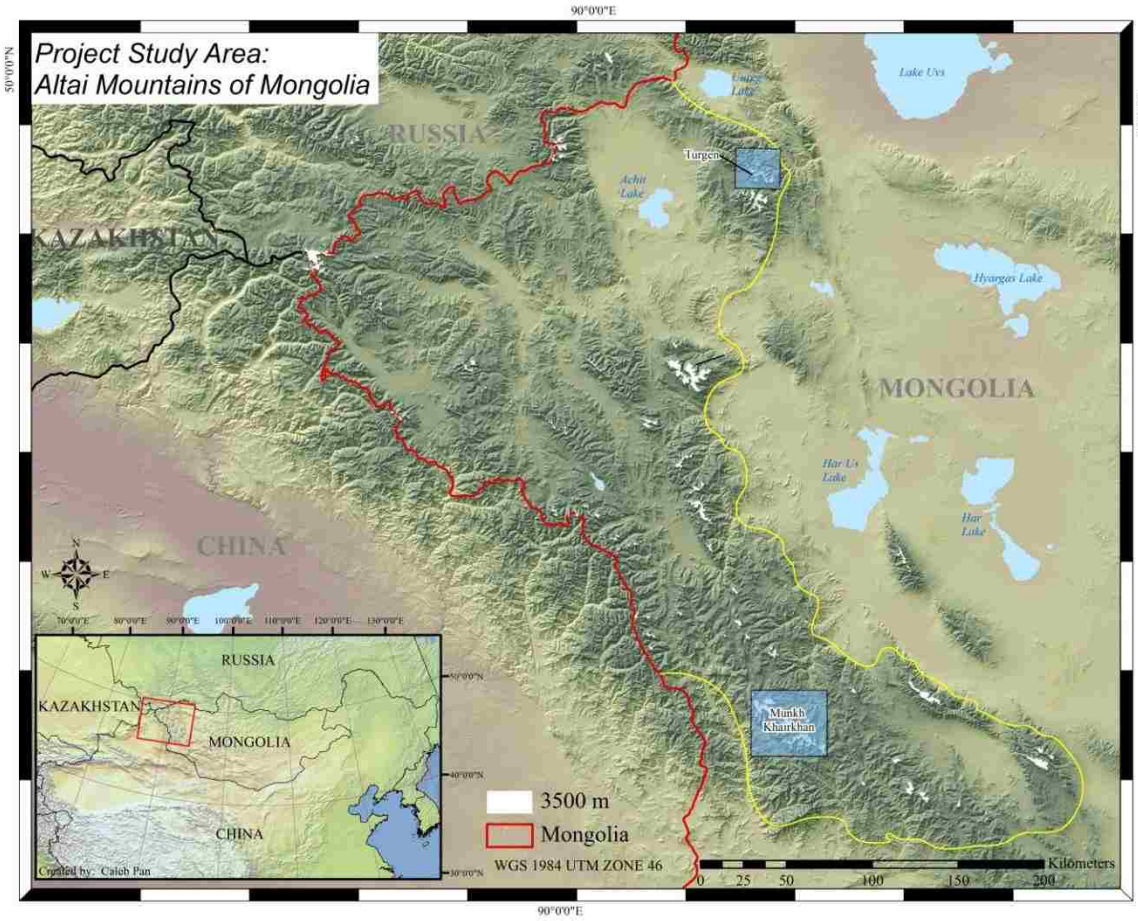

Figure 1. Map of the Altai Mountains of Mongolia. The study sites are indicated by rectangular boxes.

2.1 Turgen Mountains

The Turgen-Kharkhiraa Mountains (49–50ºN, 91–92ºE) in the northern part of the Altai Mountains represent a system of two neighbouring mountain systems that formed during the Variscan orogeny. They extend over approximately 20 km along a northwestern direction from Lake Khara-Us Nuur to the Mongun-Taiga mountain group. In the west the mountains border the Achit Nuur-Ureg Nuur systems of hollows, in the east the Great Lakes depression. During an intense tectonic uplift that continued throughout the Quaternary, the mountains were mainly shaped by glacial and fluvial erosion (Khrutsky and Golubeva, 2008). Turgen Nuruu (with a peak between 3954 and 3978 m depending on the source) and Kharkhiraa Uul (with a peak between 4037 and 4040 m depending on the source) are the highest peaks (Lehmkuhl, 1999; Khrutsky and Golubeva, 2008). The general morphology of the entire mountain system makes for relatively high ablation rates on southern and western slopes, and for relatively low ablation rates on northern and eastern slopes. Janson (2010) identified 82 % of all glaciers in the Turgen Mountains as being of valley glacier type.

Probably because of location and ease of access, the Quaternary glaciations and modern glaciers in the Turgen-Kharkhiraa Mountains are relatively well studied. One of

the most detailed such study is from Khrutsky and Golubeva (2008) who stated that these mountains represent a significant glacier center in the Altai Mountains that is not exceeded in area by any other glacial basin (Tsast-Ula, Munkh Khairkhan, and Delyun ranges).

2.2 Munkh Khairkhan Mountains

For the Munkh Khairkhan Mountains in the central Mongolian Altai, Klinge (2001) showed that the glaciated area was 25.2 km^2 in the 1980s/90s and described that mostly individual plateau glaciers, like the one at Munkh Khairkhan summit (4204 m), and snowfields were common, while cirque glaciers were rare and only three valley glaciers existed.

In the last decades, the glaciers in the Munkh Khairkhan Mountains were in general trend of recession. Krumwiede and others (in press) showed that from 1990–2006 the glacial area decreased by 30% from 40 to 28 km^2 and almost all of the glaciers receded by 20–80 m at a rate of 1.3–5 m per year; only Khar Tsunkh Glacier increased in area by 6%. However, the authors pointed out that this recession must have occurred somewhere between 1990 and 2000, because for the entire next decade from 2000–2010 the glaciers remained in a phase of stagnation.

3. Methodology

3.1 Data

Elevation data were utilized from the Shuttle Radar Topography Mission 3 (SRTM3) and were downloaded from the Consortium for Spatial Information – Consultative Group for International Agricultural Research (CSI-CGIAR). SRTM 3 data have a spatial resolution of 90 m and need to be resampled to 30 m in order to be comparable to 30 m Landsat TM data. Bishop *et al.* (2008) found that SRTM3 data are greatly affected by shadows caused by high topographic relief and that the lack of repeat coverage presents problems of DEM quality. If necessary, ASTER Global Digital Elevation Model (GDEM) data are also available and they come at finer spatial resolution of 30 m.

Four Landsat TM scenes (see table 1) were acquired using the USGS Global Visualization Viewer; the Level 1 product provides geometric and radiometric corrections. All four Landsat TM scenes were sub-sectioned to each specific mountain region. Both sub-sections were representative of the topography and land cover.

Table 1. Utilized Landsat TM scenes.

Range	Entity ID	Date	Row	Path	Sensor	CLCV
Turgen	LT41410251992177XXX02	06/25/92	25	141	TM5	0
	LT51420252010241IKR00	08/29/10	25	147	TM5	11
Munkh Khairkhan	LT51410271991198XXX03	07/17/91	27	141	TM5	0
	LT51400272011246IKR00	09/03/11	27	140	TM5	0

3.2 Lambertian and Non-Lambertian models

A Lambertian surface is presumed to be a perfectly diffuse reflector, which means that reflectance is equal in all directions (isotropic surface). Colby and Keating (1998) used an example of a piece of white paper to explain a Lambertian surface. As a piece of white matte paper is illuminated by diffuse skylight, the perceived brightness of the paper does not change in any direction. The recorded radiance in a Lambertian model is assumed to be proportional to the cosine of the incidence angle. The incidence angle (*i*) is the angle between the surface normal and the solar beam (Ekstrand 1996). The cos(*i*) can be calculated by:

$$\cos(i) = \cos e \cos z + \sin e \sin z \cos(\phi_s - \phi_n) \qquad \text{equation (1)}$$

where e = surface normal zenith angle or terrain slope
z = solar zenith angle
ϕ_s = solar azimuth angle
ϕ_n = surface aspect of the slope angle

Once the cos(*i*) is calculated, it can be used in the Lambertian cosine correction model:

$$Ln = \frac{L}{cosi} \qquad \text{equation (2)}$$

where Ln = the normal response or cosine corrected radiance values
L = band radiance

To simplify and reduce computation time, surfaces are often assumed to be Lambertian. The results of the Lambertian model using the cosine correction (equation (2)) show that the spectral variation is reduced when applied. However, multiple author groups note that the Lambertian model consistently over corrects in steep slopes, which Bishop *et al.* (2000) identified as causing problems when mapping alpine glaciers. Colby and Keating (1998) discussed that the Lambertian model may only be valid for a restricted range of incident and exitant angles.
Yet, with the downsides of the Lambertian model, the Cosine-correction has proven to be useful in regions with high solar elevation angles and low slope angles (Ekstrand 1996 and Bishop *et al.* 2000).

For a more realistic representation of the of the earth's surface, remote sensing scientists often implement a non-Lambertian model assumption. Ekstrand (1996) described that the most common way to account for non-Lambertian behavior of vegetation is to employ a Minnaert constant (*k*). The *k* constant describes the bidirectional reflection distribution function (BRDF) and is related to surface roughness (Colby 1991; Colby and Keating 1998). The BRDF is described by the following equation (Colby 1991):

$$L(n,\lambda) = \frac{L\lambda \cos e}{(\cos \hat{}\, k(i) \cos \hat{}\, k(e))} \qquad \text{equation (3)}$$

where L = radiance,
λ = wavelength
e = exitance angle = slope
Ln = radiance when $i = e = 0$
k = Minnaert constant

Before implementing equation (3), the k constant must be first calculated for each spectral band by linearizing the following equation (Colby 1991 and Ekstrand 1996):

$$\log (L \cos e) = \log Ln + k \log (\cos i \cos e) \qquad \text{equation (4)}$$

where $y = \log (L \cos e)$ response variable
$x = \log (\cos i \cos e)$ independent variable
$b = \log Ln$

By using the x and y variables in a linear regression, the k constant is equal to the slope of the regression line. Once the slope is determined (k) the value can be input into equation (3) and a BRDF model can be created.

Bishop *et al.* (2003) described the k constant as ranging from zero to one. The value of k describes the surface's departure of reflectance from a Lambertian surface. For example, a k value of 1 indicates a Lambertian surface. As the k value approaches 0, the degree of anisotropy is indicated.

This study created a globally computed k value for each sub-sectioned scene (see table 1). Some author groups (Bishop *et al.* 2003) created k values for each specific land cover. Land cover specific k values are important when examining large regions with heterogeneous land covers. In the case of the Altai Mountains of Mongolia, the land cover is relatively homogenous. The land cover transitions from grasslands, to talus slopes, and ends with glacier/snow cover (figure 2). As mentioned in the Introduction, spatial variation in topography and land cover will cause k values to vary spatially. However, Bishop *et al.* (2003) goes on to discuss that there have been many author groups who have implemented a globally computed k and were successful in reducing the topographic effect in satellite imagery.

The determined methodology for the GLIMS Mongolian Glacier Inventory is to use a NIR/SWIR band ratio with a threshold of 2. Therefore, results and analysis will only be performed for NIR and SWIR wavelengths. The outcome will be a more clear understanding of the effect of topography on the produced glacier outlines using the proposed band ratio.

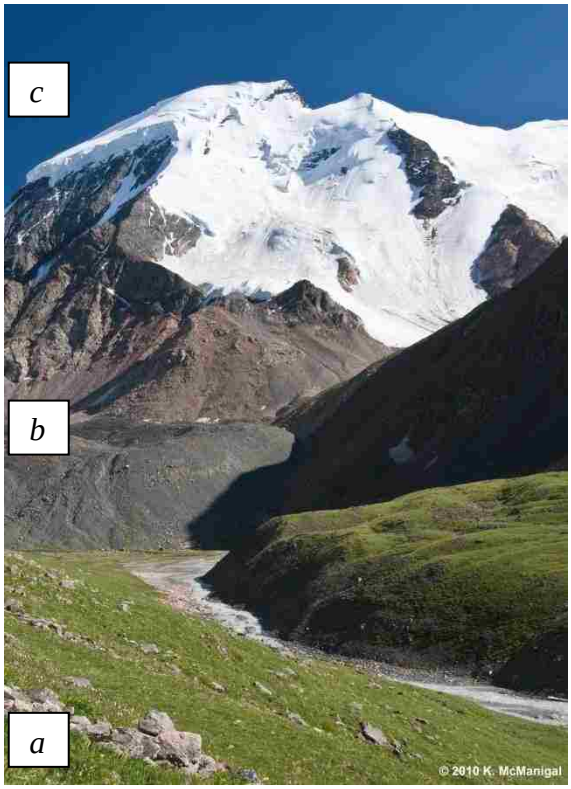

Figure 2. Turgen Range in the Altai Mountains portrays the altitudinal zonation from grasslands (*a*) to scree/talus slopes (*b*) and to glacier (*c*). Photo by Kevin McManigal

3.3 Image preprocessing

Before cosine correction and BRDF models can be created, all Landsat TM bands must be converted from Digital Numbers (DN) to radiance values. Following the Landsat-5 TM Radiometric Calibration Procedures by Chander and Markham (2003) the following equation was used:

$$L_\lambda = \left(\frac{LMAX_\lambda - LMIN_\lambda}{Q_{calmax}}\right) * Q_{cal} + LMIN_\lambda \quad \text{equation (5)}$$

where Q_{calmax} = max quantized calibrated pixel value corresponding to $LMAX_\lambda$
$LMIN_\lambda$ = spectral radiance that is scaled to Q_{calmin}
$LMAX_\lambda$ = spectral radiance that is scaled to Q_{calmax}

After the spectral bands were converted to radiance values, all images needed to be clipped to sub-sectioned study areas. By performing analysis on sub-sections rather the entire scenes, the computation time and processing was greatly reduced. And since glaciers only covered a small percentage of an entire Landsat TM scene, it was important to use sub-sectioned scenes where glacier was the dominant land cover. Focusing on glacier land cover in our sub-sectioned scenes, our Cosine and Minnaert corrections were stronger representations of the influence topography has when mapping glacier land cover. Munkh Khairkhan was clipped to 11 km X 6.5 km areas and the Turgen study

region was clipped to 10 km X 5 km areas. The extents of the study areas are a strong representation of the greater massif region's topography and land cover (figures 3 and 4).

The SRTM3 data also needed to be sub-sectioned to the same extents as the Munkh Khairkhan and Turgen extents so aspect and slope data could be derived for later use in the derivation of cos(*i*) (equation (1)). Other studies used SRTM3 data for topographic normalization by resampling their 90m DEM to 30m in order to equal the Landsat TM resolution. However, the Lambertian Reflectance Model within ERDAS Imagine 2011natively resamples the 90 m SRTM3 DEM.

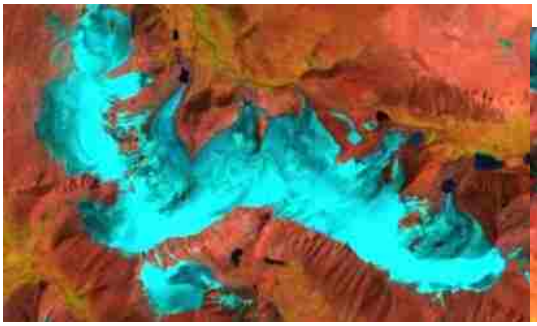

Figure 3. Munkh Khairkhan sub-section.

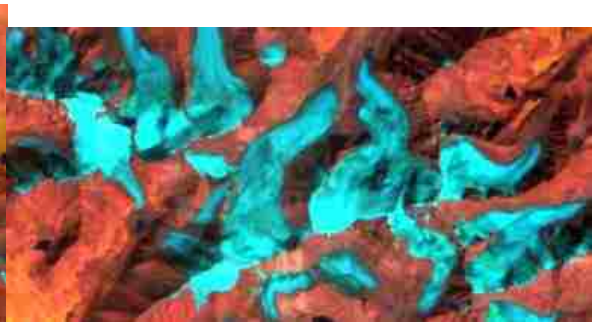

Figure 4. Turgen sub-section. (1:100,000)

3.4 Topographic normalization

The first images were processed based on a Lambertian assumption using equation (2) A native Lambertian Reflectance Model was used inside ERDAS Imagine 2011, requiring four input data sources. These data included the sub-sectioned spectral bands, converted to radiance values, sub-sectioned SRTM3 DEM, solar azimuth and the solar elevation angle. The solar azimuth and solar elevation angles are located within the Landsat TM imagery metadata and are important for denoting the spatial relationship between the satellite and the earth's surface. By using the Lambertian Reflectance Model, Lambertian corrected images were performed for all spectral bands for each study area and time period.

Due to the tendency of the cosine correction to overcorrect spectral images, a conditional statement was created to replace any pixel values greater than 255 with a value of 255. Figure 5 (*a*) is a sub-section of Munkh Khairkhan NIR band after a cosine correction. Figure 5 (*b*) is the same image with the conditional statement applied. The conditional statement allows for more visual interpretation between land cover features.

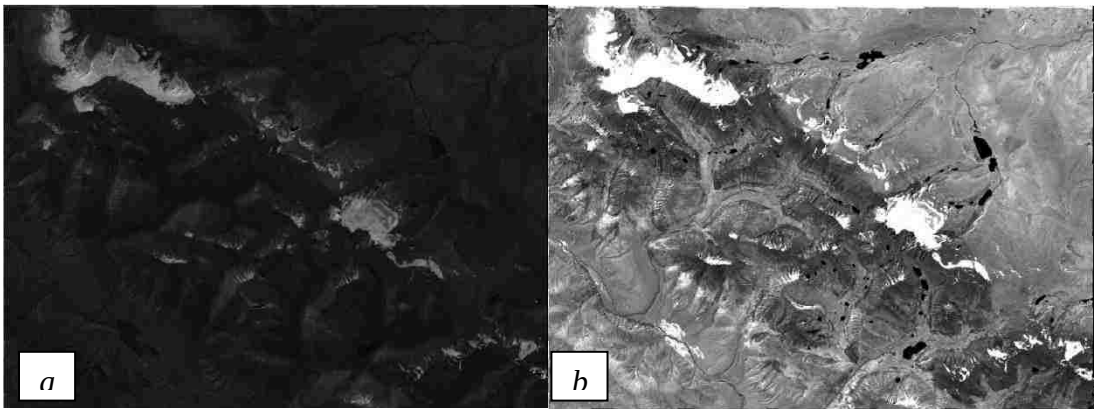

Figure 5. (*a*)NIR band with pixel values >255. (*b*) NIR band with pixel values not exceeding 255.

The non-Lambertian model requires the creation of sub-sectioned raster datasets and map algebra unlike the Lambertian model. First cos(*i*) and cos(*e*) datasets needed to be derived (equation (1)). The next step was to utilize Raster Calculator within ESRI ArcMap and multiply cos(*i*) by cos(*e*) to create a new raster dataset which would result in the *x* variable. To derive the *y* variable the radiance of the specific spectral band was multiplied by cos(*i*). The logarithms of both the *x* and *y* variables were derived in the final datasets of each and were exported to IDRISI Selva for regression analysis.

Once the new variables were imported to IDRISI the REGRESS module calculated a linear regression between the independent and dependent variables. The linear regression is important because the slope of the regression line equals the *k* constant. Linear regressions were performed for each spectral band and recorded (see table 2). The *k* values were then input into Equation 3 using Raster Calculator within ArcMap and non-Lambertian models for each spectral band and study site were created.

Table 2. Globally computed *k* values.

	Munk:07171991	Munk:09032011	Turgen:06251992	Turgen:08292010
Band	*k*	*k*	*k*	*k*
1	0.057	0.32	0.21	0.18
2	1.21	0.06	0.65	0.298
3	0.92	0.4	0.51	0.33
4	0.36	0.35	0.45	0.45
5	1.44	1.24	0.9	0.76
7	1.39	1.23	0.86	na

Semivariograms were created to analyze the variance between pixel values for non-normalized and normalized NIR and SWIR bands using the GSTAT package within R. To create semivariograms using GSTAT, the sub-sectioned normalized and non-normalized images needed to first be converted from raster data to point data. By converting the images to points, locations could be attributed to each respected reflectance value. The attribute table was then exported as a Text file and imported into R. Bishop and Colby (2002) described effective ARC methods should result in a reduced

spectral variation at lag distances where topography increases spectral variability, and greater spectral variation at lag distances associated with land cover variation.

3.5Image classification

To evaluate the topographic influence on glacier mapping, all four sub-sectioned scenes were classified; this included non-normalized and normalized scenes. The best classification method was a Max-Likelihood classification using the Image Analysis toolbar inside ESRI ArcMap. A band ratio method was considered however, determining equivalent thresholds between correction methods proved to be problematic. Training sites were created based on a glacier or non-glacier land cover classification scheme. Training sites were also derived from each normalized and non-normalized 5-4-3 Landsat TM composite.

4. Results

Bishop *et al.* (2000) describe the spectral variation of glaciers is determined by variables such as; ice structure, glacier topography, debris loads, and ice-surface velocities. Considering the aforementioned factors in glacier mapping, upon visual inspection of LandsatTM images, the Minnaert correction produced the best results (figure 6.)

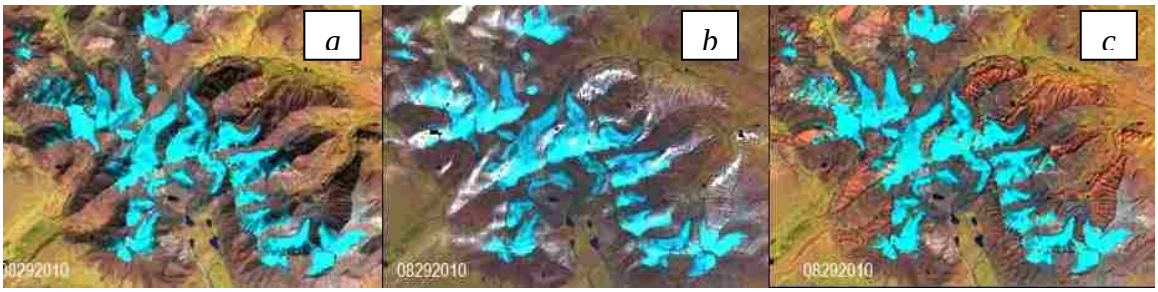

Figure 6. (*a*)Non-normalized Turgen Composite. (*b*) Cosine corrected Turgen Composite. (*c*) Minnaert corrected Turgen Composite.

Figure 6 depicts the influence of topography in (*a*), evidenced by the shadows found on the north facing slopes. By assuming the Lambertian surface (*b)*, recognized the topographic influences however overcorrected the shadowed values in (*a*) with too bright of radiance values. Like image (*b*), (*c*) also recognized the shadow slopes and corrected the north facing slopes without overcorrecting the values. For this reason, through visual interpretation, Minnaert correction was the most effective for both study areas and time periods.

Statistical analysis of the application of ARC methods to NIR and SWIR bands on Turgen and Munkh Khairkhan massif provide no evidence of a reduction of topographic influence in Landsat TM imagery. Cosine correction consistently provided higher spectral variation in both study areas, spectral bands, and time periods. Even with a

conditional statement to reduce the pixel values to no greater than 255, extreme variation persisted (figure 7). Based on semivariograms, except for few instances, Minnaert correction consistently produced results with slightly higher spectral variation compared to non-normalized images. These results are not in line with other studies that implemented a Minnaert correction (Colby 1991 and Colby and Keating 1998). However in Bishop *et al.* (2003), the group found that a globally computed *k* did not characterize the relationship between topography, land surface cover, and surface radiance.

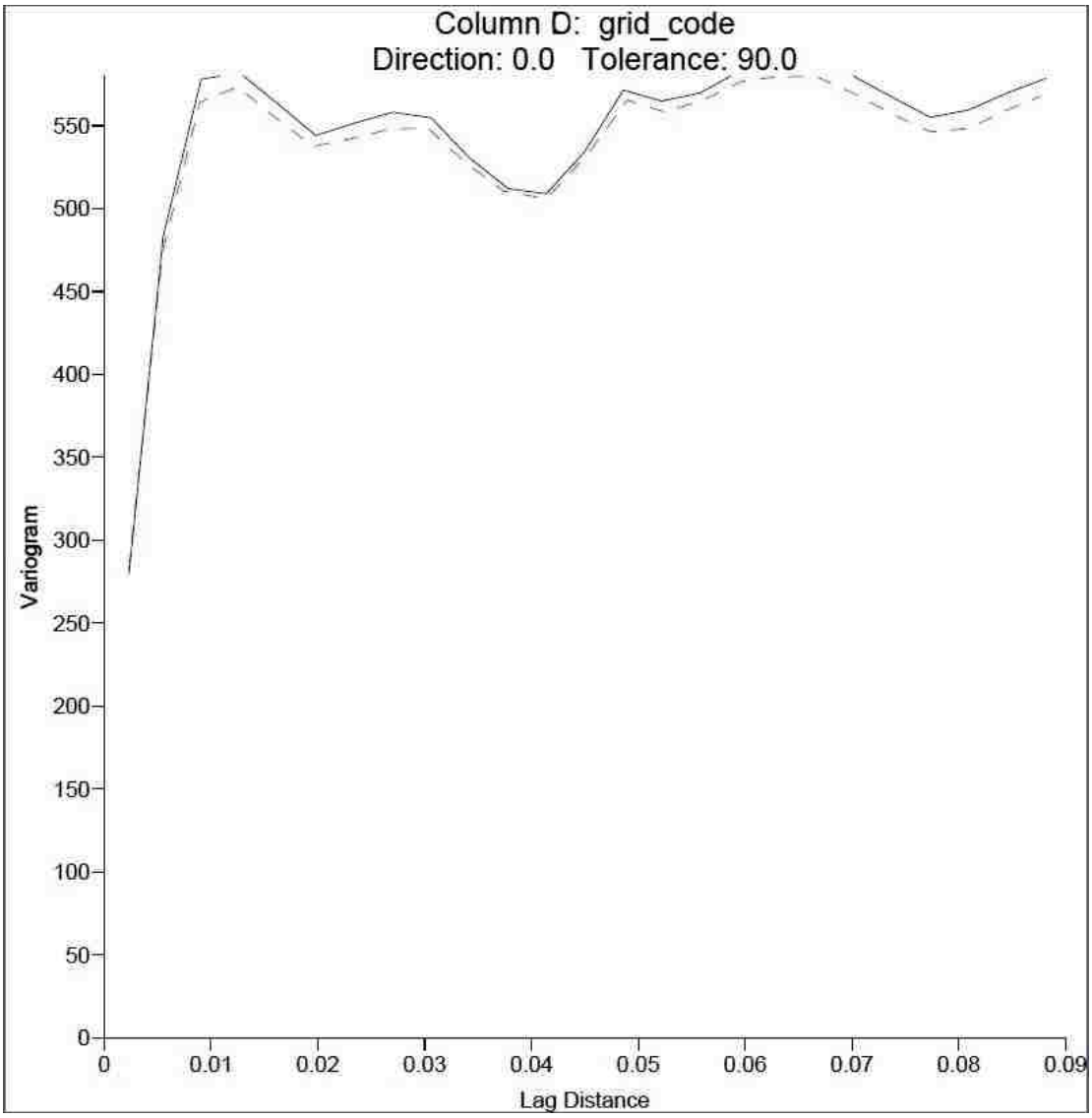

Figure 7. Turgen (2010) NIR semivariogram. Minnaert correction is in black and the non-normalized radiance is in the dotted red-line.

Using the REGRESS module within IDRISI Selva, r^2 values were also calculated between the cos(*i*) and reflectance values. The r^2 values between the tested variables represent a weak or strong correlation. If the r^2 values are reduced from the non-

normalized values than topographic influence is reduced. Tables 3 - 6 demonstrate that in all circumstances r^2 values have been dramatically reduced once an ARC method was applied. The exception is the Cosine corrected NIR band where r^2 values severely increased. Even though semivariograms quantify conflicting results, based on visual interpretation and r^2 values, the Minnaert constant using a globally computed *k* value is the most effective at reducing the influence of topography.

Table 3. r^2 Turgen Massif: 06251992

	NonNorm	Cosine	Minnaert
Band1	0.6	NA	0.06
Band2	1.29	9.37	1.46
Band3	6.54	3.55	0.43
Band4	3.35	13.07	0.21
Band5	23.25	0.29	0.04
Band7	23.93	0.87	0.02

Table 4. r^2 Turgen Massif: 08292010

	NonNorm	Cosine	Minnaert
Band1	0.94	42.46	0.09
Band2	1.29	9.37	0.19
Band3	3.02	32.13	0.23
Band4	9.9	34.33	0.48
Band5	39.8	0.9	0.04
Band7	NA	NA	NA

Table 5. r^2 Munkh Khairkhan: 07171991

	NonNorm	Cosine	Minnaert
Band1	0.15	11.1	0.29
Band2	26.62	5.67	2.91
Band3	11.8	0.38	0.8
Band4	0.38	6.41	0.21
Band5	12.99	0.63	0.53
Band7	11.69	0.26	0.72

Table 6. r^2 Munkh Khairkhan:09032011

	NonNorm	Cosine	Minnaert
Band1	0.91	10.49	0.05
Band2	0.88	21.65	1.43
Band3	0.48	19.65	4.69
Band4	0.18	18.07	1.55
Band5	28.92	0.62	0.55
Band7	29.4	0.37	0.78

4.1 Glacier mapping comparison

To test the effectiveness of ARC methods, Colby and Keating (1998) performed supervised land cover classifications and compared decreases or improvements in overall land cover accuracy. In their study, the implementation of a Minnaert correction improved the accuracy of the overall land cover classification by almost 5%.

This study compared the effectiveness of ARC methods based on variations in output glacier land cover area. The results (see tables 7 - 8) show that the Cosine correction method consistently mapped larger glacier areas compared to Minnaert correction and non-Normalized. This is due to the tendency of the Cosine correction method to overcorrect with higher pixel values on north facing slopes. High pixel values are often associated with glacier land cover and therefore, over-exposed slopes were mapped as glaciers leading to higher glacier land cover areas.

Table 7. Turgen Massif: Glacier area using a Max Likelihood classification.

Date	*6251992*	*8292010*	
Method	**Area (km^2)**	**Area (km^2)**	**Percent Change**
Non Normalized	59.19	33.28	56.23
Lambertian	64.6	33.56	51.95
Non-Lambertian	62.4	33.29	53.35

Table 8. Munkh Kharikhan: Glacier area using a Max Likelihood classification

Date	*7171991*	*9032011*	
Method	**Area (km^2)**	**Area (km^2)**	**Percent Change**
Non Normalized	44.88	28.29	63.03
Lambertian	47.69	28.15	59.03
Non-Lambertian	45.18	28.79	63.72

Overall, glacier mapping inconsistencies are most prevalent in the early scenes in both Turgen and Munkh Khairkhan. Glacier areas range from 59.19 km^2 to 64.69 km^2 in Turgen and 44.88 km^2 to 47.69 km^2 in Munkh Khairkhan. The Minnaert corrected areas consistently produced results in between the non-Normalized and Cosine corrected areas, in the early years. When results in the recent images were compared (2010 and 2011), there was little change between areas produced from different methods. The Turgen areas ranged from 33.28 km^2 to 33.56 km^2 and Munkh Khairkhan produced glacier areas ranging from 28.15 km^2 to 28.79 km^2. The glacier area differences in the recent years are quite negligible and too narrow to place any preference for one particular ARC method.

A percentage error of area determination, A_{er}, was also calculated based on the glacier land cover mapping. A_{er} is calculated from the following equation:

$$A_{er} = 100\% \cdot (n \cdot m)/A_{gl} \qquad \text{equation (6)}$$

where: n = number of pixels defining the perimeter of the glacier area
m = pixel resolution (e.g., 900 m^2 for a 30 x 30 m TM pixel)
A_{gl} = glacier area

The percent error of area determination was more consistent between correction methods than glacier mapping area during the earlier scenes for both Turgen and Munkh Khairkhan (see tables 10 - 12). Only when mapping glaciers in the 1991 Munkh Khairkhan scene did any correction method perform better than others by greater than 1%. Both the glacier area results and percent error results demonstrate strong consistencies using a Max-Likelihood supervised classification scheme within non-normalized and normalized scenes. However, it has been documented that small glaciers will disproportionally increase percent error calculations (Krumwiede *et al.* in press). Therefore these results demonstrate that ARC methods are more effective at improving mapping of land cover that is in excess of at least 0.1 km^2. When mapping land cover objects that are between 0.01 km^2 and 0.1 km^2, the correction methods are not effective.

Table 9. Munkh Khairkhan 1991: Percent Error of Area Determination

Correction Method	Pixel Number	Glacier Area (m^2)	Aer
Non Normalized	11017	44881866.79	22.09
Cosine	13701	47695977.60	25.85
Minnaert	12317	45183705.20	24.53

Table 10. Munkh Khairkhan 2011: Percent Error of Area Determination

Correction Method	Pixel Number	Glacier Area (m^2)	Aer
Non Normalized	4875	28298028.84	15.50
Cosine	5057	28146513.64	16.17
Minnaert	5062	28792311.66	15.82

Table 11. Turgen 1992: Percent Error of Area Determination

Correction Method	Pixel Number	Glacier Area (m^2)	Aer
Non Normalized	15478	59164263.21	23.54
Cosine	16655	64601598.48	23.20
Minnaert	16773	62401222.77	24.19

Table 12. Turgen 2010: Percent Error of Area Determination

Correction Method	Pixel Number	Glacier Area (m^2)	Aer
Non Normalized	7400	33279739.78	20.01
Cosine	7851	33562969.67	21.05
Minnaert	7268	33294348.93	19.65

5. Discussion

Based on the presented evidence collected from visual interpretation, r^2 values, and glacier mapping, the Minnaert corrected images produced the best results pertaining to glacier mapping in both study sites. However, there are no conclusive results that demonstrate the retreat Mongolian glaciers decreased or increased the influence of topography on spectral signatures. The results produced from the semivariograms consistently quantified high spectral variance between Cosine correction and the other methods. Yet, the semivariance was consistently higher for Minnaert corrected spectral bands at the same lag distance when compared to non-Normalized images. Before any conclusions can be drawn from the created semivariograms, further research needs to be conducted to determine the best lag distance at which to observe spectral variance.

Even though this study successfully quantified the influence of topography in Landsat TM scenes through multiple measurement techniques, no ARC method will be applied when mapping Mongolian glaciers for the GLIMS inventory. Currently, there is no documented methodology that implements either a Cosine or Minnaert correction within the GLIMS Program. The reason for the lack of ARC methods is the majority of GLIMS contributors implement a band ratio classification scheme (Bolch *et al.* 2009 and Paul *et al.* 2009). Band ratios have been noted as being a common method for minimizing differences in brightness values from similar surface materials due to topographic conditions (Colby 1991). The use of a band ratio is far more intuitive than an ARC method. As this research has presented, within the Altai Mountains of Mongolia, the difference between glacier mapping results before and after ARC methods are applied is not significant.

Unlike the Himalayas, Andes, and Alaskan Range where massive glaciers develop at high altitudes and flow downwards, the nature of glacier types are important when considering the effectiveness of ARC methods. As of 2011, glaciers in Mongolia only cover an area of ~375 km^2 and over 70% of the total number of glaciers is smaller than 0.125 km^2 (Pan *et al.* in prep). The issue of scale is why ARC methods do not clearly improve glacier mapping accuracies and this is reflected in the A_{er} results. If the glacier area and individual glaciers were larger, the A_{er} would have improved more than 1% when an ARC is applied. With the current state of glaciers in the Altai Mountains as they are today, ARC methods would be more effective when using a platform with a smaller pixel resolution then Landsat TM. This research has also supported that the influence of topography on outgoing radiance is spatially variable. This translates into spatially specific *k* constants for each of the eighteen glaciated regions within the Altai. To perform ARC methods, this project in particular involved four separate software packages and program coding knowledge. To incorporate ARC methods into the Mongolian Glacier Inventory would not be feasible. The main methodology objective is

to retain an intuitive nature and affordability. If ARC methods are incorporated into the methodology it will no longer be cheap or intuitive.

6. Conclusion

Scientists have been working to discover a definitive solution to anisotropic reflectance for over thirty years now. There are methods such as the Cosine correction and Minnaert correction that have been proven to be successful, yet are still hampered by inconsistencies. This paper was the first to test ARC methods at study sites within the Altai Mountains of Mongolia. The ARC methods were applied over a time period spanning twenty years. Within this research it was proven that the Minnaert correction was most effective at both study sites, over both time periods, and when applied to both NIR and SWIR spectral bands. However, based on percent error and glacier area calculations, results between correction methods were minor. This study also demonstrated the issues of scale when performing ARC methods in relation to land cover phenomena and sensor spatial resolution. Currently, there is no automated method to apply a Minnaert correction, therefore it will not be implemented in the Mongolian Glacier Inventory.

References

BOLCH, T., MENOUNOS, B., and WHEATE, R., 2010, Landsat-based inventory of glaciers in western Canada, 1985-2005. *Remote Sensing of Environment,* **114**, pp. 127-137.

BISHOP, M.P., and COLBY, J.D., 2002, Anisotropic reflectance correction of SPOT-3 HRV imagery. *International Journal of Remote Sensing,* **23,** pp. 2125-2131.

BISHOP, M.P., KARGEL, J.S., KIEFFER, H.H., MACKINNON, D.J., RAUP, B.H., and SHRODER, J.F., 2000, Remote-sensing science and technology for studying glacier processes in high Asia. *Annals of Glaciology*, **31** pp. 164-170.

BISHOP, M.P., SCHRODER, J.F., and COLBY, J.D., 2003, Remote sensing and geomorphometry for studying relief production in high mountains. *Geomorphology,* **55**, pp. 345-361.

BISHOP, M.P., OLSENHOLLER, J.A., SHRODER, J.F., BARRY, R.G., RAUP, B.H., BUSH, A.B.G., COPLAND, L., DWYER, D.L., FOUNTAIN, A.G., HAEBERLI, W., KAAB, A., PAUL, F., HALL, D.K., KARGEL, J.S., MOLNIA, B.F., TRABANT, D.C., and WESSELS, R., 2008, Global land ice measurements from space (GLIMS): remote sensing and GIS investigations of the earth's cryosphere. *Geocarto International*, **19-2**, pp. 57-84.

CHANDER, G. and MARKHAM B., 2003, Revised Landsat-5 TM radiometric calibration procedures and postcalibration dynamic ranges. *IEEE Transactions on Geosciences and Remote Sensing*, **41**, pp. 2674 – 2677.

COLBY, J.D., 1991, Topographic normalization in rugged terrain. *Photogrammetric Engineering and Remote Sensing*, **57**, pp. 531-537.

COLBY, J.D., and KEATING, P.L., 1998, Land cover classification using Landsat TM imagery in the tropical highlands: the influence of anisotropic reflectance. *International Journal of Remote Sensing,* **19**, pp. 1479-1500.

EKSTRAND, S., 1996, Landsat TM-based forest damage assessment: Correction for topographic effects. *Photogrammetric Engineering and Remote Sensing,* **62**, pp. 151-161.

DAVAA, G., and BASANDORJ, D., 2005, Changes in hydrological systems of Mongolia. *UNESCO, 13th International Hydrological Programme (IHP) Regional Steering Committee Meeting for Southeast Asia and Pacific, Final Report,* 25 November 2005, Bali, Indonesia, (Jakarta: UNESCO) pp. 113-122.

DAVAA, G., MIJIDDORJ, R., KHUDULMUR, S., ERDENETUYA, M., KADOTA, T., and BAATARBILEG, N., 2005, Responses of the Uvs lake regime to the air temperature fluctuations and the environment changes: Ulaanbaatar, *Proceedings of the First International Symposium on Terrestrial and Climate Changes in Mongolia*, (Institute of Meteorology and Hydrology), pp. 130-133.

DAVAA, G., OYUNBAATAR, D. and SUGITA, M., 2007, Surface Water of Mongolia. In: Konagaya, Y. (ed.), *A Handbook of Mongolian Environments*, 55-68.

ENKHTAIVAN, D., 2006, Physical-geographical characteristics of the Altai region. In *Environmental Security and Sustainable Land Use – with Special Reference to Central Asia*, H. Vogtmann and N. Dobrestov (Ed.), pp. 349-351 (Doodrecht, Springer).

KAMP, U., and PAN, C., in prep. First satellite-derived glacier inventory for Mongolia. *Remote Sensing of Environment.*

KAMP U., KRUMWIEDE B., McMANIGAL K., PAN, C., WALTHER M., and DASHTSEREN A., 2013, Glaciers of Mongolia. *Institute for Arctic and Alpine Research (INSTAAR).* Occasional Paper 61.

KADOTA, T., and DAVAA, G., 2004, A preliminary study on glaciers in Mongolia: Ulaanbaatar, *Proceedings of the 2nd International Workshop on Terrestrial Change in Mongolia*, (Institute of Meteorology and Hydrology), pp. 100-102.

KADOTA, T., and DAVAA, G., 2007, Recent glacier variations in Mongolia. *Annals of Glaciology*, **46**, pp. 185-188.

KHRUTSKY, V.S., and GOLUBEVA, E.I., 2008, Dynamics of the glaciers of the Turgen-Kharkhira Mountain range (Western Mongolia): *Geography and Natural Resources*, **29**, pp. 278-287.

KLINGE, M., 2001, Glazialgeomorphologische Untersuchungen im Mongolischen Altai als Beitrag zur jungquartären Landschafts- und Klimageschichte der Westmongolei: Aachener Geographische Arbeiten, vol. 35, Aachen: Geographisches Institut der RWTH Aachen, 125 p. (In German).

KRUMWIEDE B.S., KAMP U., LEONARD G.J., DASHTSEREN A., WALTHER M., (in press), Recent glacier changes in the Altai Mountains, western Mongolia: case studies from Tavan Bogd and Munkh Khairkhan. In *Global Land Ice Measurements from Space*, J.S. Kargel, G.J. Leonard, M.P. Bishop, A. Kaab, B. Raup (Ed.), pp. (Praxis-Springer, Heidelberg).

LEHMKUHL, F., 1998, Quaternary glaciations in central and western Mongolia. *Journal of Quaternary Science*, **13**, pp. 153-167.

LEHMKUHL, F., and HASELEIN, F., 2000, Quaternary paleoenvironmental change on the Tibetan Plateau and adjacent areas (Western China and Western Mongolia). *Quaternary International*, **65-6**, pp. 121-145.

LEHMKUHL, F., and LANG, A., 2001, Geomorphological investigations and luminescence dating in the southern part of the Khangay and the Valley of the Gobi Lakes (Central Mongolia). *Journal of Quaternary Science*, **16**, pp. 69-87.

PAN, C., in prep, Inventory of Mongolian glaciers for the global land ice measurements from space (GLIMS) program. Master's Thesis. The University of Montana, U.S.A.

PAUL, F., and SVOBODA, F., 2009, A new glacier inventory on southern Baffin Island, Canada, from ASTER data: II. Data analysis, glacier change and applications. *Annals of Glaciology*, **50**, pp. 22-31.